Characterization of ultrashort pulses

Günter Steinmeyer
Max-Born-Institut für Nichtlineare Optik und Kurzzeitspektroskopie, Berlin
steinmey@mbi-berlin.de

MBI
Max-Born-Institute

Varenna, Italy

Enrico Fermi Summer School ***Saturday, July 5, 2014***

Overview

- **Fundamental Definitions, electric field, SVEA**
- **Classical methods: autocorrelation and Decorrelation**
- **Frequency-resolved optical gating (FROG)**
- **Spectral phase interferometry for direct electric field reconstruction (SPIDER)**
- **MIIPS, d-scan, etc.**
- **The coherent artifact**
- **Carrier-envelope phase**

Characterization of short light pulses

- **generally:** How can I measure events on femtosecond time scales?

- How can I characterize the shortest event ever?
- **Methods:**
  - Autocorrelation
  - Tomography-like methods (FROG)
  - Interferometry-based methods (SPIDER)

- **Limits:** The coherent artifact
- **Limits:** The carrier-envelope phase

Measuring on short time scales

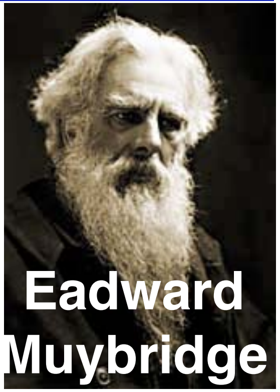

Eadward Muybridge
(1830-1904)

Electro-mechanical methods

⇒ electrically triggered mechanical shutters
⇒ 1/1000s temporal shutters

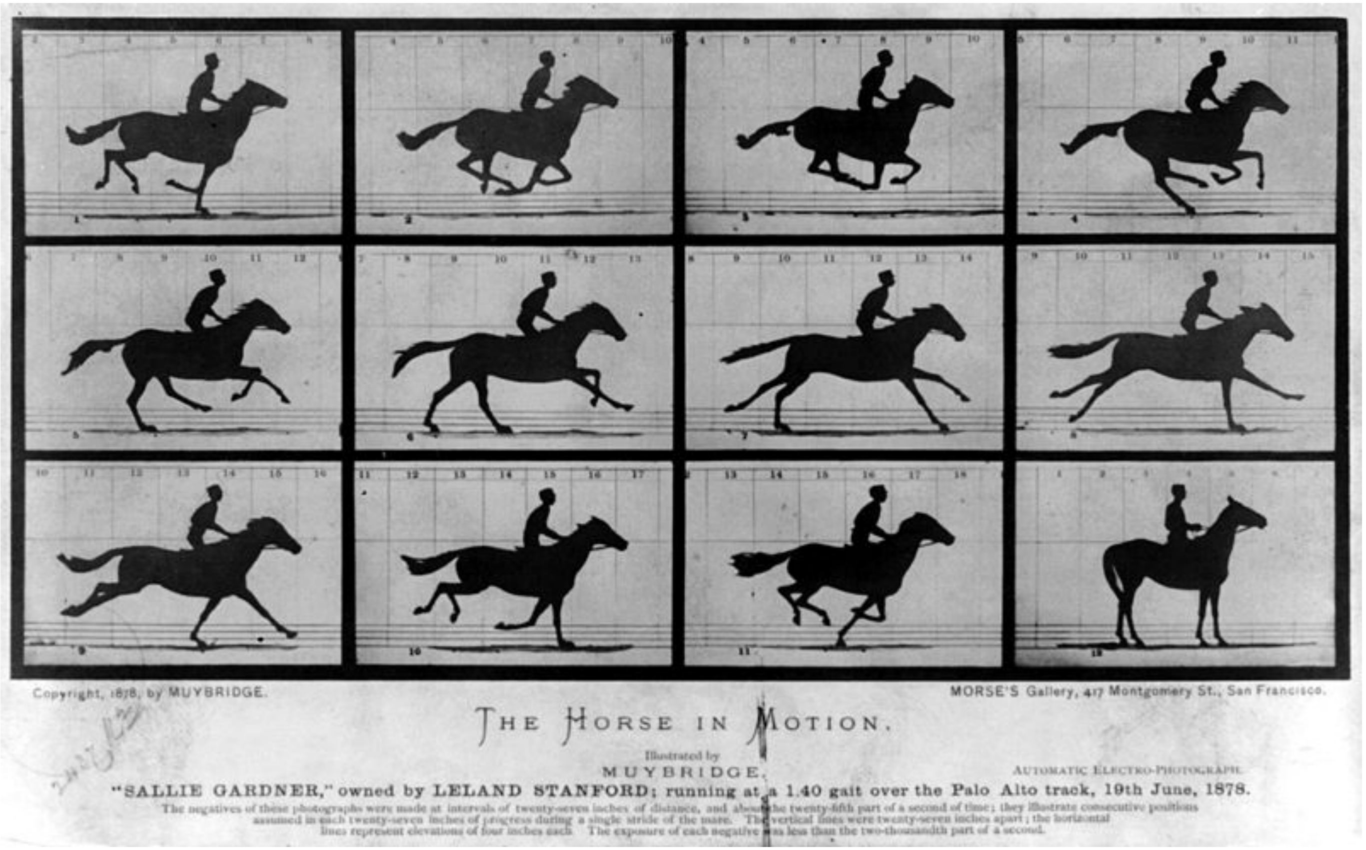

First movie ever
Horse: Sallie Gardner
June 19, 1878

12 trip wires and cameras

Microsecond time scales

Elektronics

⇒ triggered flash lamps

⇒ <μs temporal resolution

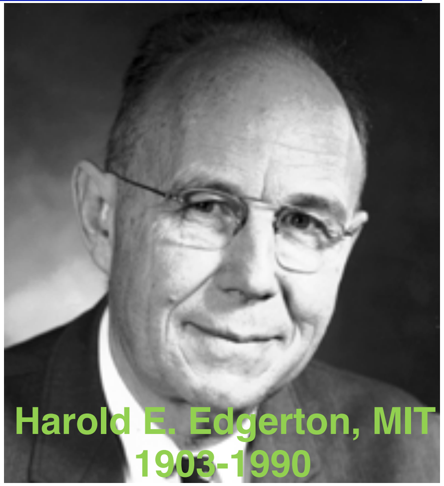

Harold E. Edgerton, MIT
1903-1990

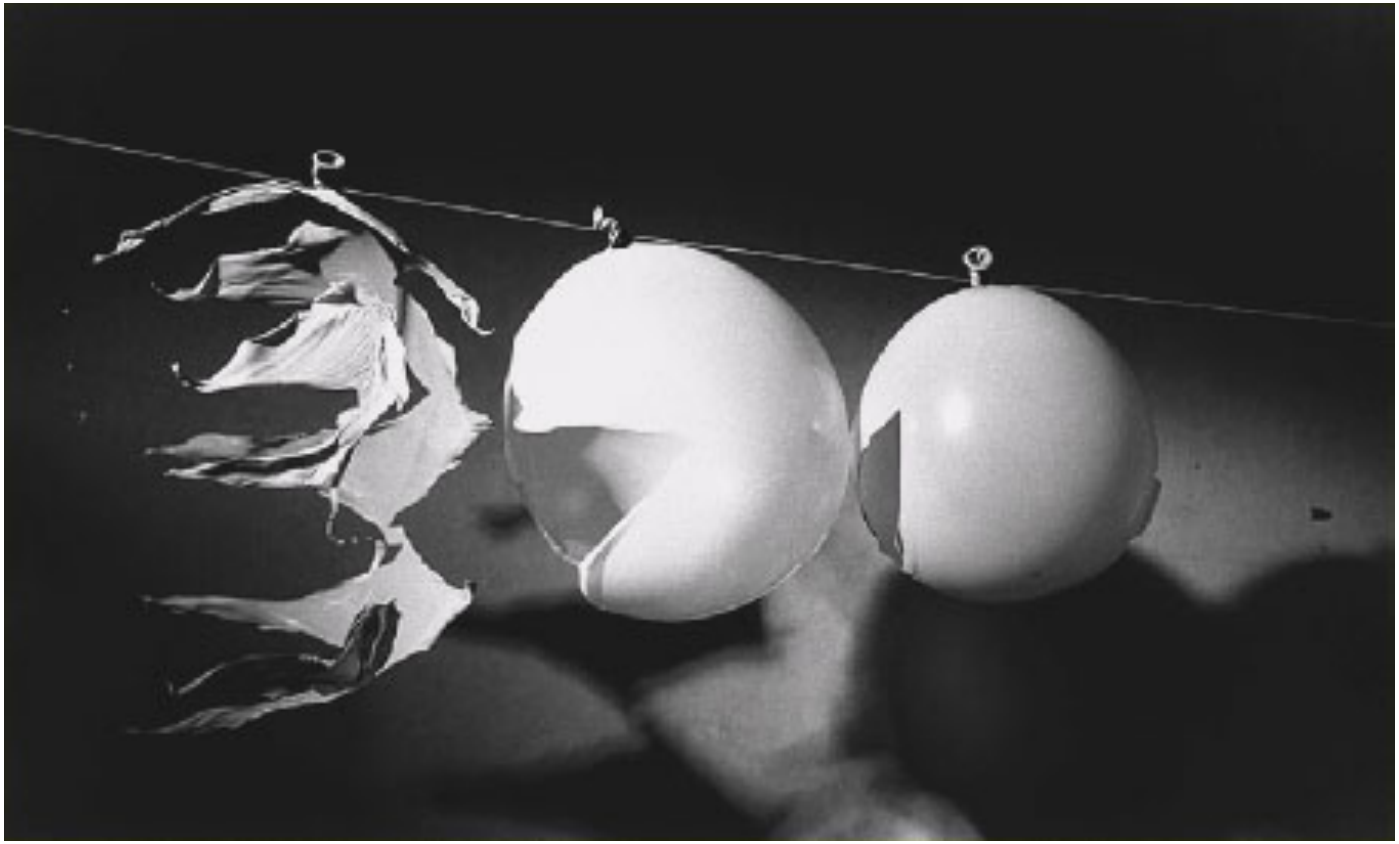

Stroboscopy with femtosecond lasers

Photonics

⇒ mode-locked lasers
⇒ a few 10^{-15} s temporal resolution

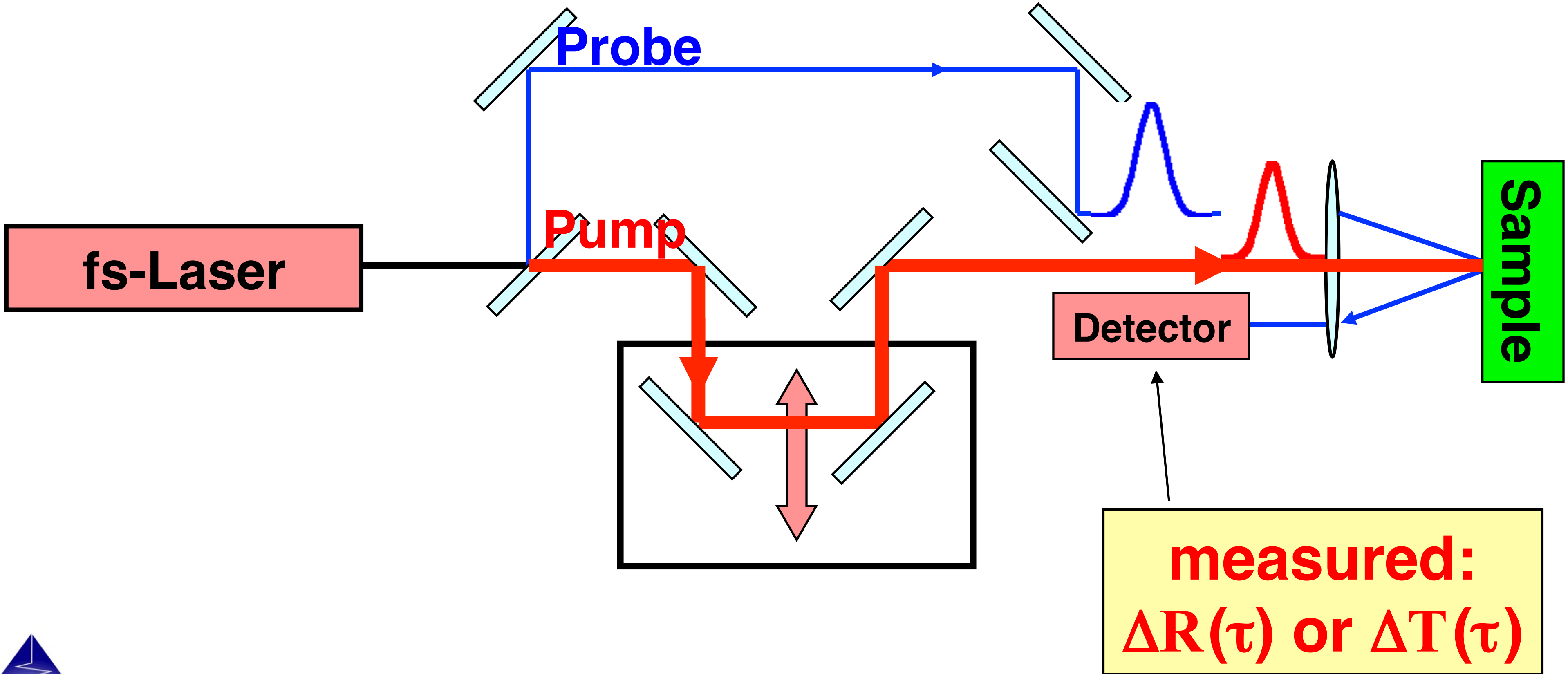

Ultrafast Pump-Probe Spectroscopy

Ref.: Mokhtari, Cong, Herek, Zewail, Nature **348**, 225 (1990)

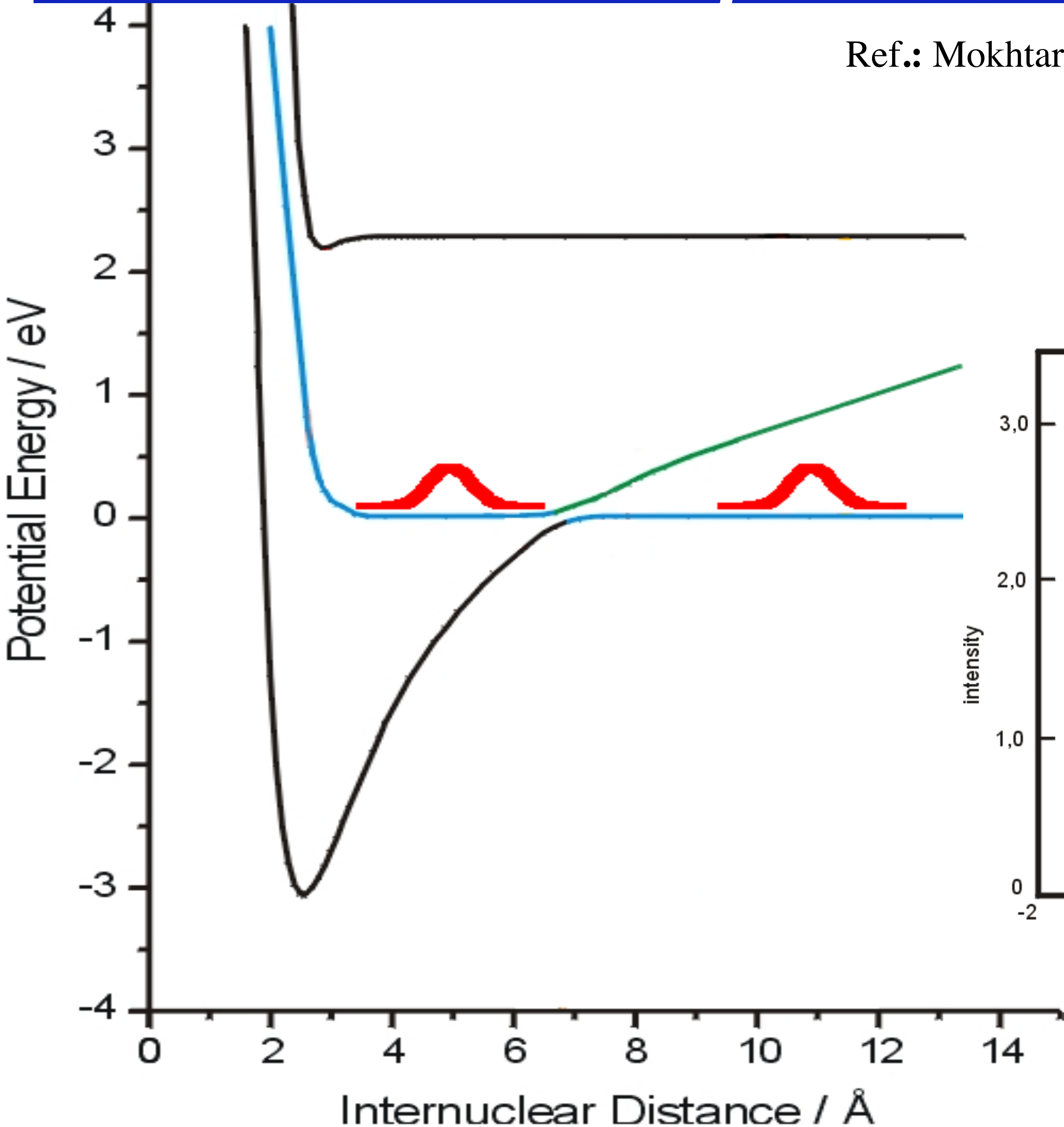

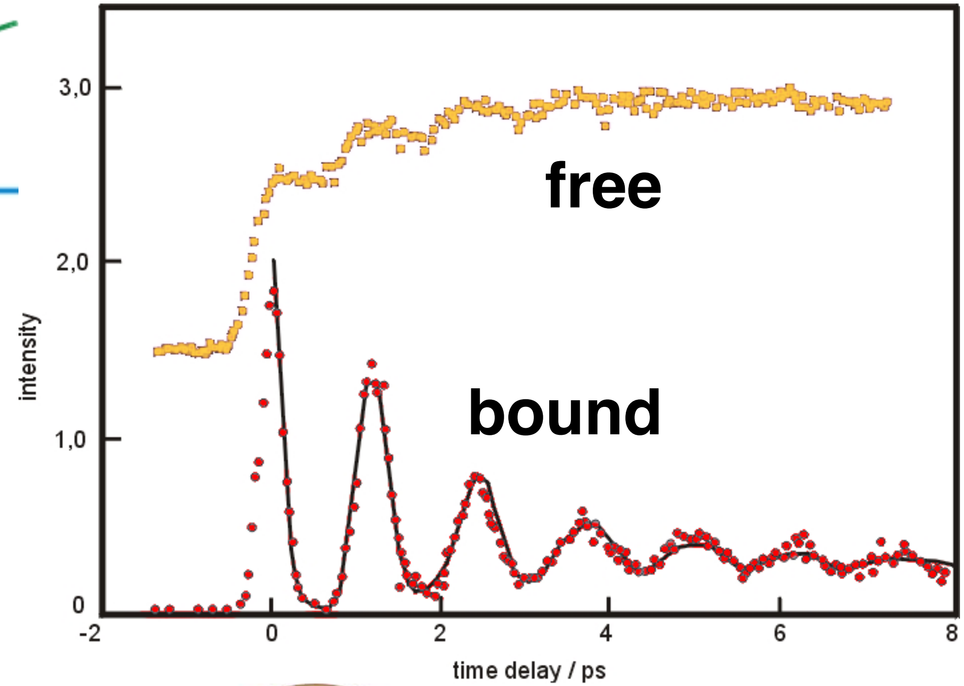

Nobel Prize in Physics 1999

Fundamental definitions and concepts

An ultrashort laser pulse has an intensity and phase vs. time.

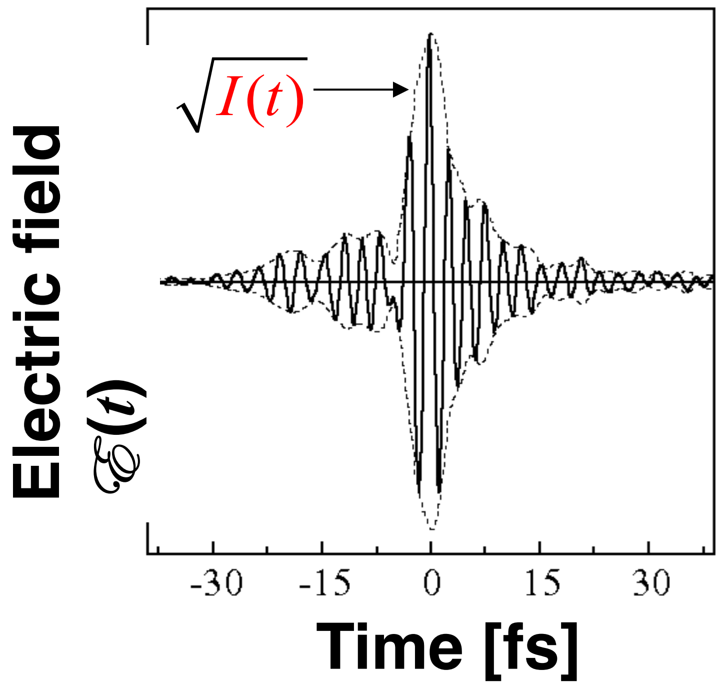

Neglecting the spatial dependence for now, the pulse electric field is given by:

$$\mathscr{E}(t) = \tfrac{1}{2}\sqrt{I(t)}\,\exp\{i[\omega_0 t - \phi(t)]\} + c.c.$$

Intensity

Carrier frequency

Phase

A sharply peaked function for the intensity yields an ultrashort pulse.

The phase tells us the color evolution of the pulse in time.

The real and complex pulse amplitudes

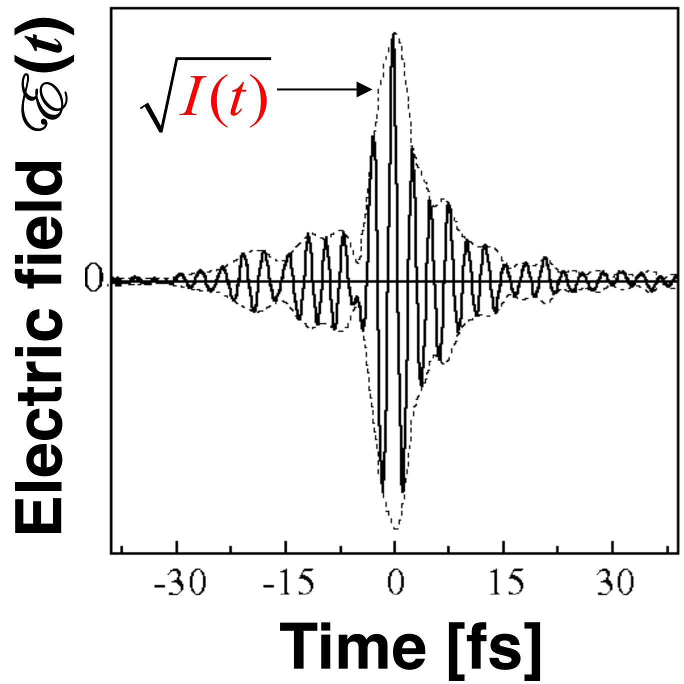

Removing the 1/2, the c.c., and the exponential factor with the carrier frequency yields the *complex amplitude, $E(t)$,* of the pulse:

$$E(t) = \sqrt{I(t)}\,\exp\{-i\phi(t)\}$$

This removes the rapidly varying part of the pulse electric field and yields a complex quantity, which is actually easier to calculate with.

$\sqrt{I(t)}$ is often called the *real amplitude, $A(t)$,* of the pulse.

Intensity vs. amplitude

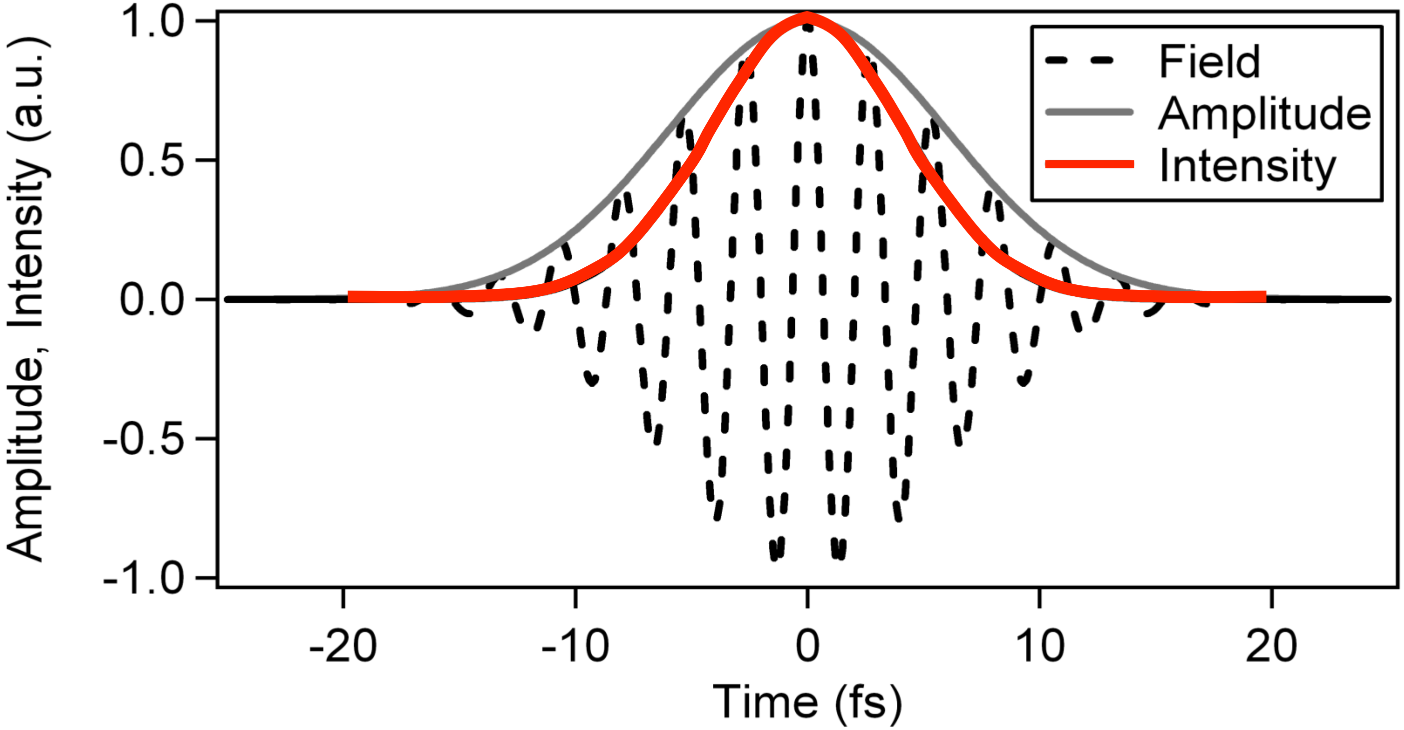

The phase of this pulse is constant, $\phi(t)$ = 0, and is not plotted.

The intensity of a Gaussian pulse is √2 shorter than its real amplitude. This factor varies from pulse shape to pulse shape.

Second-order phase: the linearly chirped pulse

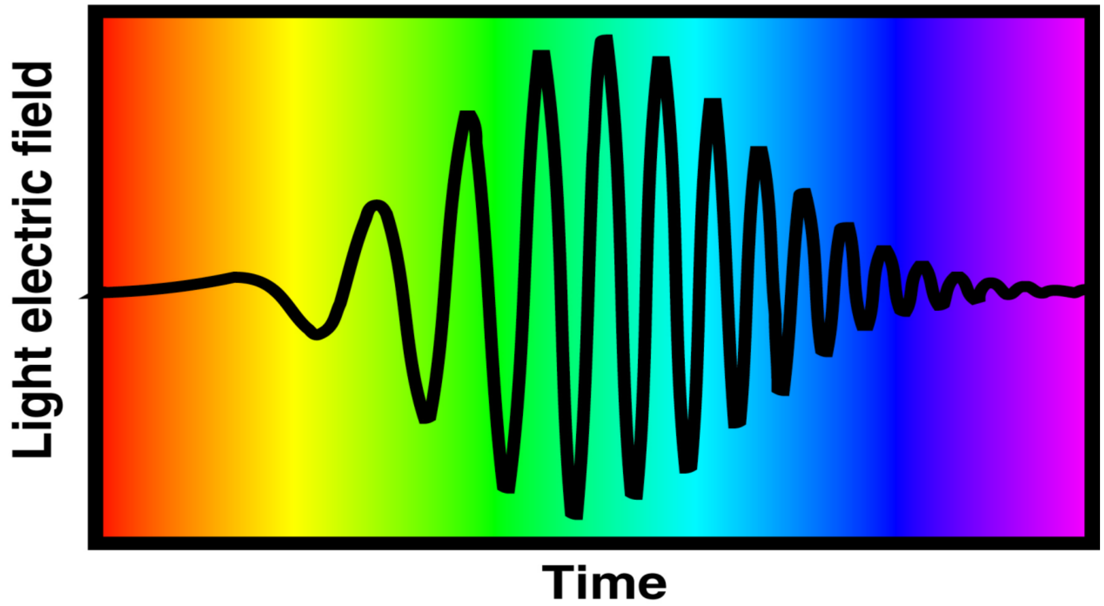

This pulse increases its frequency linearly in time (from red to blue).

In analogy to bird sounds, this pulse is called a "chirped" pulse.

The linearly chirped Gaussian pulse

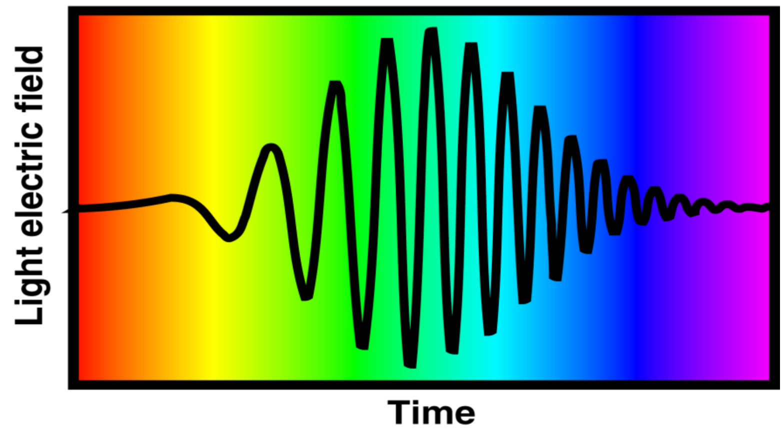

We can write a linearly chirped Gaussian pulse mathematically as:

$$E(t) = E_0 \underbrace{\exp\left[-(t/\tau_G)^2\right]}_{\text{Gaussian amplitude}} \exp\left[i\left(\underbrace{\omega_0 t}_{\text{Carrier wave}} + \underbrace{\beta t^2}_{\text{Chirp}}\right)\right]$$

Note that for $\beta > 0$, when $t < 0$, the two terms partially cancel, so the phase changes slowly with time (so the frequency is low). And when $t > 0$, the terms add, and the phase changes more rapidly (so the frequency is larger).

The Fourier Transform

$$\tilde{\mathcal{E}}(\omega) = \int_{-\infty}^{\infty} \mathcal{E}(t) \exp(-i\omega t)\, dt$$

$$\mathcal{E}(t) = \frac{1}{2\pi} \int_{-\infty}^{\infty} \tilde{\mathcal{E}}(\omega) \exp(i\omega t)\, d\omega$$

We always perform Fourier transforms on the real or complex pulse electric field, and not the intensity, unless otherwise specified.

The complex frequency-domain pulse field

Since the negative-frequency component contains the same infor-mation as the positive-frequency component, we usually neglect it.

We also center the pulse on its actual frequency, not zero. So the most commonly used complex frequency-domain pulse field is:

$$\tilde{\mathcal{E}}(\omega) \equiv \sqrt{S(\omega)}\,\exp\{-i\,\varphi(\omega)\}$$

Thus, the frequency-domain electric field also has an intensity and phase.

S **is the spectrum, and** φ **is the spectral phase.**

Method I

Characterizing the pulse by using one and the same pulse for the gate function

aka

Autocorrelation

Autocorrelator

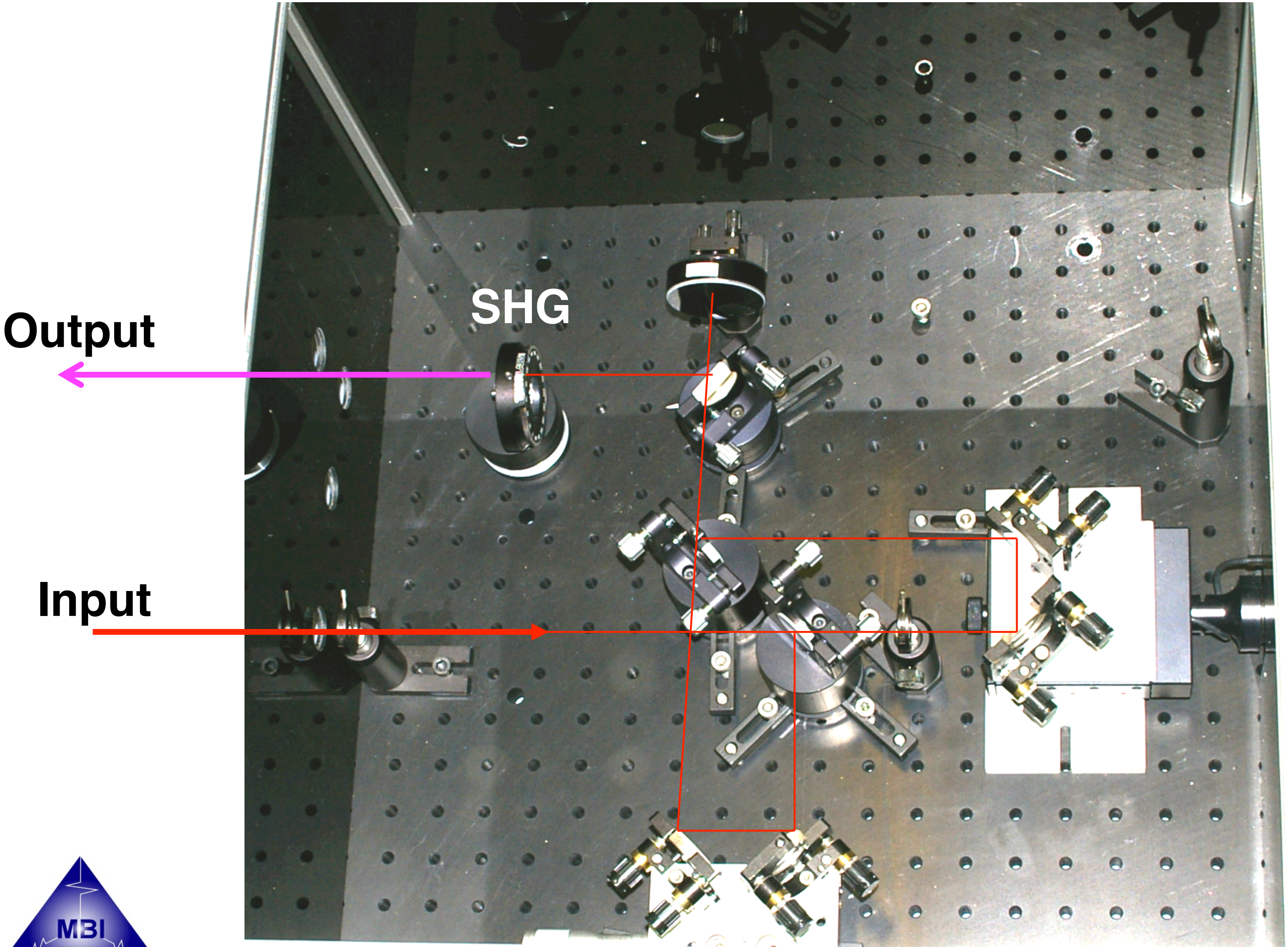

Double balanced scheme

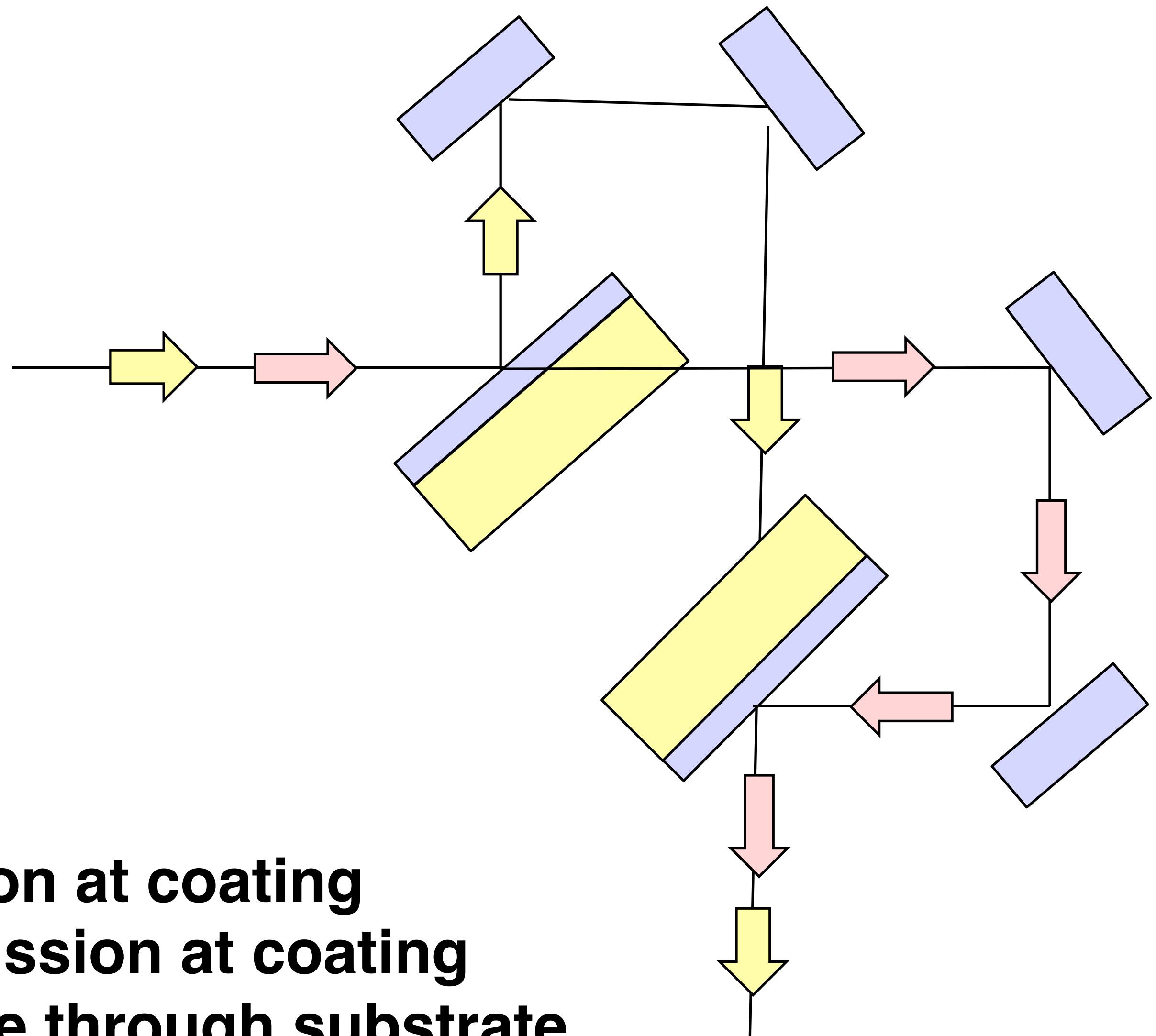

1 reflection at coating
1 transmission at coating
1 passage through substrate

Interferometric Autocorrelation

Interferometric autocorrelation

OR

Fringe-resolved autocorrelation

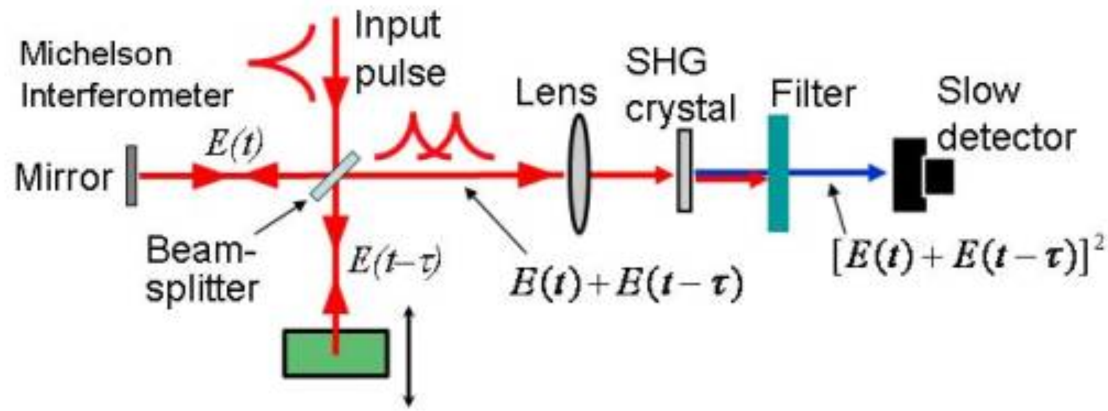

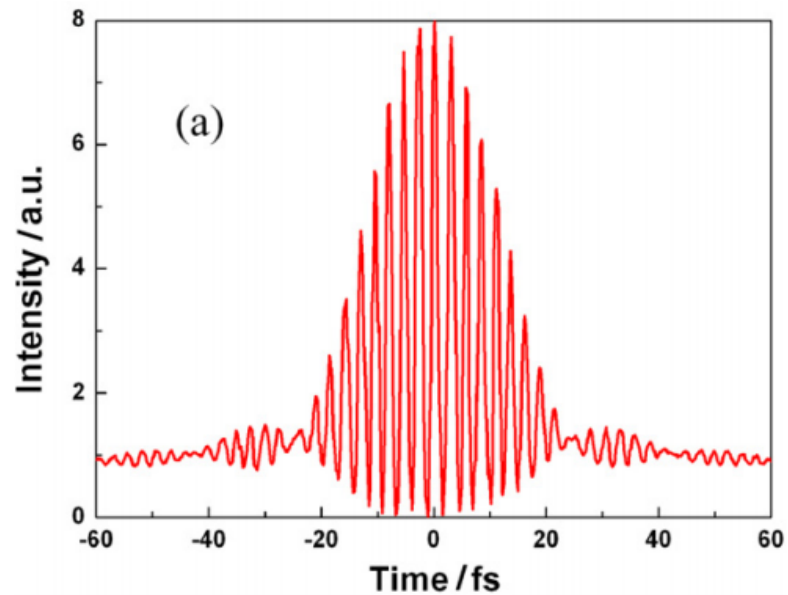

Suitable for few-cycle pulses
Maximum information

Ref. J.-C. Diels et al., Appl. Opt. 24, 1270 (1985)

Background-free autocorrelation

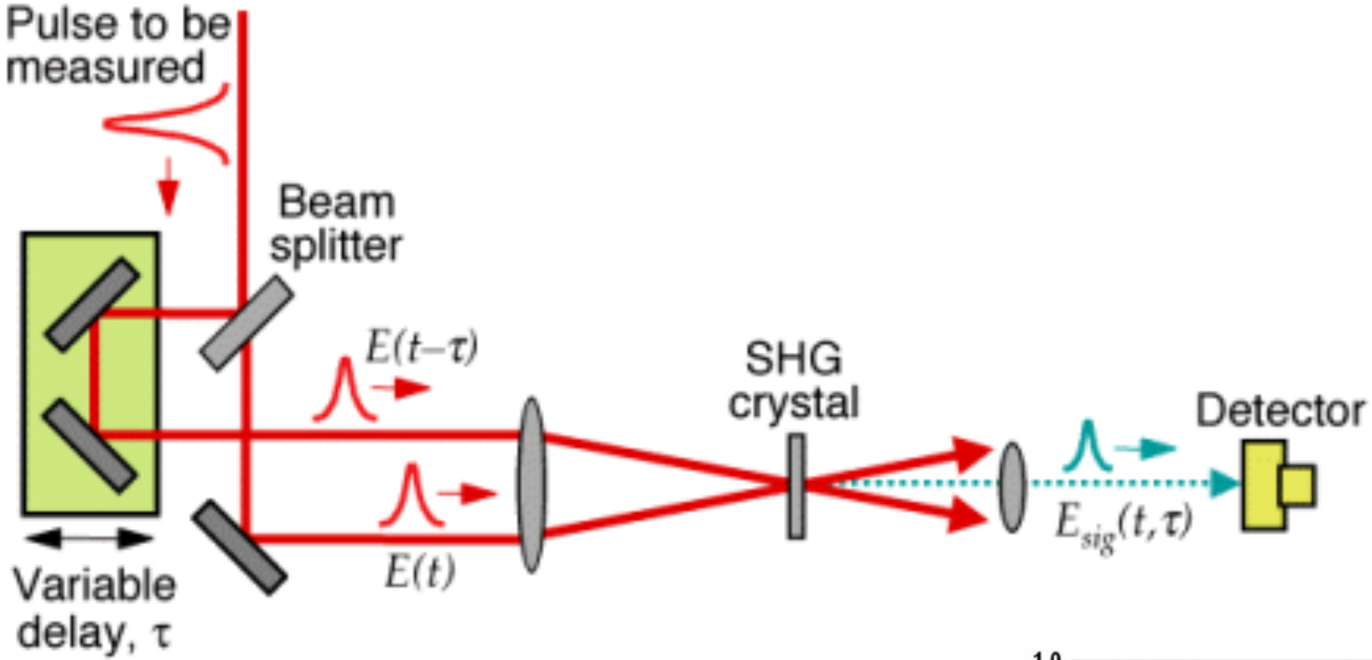

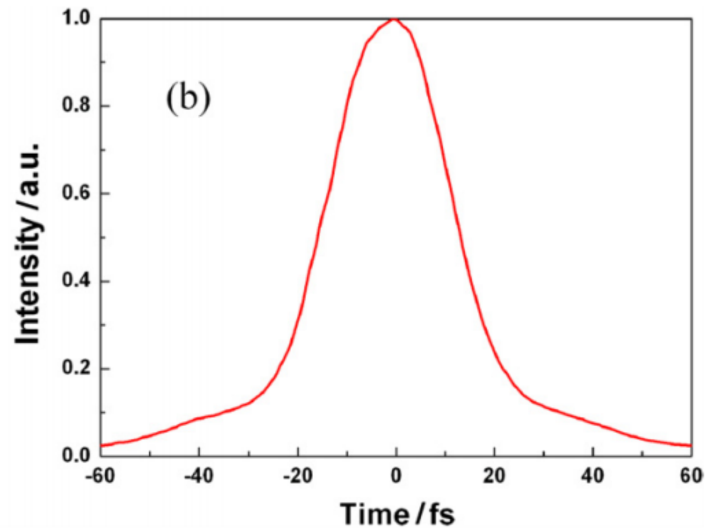

High dynamic range
Pulse contrast estimation
Not suitable for shortest pulses

Not background free but not necessarily interferometric…

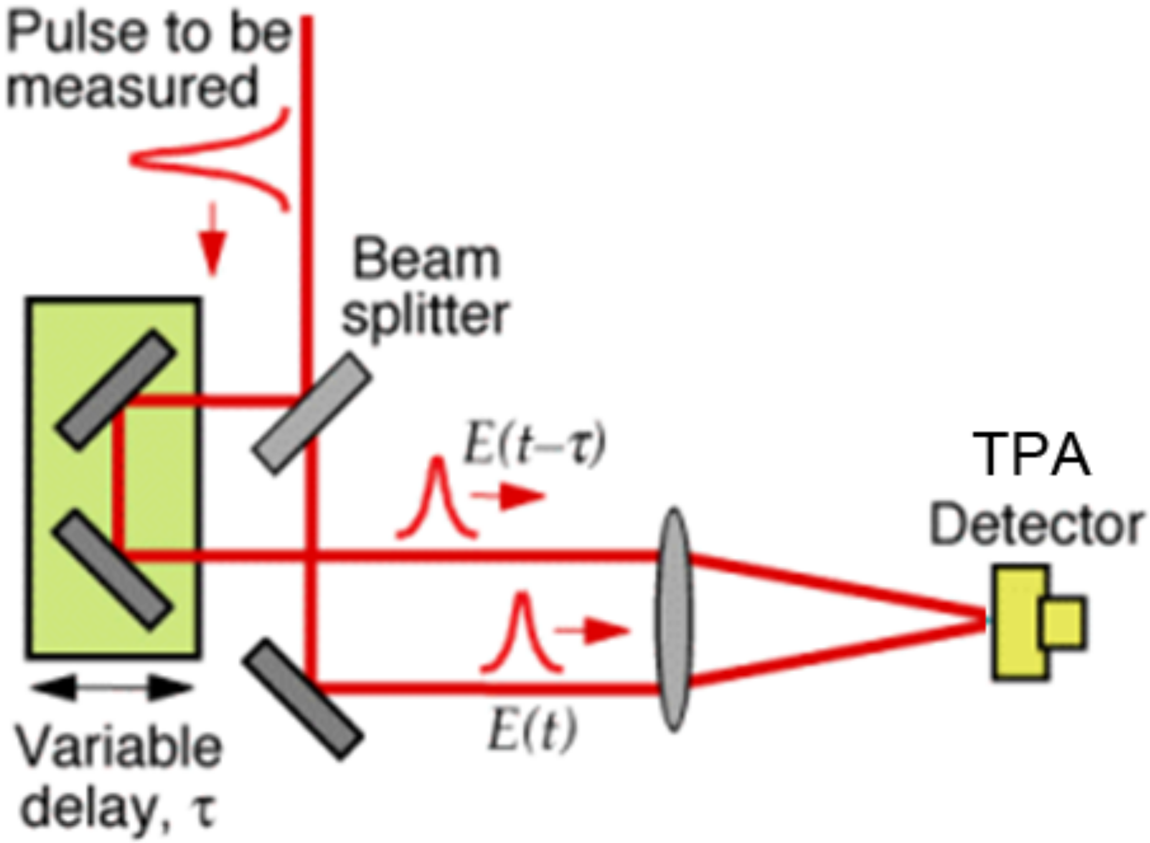

Basic Idea: Use a silicon photo diode at 1.5 μm wavelength

J. K. Ranka et al., Opt. Lett. **22**, 1344-1346 (1997)
D.T. Reid et al., Appl. Opt. **37**, 8142-8144 (1998)

Mathematical form of autocorrelation

I(t)=Intensity Envelope of Pulse

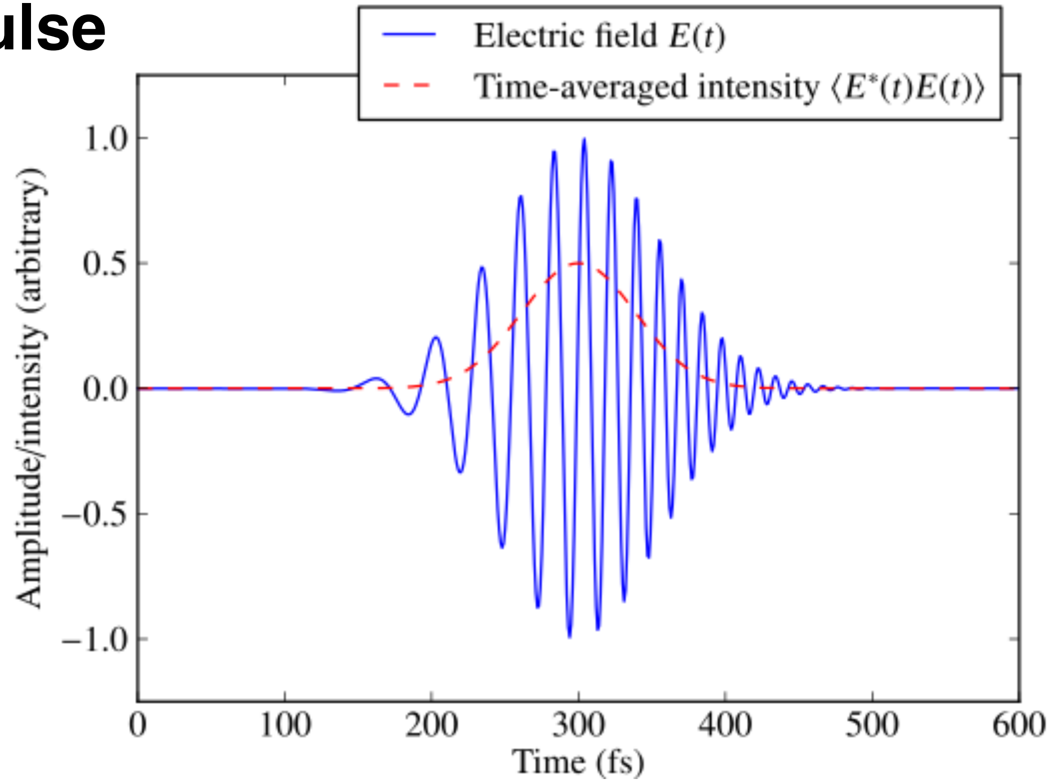

Intensity autocorrelation:

$$I(t) \otimes I(t) = \int I(t')\, I(t'-t)\, \mathrm{d}t' =: \mathcal{AC}(t)$$

Loss of symmetry information on I(t)

Impossible to retrieve I(t)

Evaluating autocorrelation traces

traditional: assumption of a pulse shape

$$I(t) := \mathrm{sech}^2(t/t_0)$$

$$\Rightarrow \mathrm{FWHM}[\mathcal{AC}(t)] = 1.763\ \mathrm{FWHM}[I(t)]$$

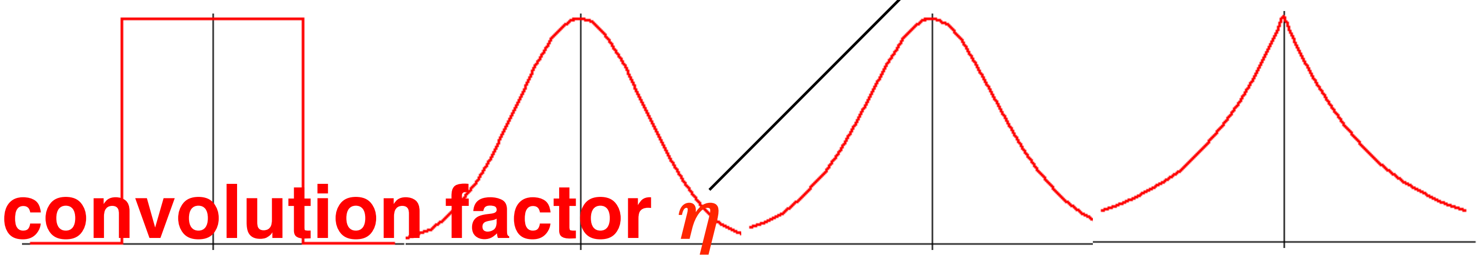

deconvolution factor η

η	rect	gaussian	sech	dbl exp
	1.0	**1.177**	**1.763**	**2.0**

Extensive tables for pulse shape guessing

Table I. Diagnostic Functions Corresponding to Various Pulse Shapes

$I(t)$	Δt	$I(\omega)$	$\Delta\omega$	$\Delta\omega/\Delta t$	$g_1(\tau)$	$\Delta\tau$	$\Delta\tau/\Delta t$	$G_2(\tau)$	$\Delta\tau$	$\Delta\tau/\Delta t$	$g_2(\tau)$
e^{-t^2}	1.665	$e^{-\omega^2}$	1.665	2.772	$1 + e^{-\frac{\tau^2}{4}}$	3.330	2	$e^{-\frac{\tau^2}{2}}$	2.355	1.414	$1 + 3G_2(\tau) \pm 4e^{-\frac{3}{8}\tau^2}$
$\mathrm{sech}^2 t$	1.763	$\mathrm{sech}^2 \frac{\pi\omega}{2}$	1.122	1.978	$1 \pm \frac{\tau}{\sinh\tau}$	4.355	2.470	$\frac{3(\tau\cosh\tau - \sinh\tau)}{\sinh^3\tau}$	2.720	1.543	$1 + 3G_2(\tau) \pm \frac{3(\sinh 2\tau - 2\tau)}{\sinh^3\tau}$
$\frac{1}{\left(e^{\frac{t}{1+A}} + e^{-\frac{t}{1-A}}\right)^2}$ A = ¼	1.715	$\frac{1 + 1/\sqrt{2}}{\cosh\frac{15\pi}{16}\omega + 1/\sqrt{2}}$	1.123	1.925	$1 \pm 4\frac{\sinh\frac{1}{3}\tau}{\sinh\frac{4}{3}\tau}$	3.405	1.985	$\frac{1}{\cosh^3\frac{8}{15}\tau}$	2.648	1.544	$1 + 3G_2(\tau) \pm 4\frac{\cosh^3\frac{4}{15}\tau}{\cosh^3\frac{8}{15}\tau}$
A = ½	1.565	$\mathrm{sech}\frac{3\pi}{4}\omega$	1.118	1.749	$1 \pm 2\frac{\sinh\tau}{\sinh 2\tau}$	2.634	1.683	$\frac{3\sinh\frac{8}{3}\tau - 8\tau}{4\sinh^3\frac{4}{3}\tau}$	2.424	1.549	$1 + 3G_2(\tau) \pm 4\frac{\tau\cosh 2\tau - \frac{3}{2}\cosh^2\frac{2}{3}\tau\sinh\frac{2}{3}\tau(2 - \cosh\frac{4}{3}\tau)}{\sinh^3\frac{4}{3}\tau}$
A = ¾	1.278	$\frac{1 - 1/\sqrt{2}}{\cosh\frac{7\pi}{16}\omega - 1/\sqrt{2}}$	1.088	1.391	$1 \pm \frac{4\sinh 3\tau}{3\sinh 4\tau}$	1.957	1.531	$\frac{2\cosh\frac{16}{7}\tau + 3}{5\cosh^3\frac{8}{7}\tau}$	2.007	1.570	$1 + 3G_2(\tau) \pm 4\frac{\cosh^3\frac{4}{7}\tau\,(6\cosh\frac{8}{7}\tau - 1)}{5\cosh^3\frac{8}{7}\tau}$
$\frac{1}{(e^t + e^{-rt})^2}$		$\frac{2(1-y)x}{x^2 - 2yx + 1}$ where, $x = \exp(\frac{2\pi\omega}{1+r})$, $y = \cos(\frac{2\pi r}{1+r})$			$1 \pm \frac{r+1}{r-1}\frac{\sinh(\frac{r-1}{2}\tau)}{\sinh(\frac{r+1}{2}\tau)}$						

$I(t)$ and $I(\omega)$ are the intensities in the time and (angular) frequency domains, respectively. $g_1(\tau)$ is the first-order autocorrelation of the field envelope. $G_2(\tau)$ is the intensity autocorrelation, and $g_2(\tau)$ the envelope of the interferometric [illegible]ation. The FWHM is indicated in the next column to the right for each function.

Ref. J.-C. Diels et al., Appl. Opt. 24, 1270 (1985)

Time-bandwidth product

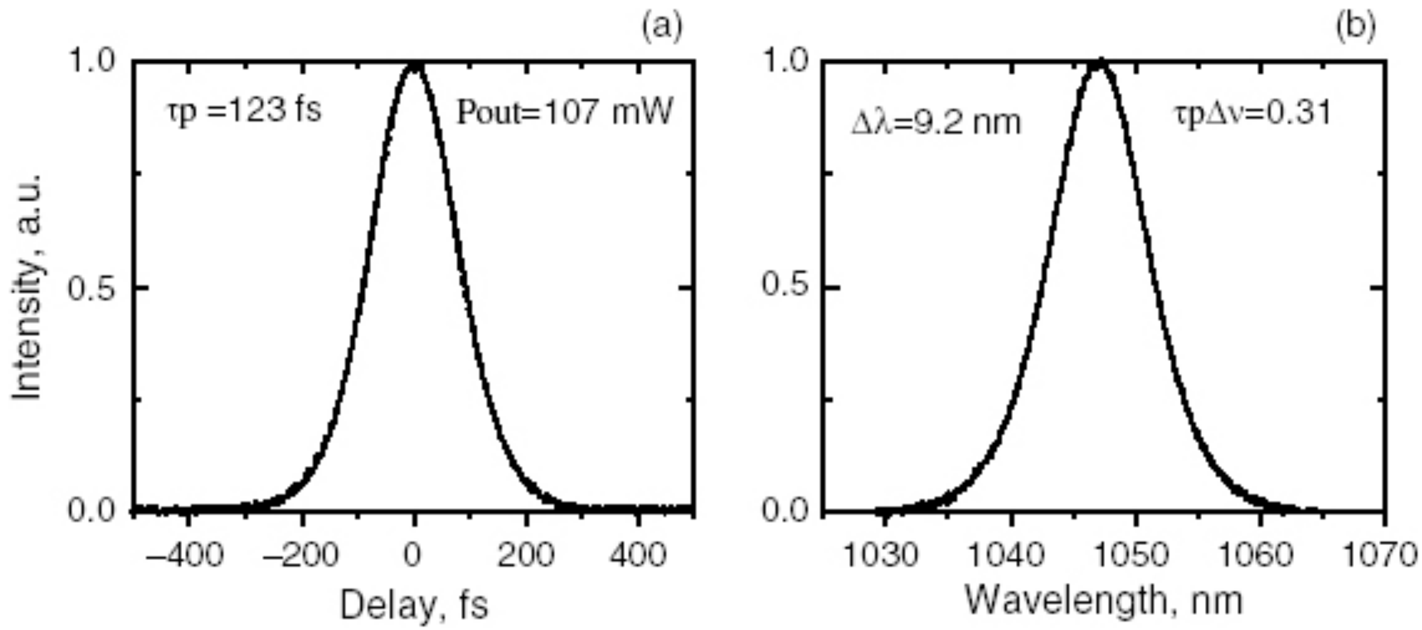

TBP = FWHM(Spectrum) x FWHM(ACF) x deconv. factor

Ideal sech^2 pulse: TBP = 0.32

Careful: TBP can be as small as 0.2 for asymmetric pulses

Example taken from Brown et al., New J. Phys. **6** (2004) 175

MBI

The autocorrelation paradox

It's simply impossible to measure the <u>shortest pulse</u> without having an even shorter event at hand...

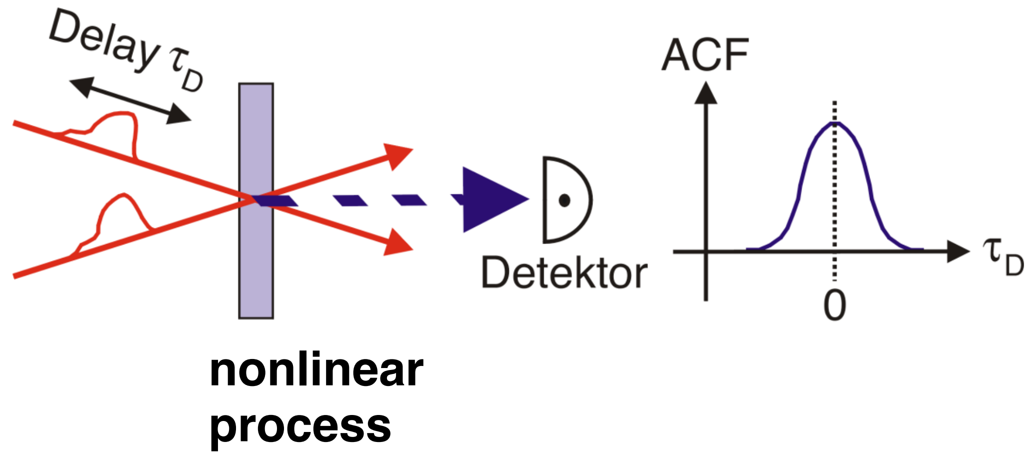

...therefore one has to escape the swamp by pulling oneself up by one's own hair...

Method Ia

Can we fix the problem of autocorrelation?

Decorrelation

The decorrelation problem

Wiener-Khinchin theorem

$$\mathfrak{AC}[f(t)] = \mathcal{F}^{-1}[\,|\,\mathcal{F}[f(t)]\,|^2]$$

$$f \otimes f \overset{\mathcal{F}}{\Longleftrightarrow} f \cdot f$$

"Convolution is multiplication in the Fourier domain"

$$f(t) = \mathcal{F}^{-1}\left[\sqrt{\mathcal{F}[\mathfrak{AC}[f(t)]]}\right] \;\; ??$$

The Decorrelation dilemma

$$f(t) = (\exp(t) + \exp(-\alpha\, t))^{-1} \qquad f(t) = \mathcal{F}^{-1}\left[\sqrt{\,|\,\mathcal{F}[\mathfrak{AC}[f(t)]]\,|}\,\right]$$

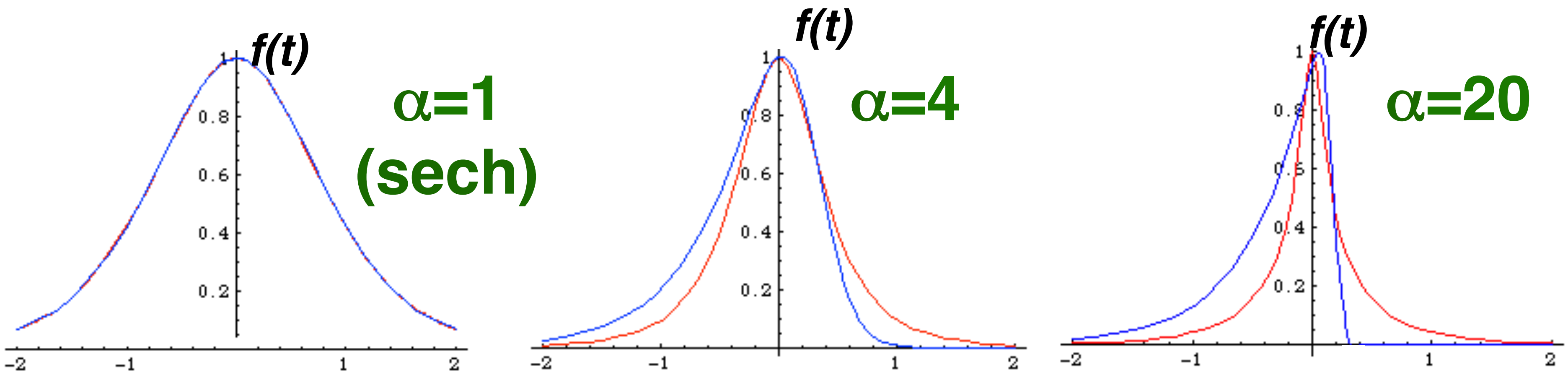

$$\frac{\mathrm{FWHM}(f)-\mathrm{FWHM}(f)}{\mathrm{FWHM}(f)}$$

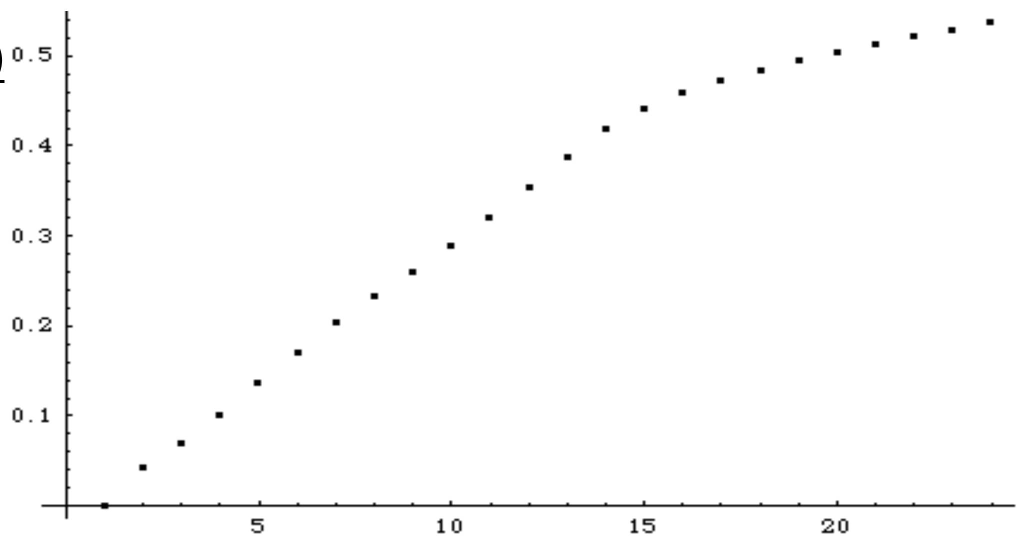

Decorrelation from ACF+spectrum

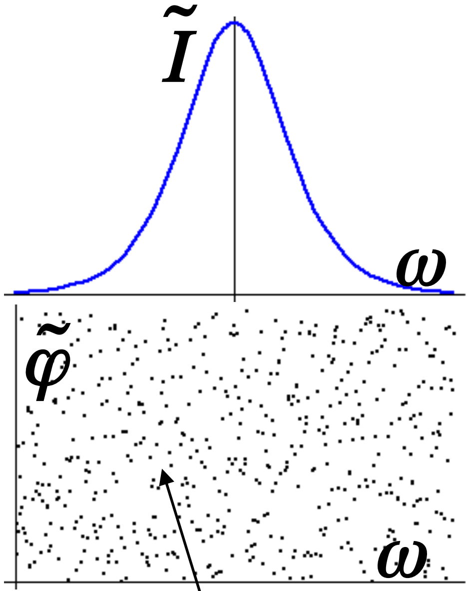

random
phase
to start

$$|\tilde{I}(\omega)| = \sqrt{\tilde{I}_{ACF}(\omega)}$$
$$\phi(\omega)$$

$\xrightarrow{FT}$

$$I(t)$$

force
$$I(t) \geq 0$$

$\xleftarrow{FT^{-1}}$

$$|\tilde{I}(\omega)|$$
$$\phi(\omega)$$

TIVI-algorithm, Peatross et al., JOSA B **15**, 216 (1998)
R.W. Gerchberg & W.O. Saxton, Optik **35**, 237 (1972)

decorrelation from ACF+Spectrum

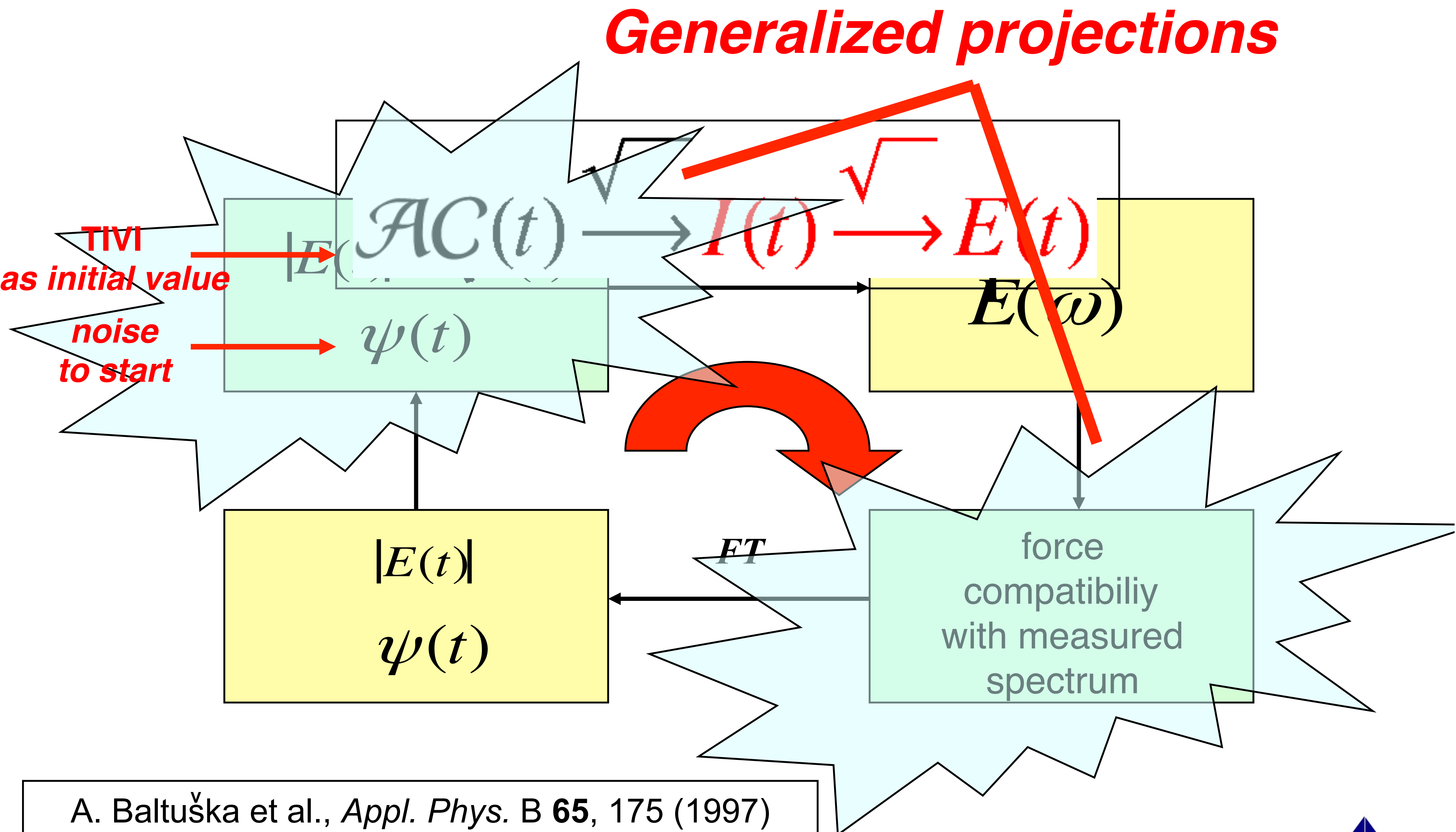

A. Baltuška et al., *Appl. Phys.* B **65**, 175 (1997)

http://www.chem.rug.nl/spectro/Projects/decorrelation.htm

decorrelated measurements

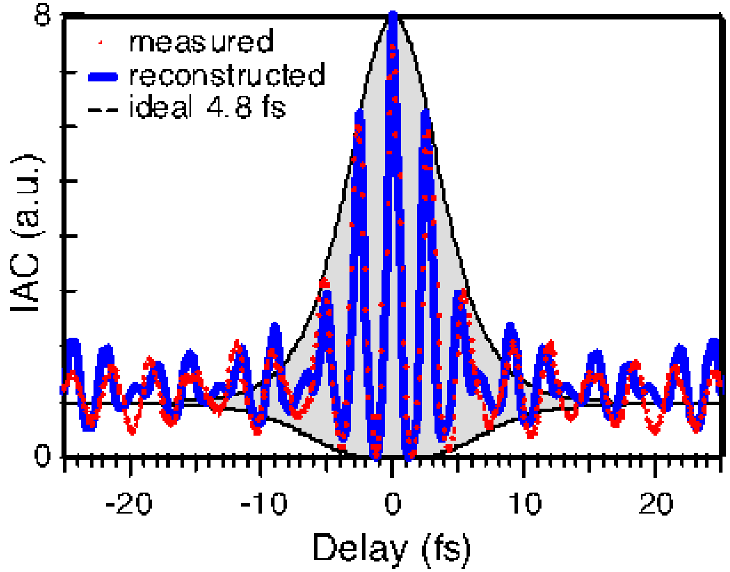

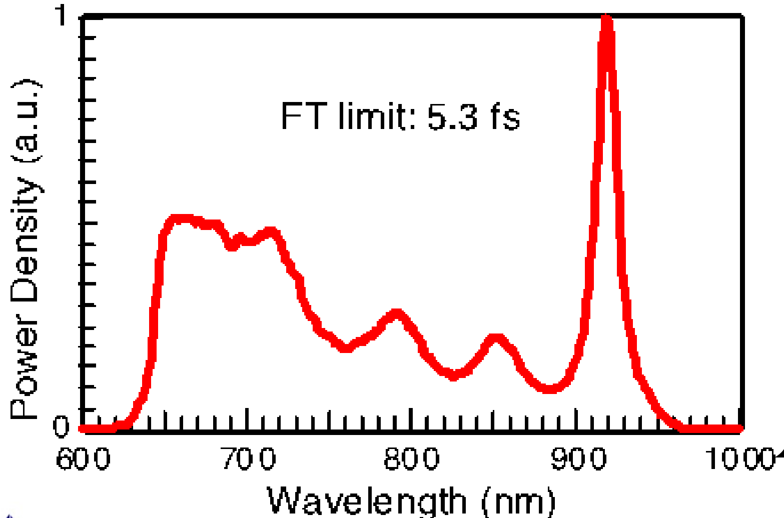

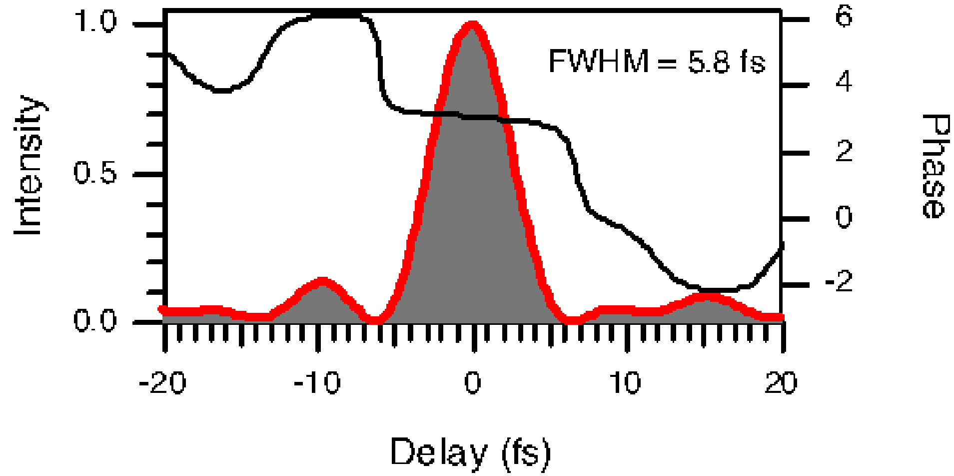

Certainly better than assumption of some arbitrary deconvolution factor, yet very susceptible to experimental noise and positively not unambiguous...

D.Sutter et al., *Opt. Lett.* **24**, 631 (1999)

Chung & Weiner, IEEE J. Sel. Top. QE **7**, 656 (2001)

PICASO method

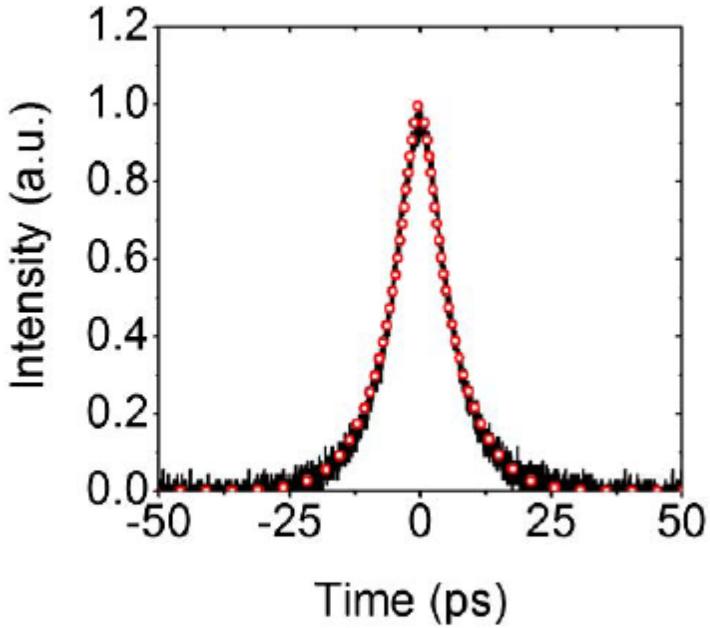

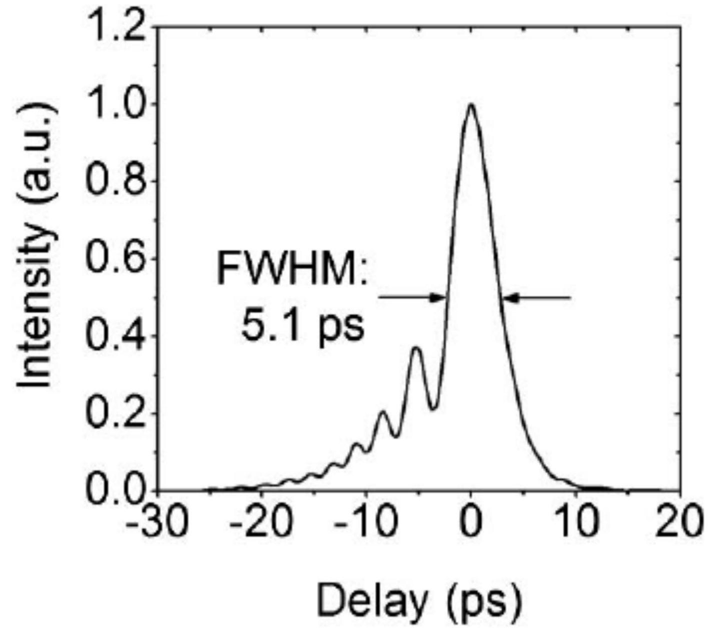

Iteratively fit phase to E(ω) until autocorrelation is retrieved

J. W. Nicholson and W. Rudolph, J. Opt. Soc. Am. B 19, 330 (2002).
S. Ranta et al., Opt. Lett. **38**, 2289-2291 (2013).

PICASO = Phase and Intensity from Correlation and Spectrum Only

Summary decorrelation

1. Assumption of a particular pulse shape ("$sech^2$-deconvolution")

- simple
- large error
- not really characterization of the pulse shape

2. Decorrelation via generalized projection

- simple application of Wiener-Khinchin theorem ignores pulse asymmetry
- may cause unphysical pulse shapes ($I(t)<0$)
- TIVI algorithm forces $I(t)$ to be >0
- has to be used with great care in the interpretation

In general:

- too little information for reconstructing the complete pulse shape
- pulse shape not unambiguously determined by measured data
- methods are helpful if FROG or SPIDER cannot be done

Method II

Spectrally resolved autocorrelation

aka

Frequency-resolved optical gating

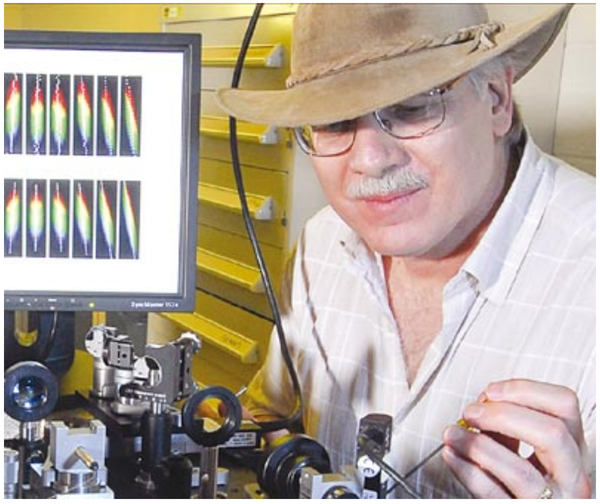

FROG

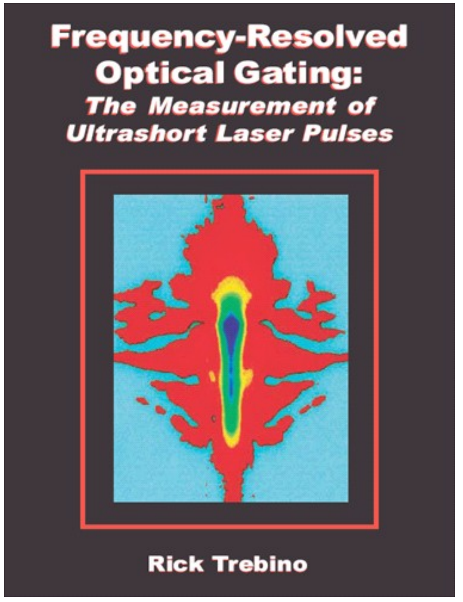

Spectrally resolved autocorrelation

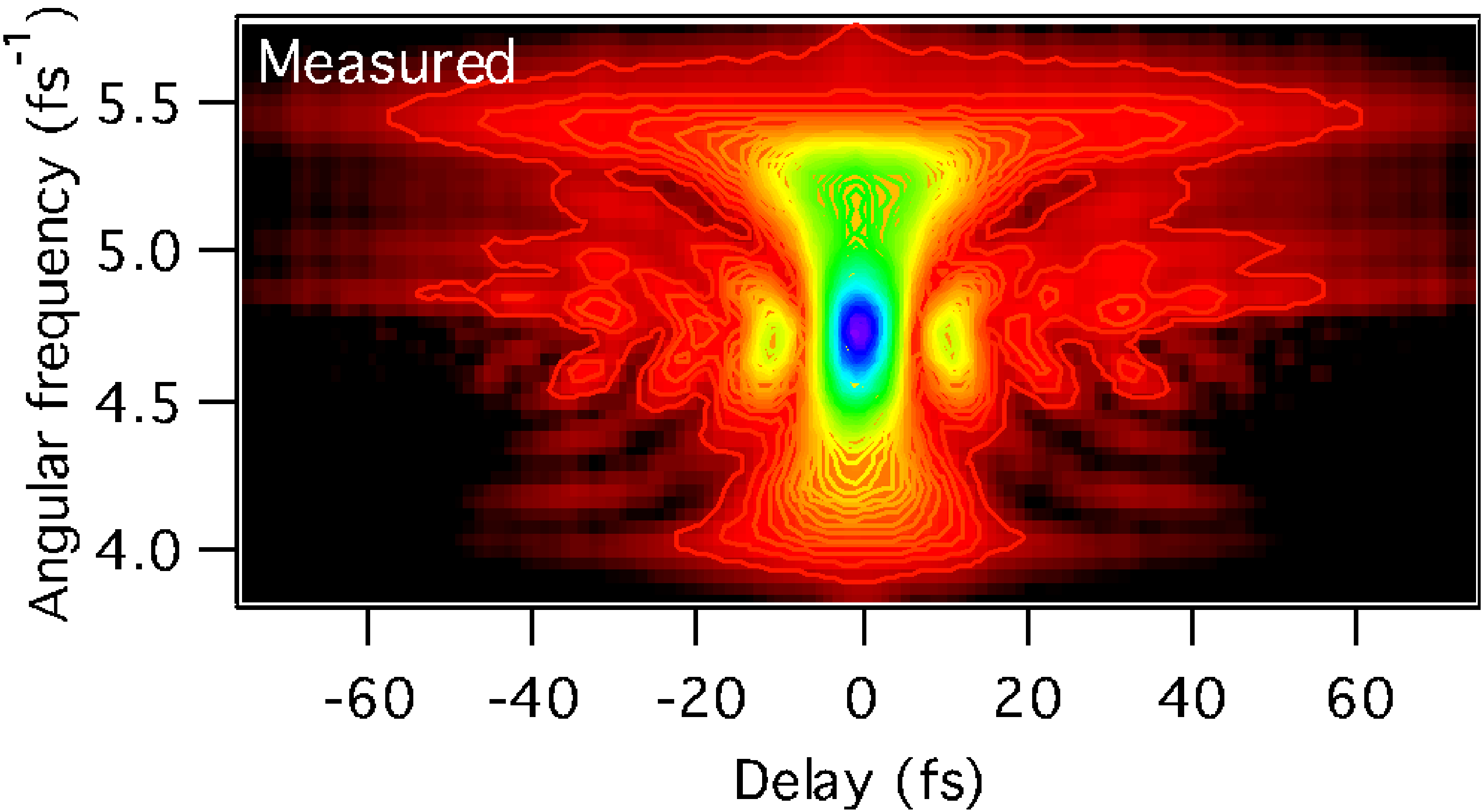

Core idea of FROG

1. **Simple autocorrelation data ACF(t) is not sufficient to unambiguously define the pulse shape.**

2. **Simply adding the spectrum does not suffice either.**

3. **Spectrally resolved autocorrelation data ACF(ω,t), however, essentially unambiguously defines the pulse shape**

4. **FROG trace retrieval is an inverse problem. You have the answer, but have to find the one matching question that yields this very answer....**

Various nonlinearities can be employed:

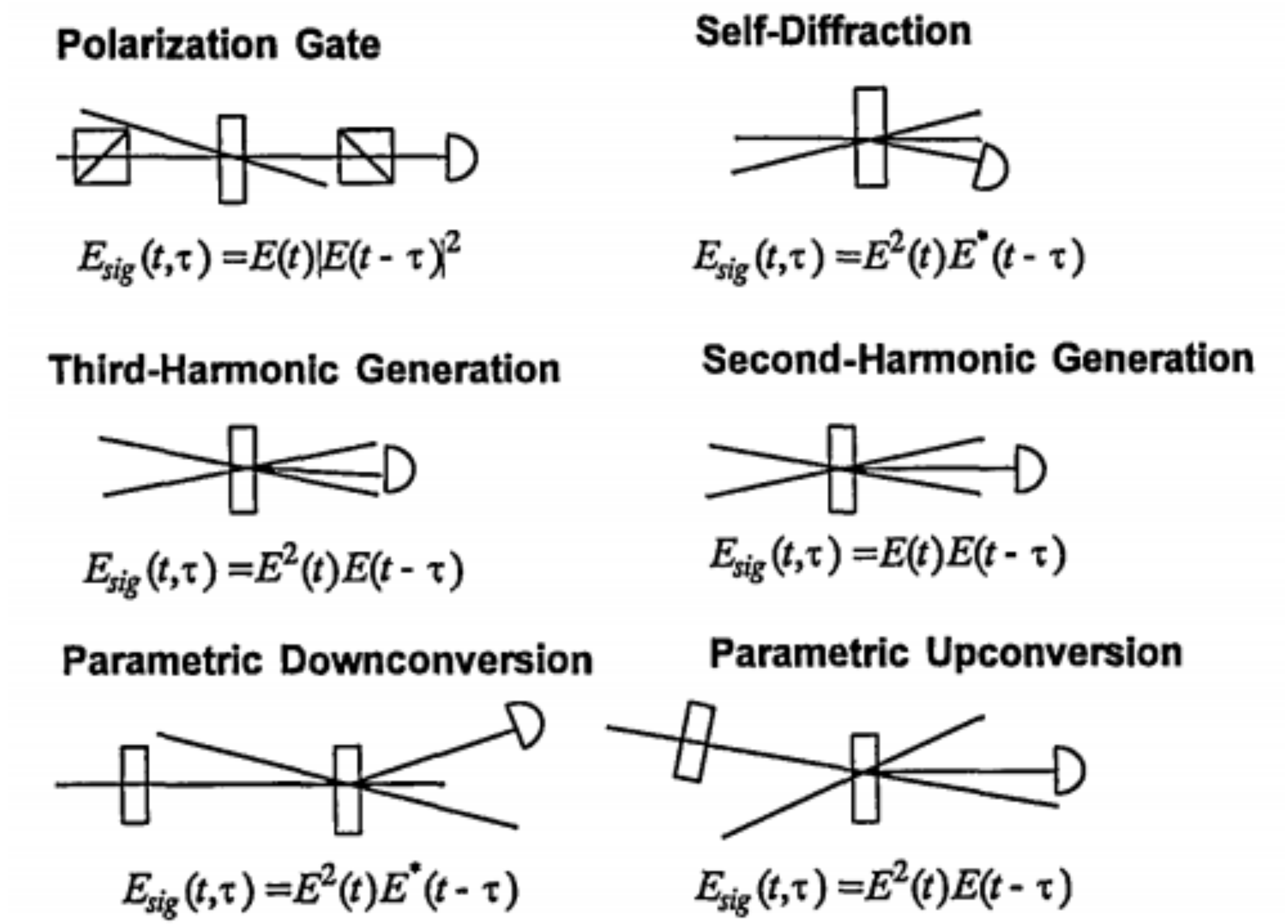

Fig. 1. Schematic of the various experimental geometries for generating FROG traces. The nonlinear mixing signal is spectrally resolved as a function of delay time between the two replicas of the beam to be measured. The parametric conversion geometries use two crystals with a second-order nonlinearity, cascaded to produce an effective third-order nonlinearity.

Frequency-resolved optical gating (FROG)

Measuring the spectrogram of the autocorrelation

$$I_{FROG}^{SHG}(\omega,\tau) = \left| \int \underbrace{E(t)E(t-\tau)}_{=E_{sig}(t,\tau)} \exp(-i\omega t)\mathrm{d}t \right|^2$$

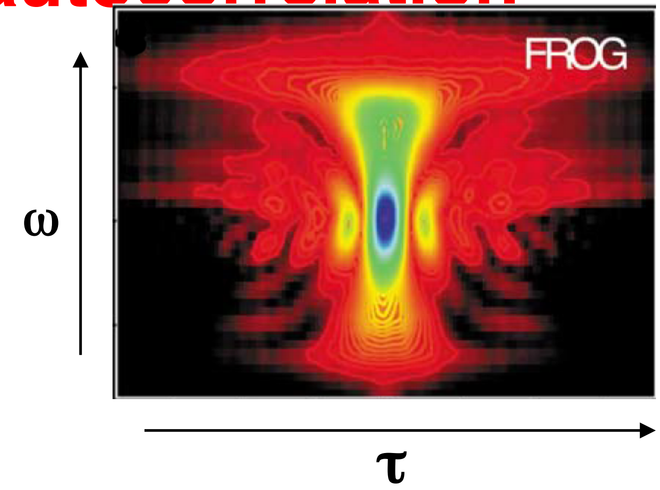

- Phase information of signal field $E_{sig}(t,\tau)$ gone
- However: phase is redundant and unambiguously defined by FROG trace
- Generalized Projections Algorithm

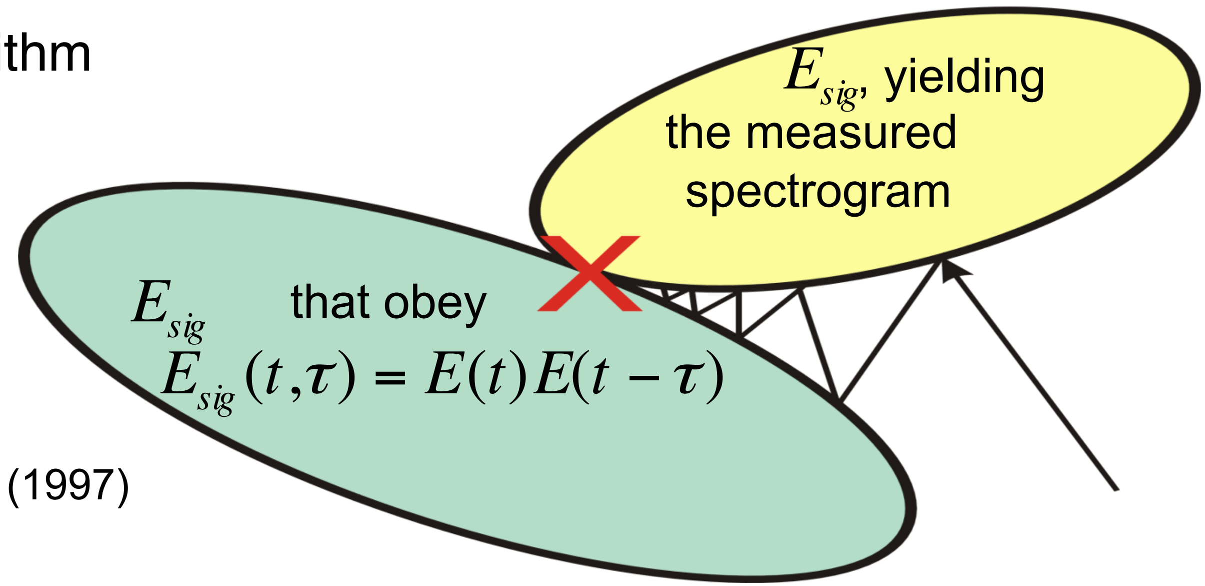

R. Trebino et al., *Rev. Sci. Instrum.* **68**, 3277 (1997)

http://www.wco.com/~fsoft/

FROG software

It is very instructive to write your own FROG software…

but there are much quicker alternatives:

Freely available Matlab code

http://frog.gatech.edu/code.html

Commercial retrieval code

http://www.swsciences.com/

Example FROG measurements

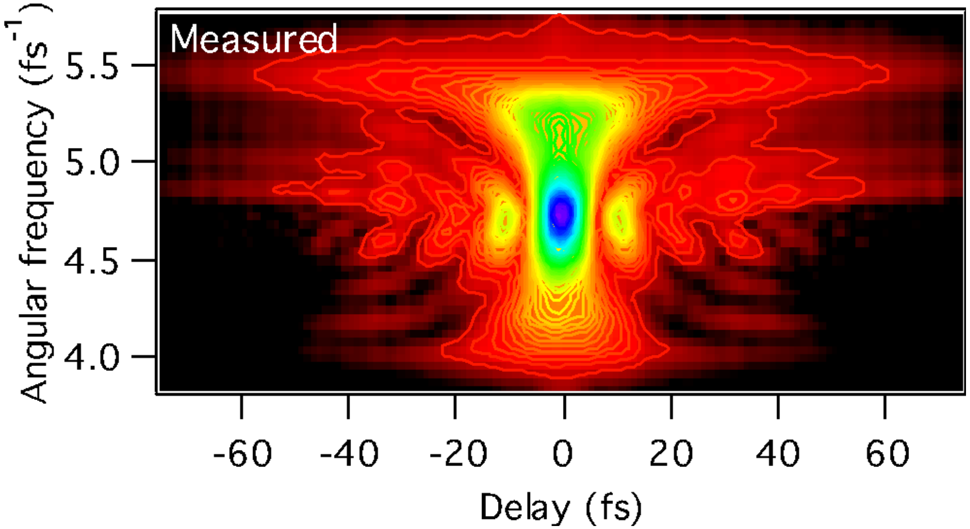

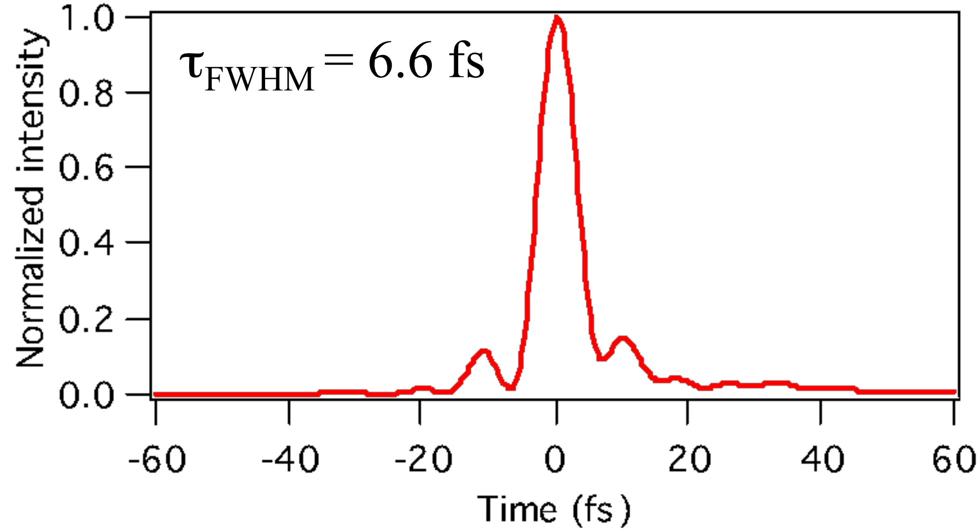

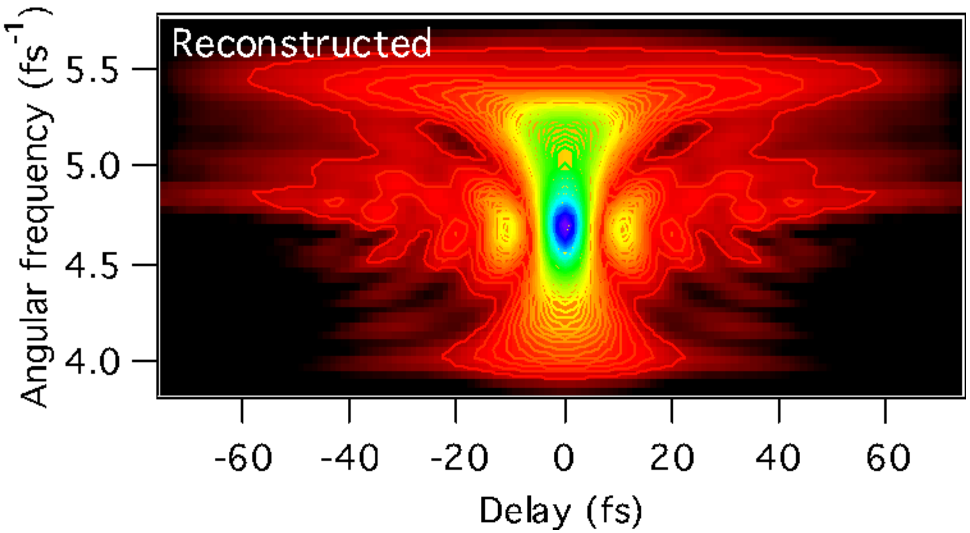

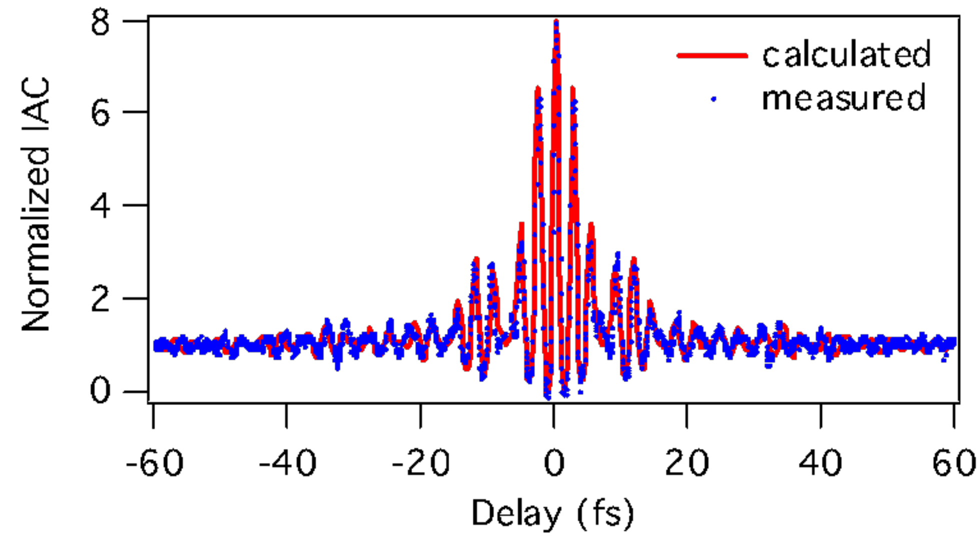

transform limit: 5.3 fs

sech^2-Fit: 4.5 fs!!

Marginal tests in FROG

Delay marginal

$$M_\tau(\tau) \equiv \int_{-\infty}^{\infty} \mathrm{d}\omega I_{\mathrm{FROG}}(\omega, \tau)$$

(to be compared w/ independently measured autocorrelation)

Frequency marginal

$$M_\omega(\omega) \equiv \int_{-\infty}^{\infty} \mathrm{d}\tau I_{\mathrm{FROG}}(\omega, \tau)$$

to be compared w/ independently measured spectrum via

$$M_\omega{}^{\mathrm{SHG}}(\omega) = 2I(\omega) * I(\omega)$$

autoconvolution

Ref.: K. De Long et al., JOSA B 11, 1595 (1994).

Marginals can be used to compensate for phase matching bandwidth…

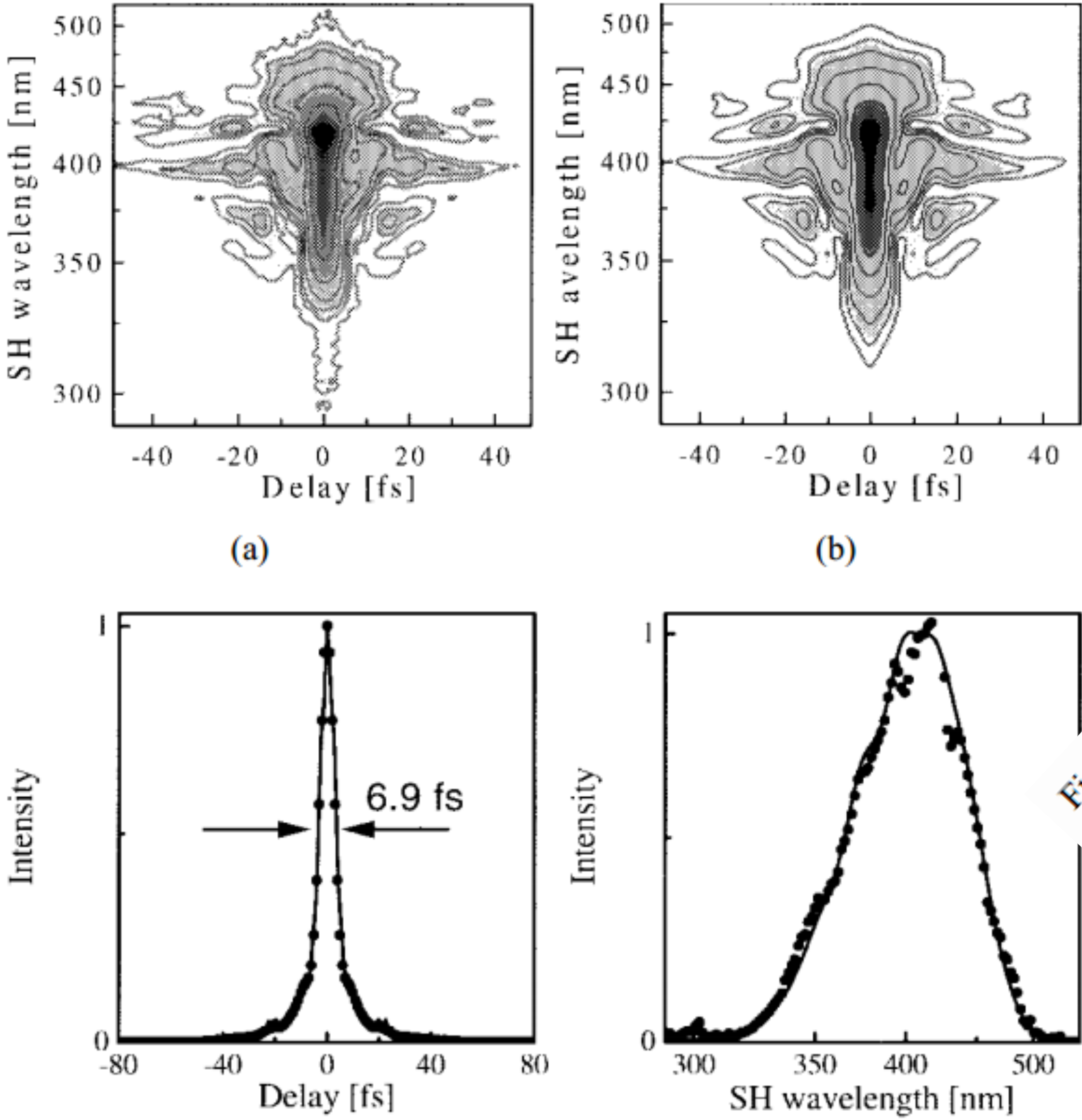

Fig. 17. The results of SHG FROG characterization of compressed pulses. (a) Experimental and (b) retrieved traces. (c) Temporal marginal (filled circles) and independently measured autocorrelation of 4.5-fs pulses (solid curve). (d) Frequency marginal (filled circles) and autoconvolution of the fundamenta spectrum (solid curve).

Ref.: A.Baltuska, IEEE JQE 35, 459 (1995)

λ^2 correction

Spectral power density

$$\frac{\partial P}{\partial \lambda} = \frac{\partial \nu}{\partial \lambda}\frac{\partial P}{\partial \nu} = -\frac{c}{\lambda^2}\frac{\partial P}{\partial \nu}$$

this is what your (calibrated) spectrograph gives you

but this is what you need for the marginal test

XFROG

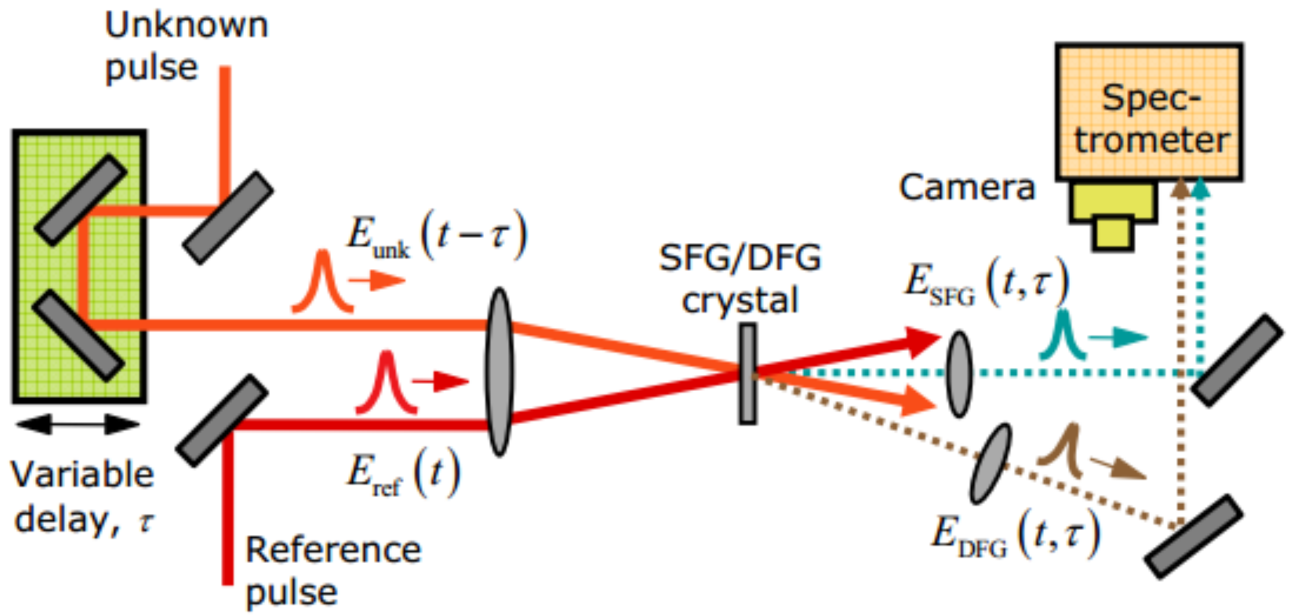

(picture from thesis Xun Gu, Georgiatech)

Crosscorrelation

DFG or SFG

Well-defined reference pulse

Most powerful FROG method

Can resolve very complex pulses

S. Linden et al., phys. stat. sol. (b) 206, 119 (1998)

XFROG

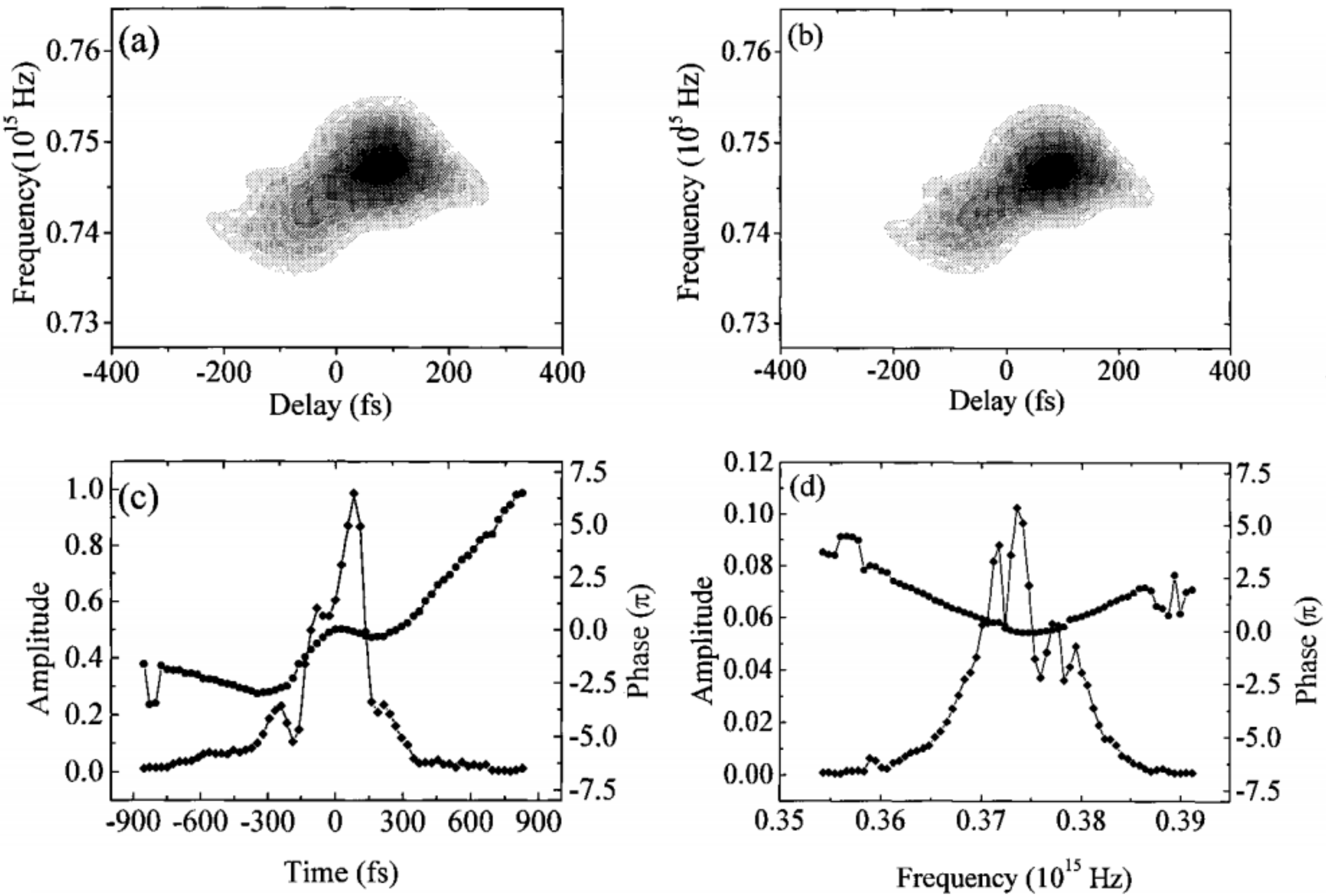

S. Linden et al., phys. stat. sol. (b) 206, 119 (1998)

XFROG can measure extremely complex pulses

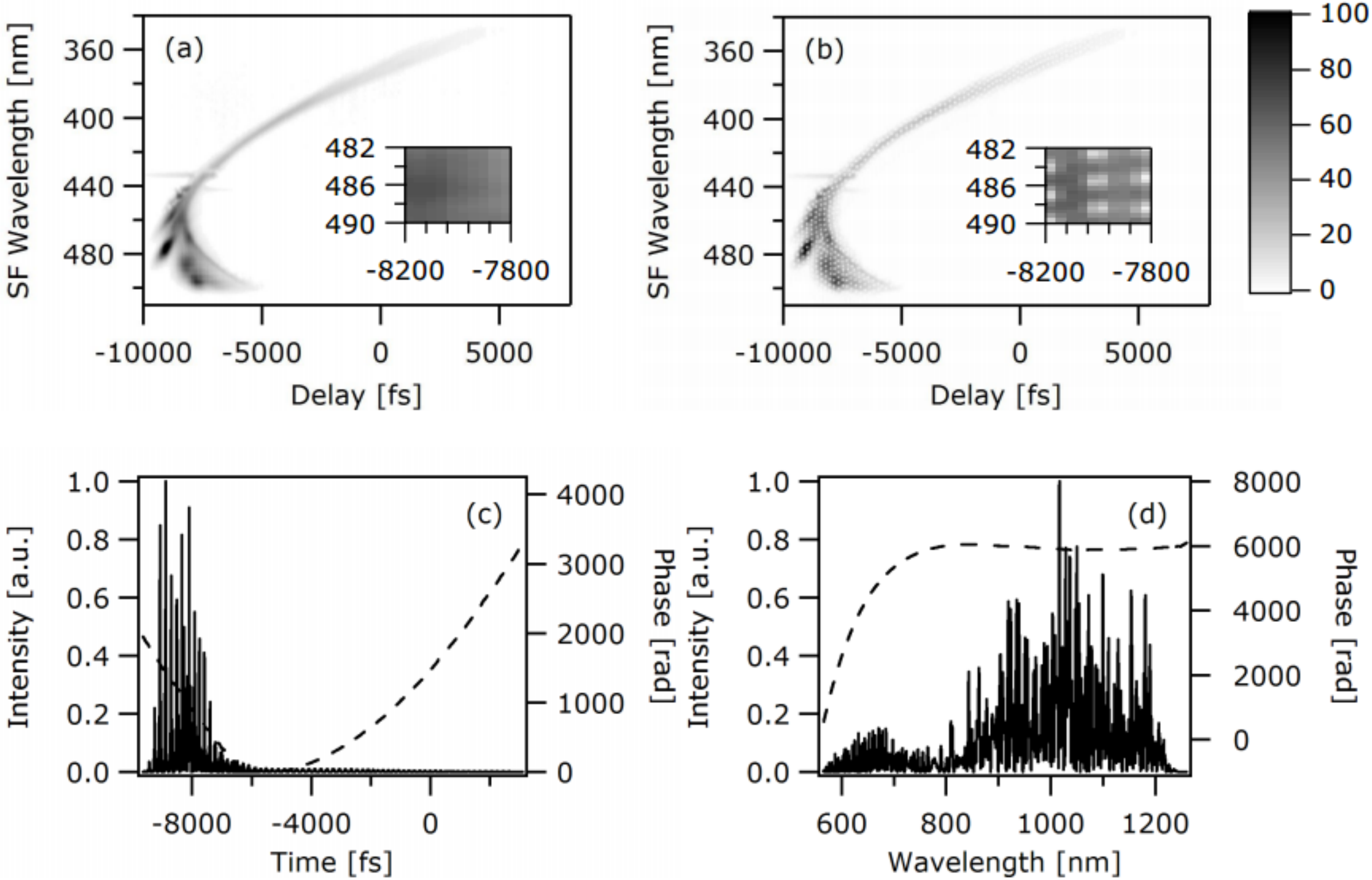

thesis Xun Gu, Georgiatech

Interferometric FROG

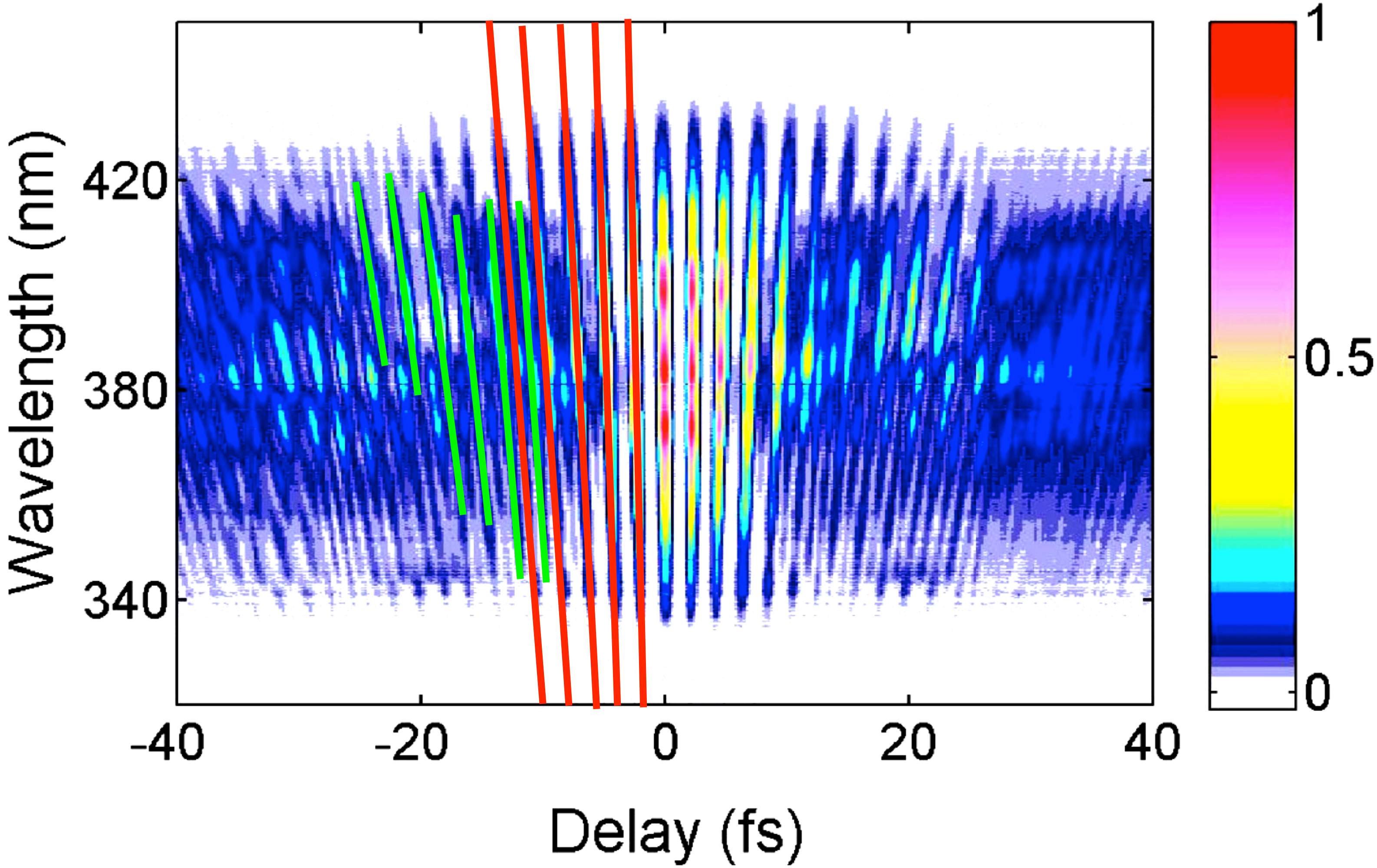

Source: Hollow fiber continuum, compressed w/ chirped mirrors

G.Stibenz and G.Steinmeyer, Opt. Express **13**, 2617 (2005).

Interferometric FROG

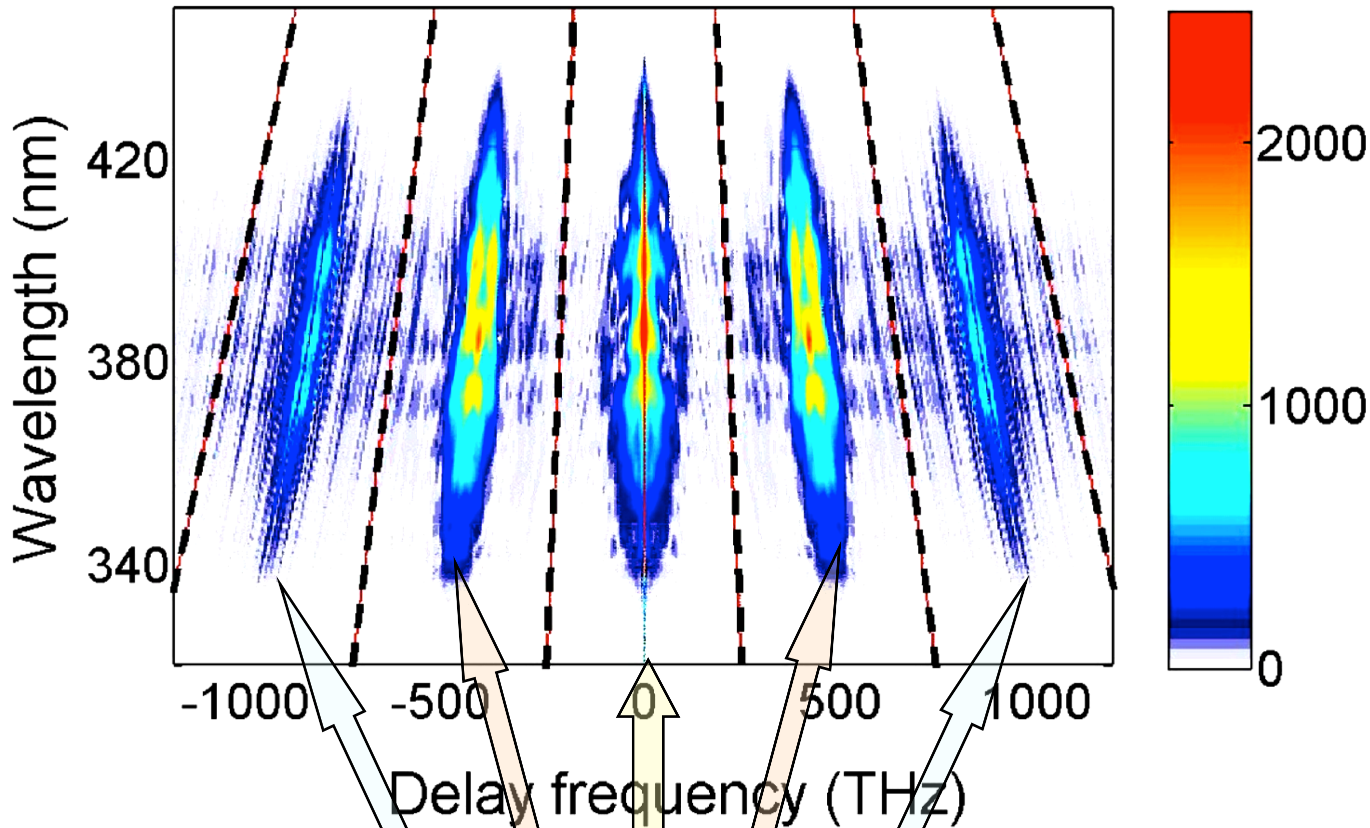

3 components:

1.) DC

2.) fund. mod.

3.) SH mod.

$$
\begin{aligned}
I_{\mathrm{IFROG}}(\omega,\tau) = {} & 2\,|E_{\mathrm{SH}}(\Delta\omega)|^2 + 4\,|E_{\mathrm{FROG}}(\Delta\omega,\tau)|^2 \\
& + 8\cos\left[\left(\omega_0 + \frac{\Delta\omega}{2}\right)\tau\right] \mathrm{Re}\left[E_{\mathrm{FROG}}(\Delta\omega,\tau)\,E^*_{\mathrm{SH}}(\Delta\omega)\exp\left(i\frac{\Delta\omega}{2}\tau\right)\right] \\
& + 2\cos\left[(2\omega_0 + \Delta\omega)\,\tau\right]|E_{\mathrm{SH}}(\Delta\omega)|^2 .
\end{aligned}
$$

Ref.: I.A. Roldan et al., *Opt.Express* **12**, 1169 (2004)

Interferometric FROG

standard SH-FROG
extracted from IFROG

negative signals
as in Wigner trace

new kind of FROG-trace
from modulation

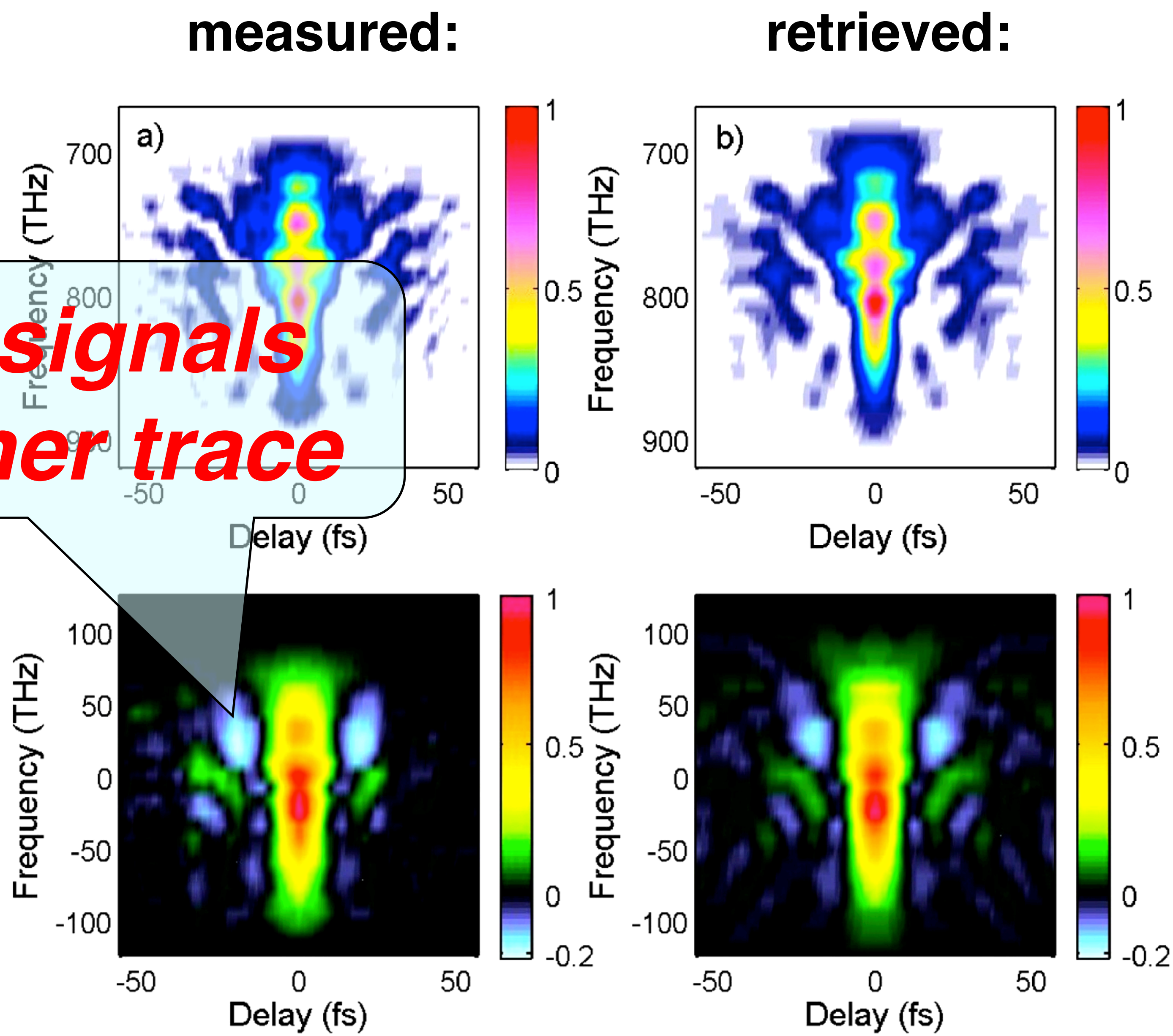

Retrieval

- Don‘t use the full IFROG trace
- Extract the **F**undamental **M**odulation part
- Resample on smaller grid

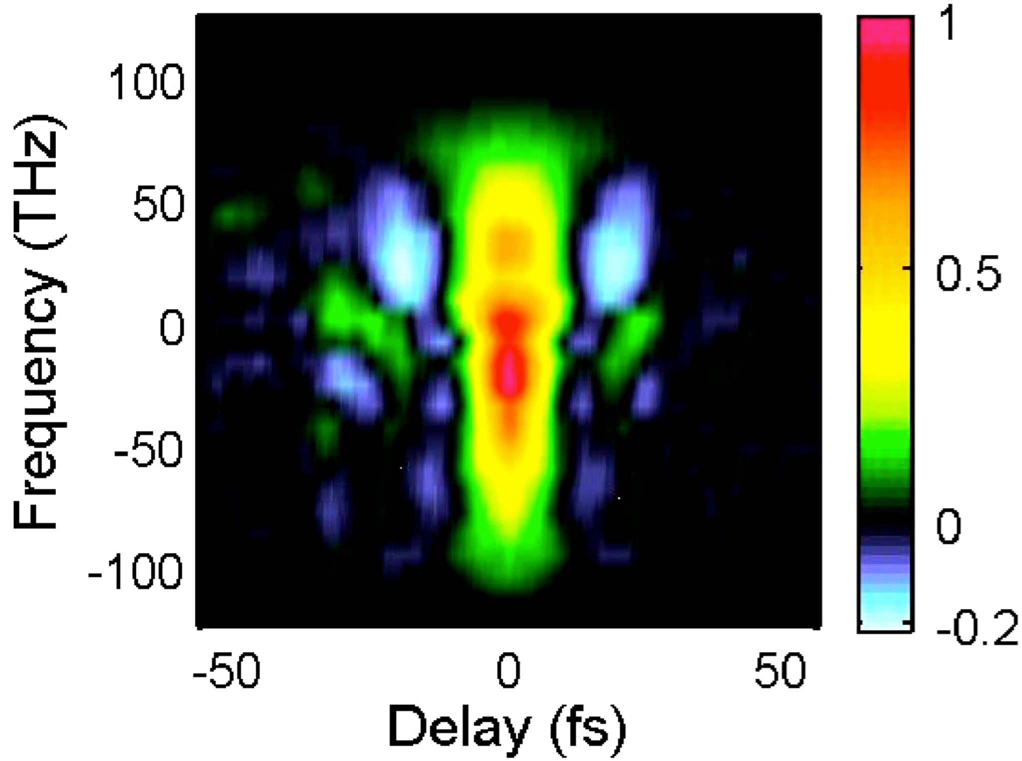

A complicated pulse

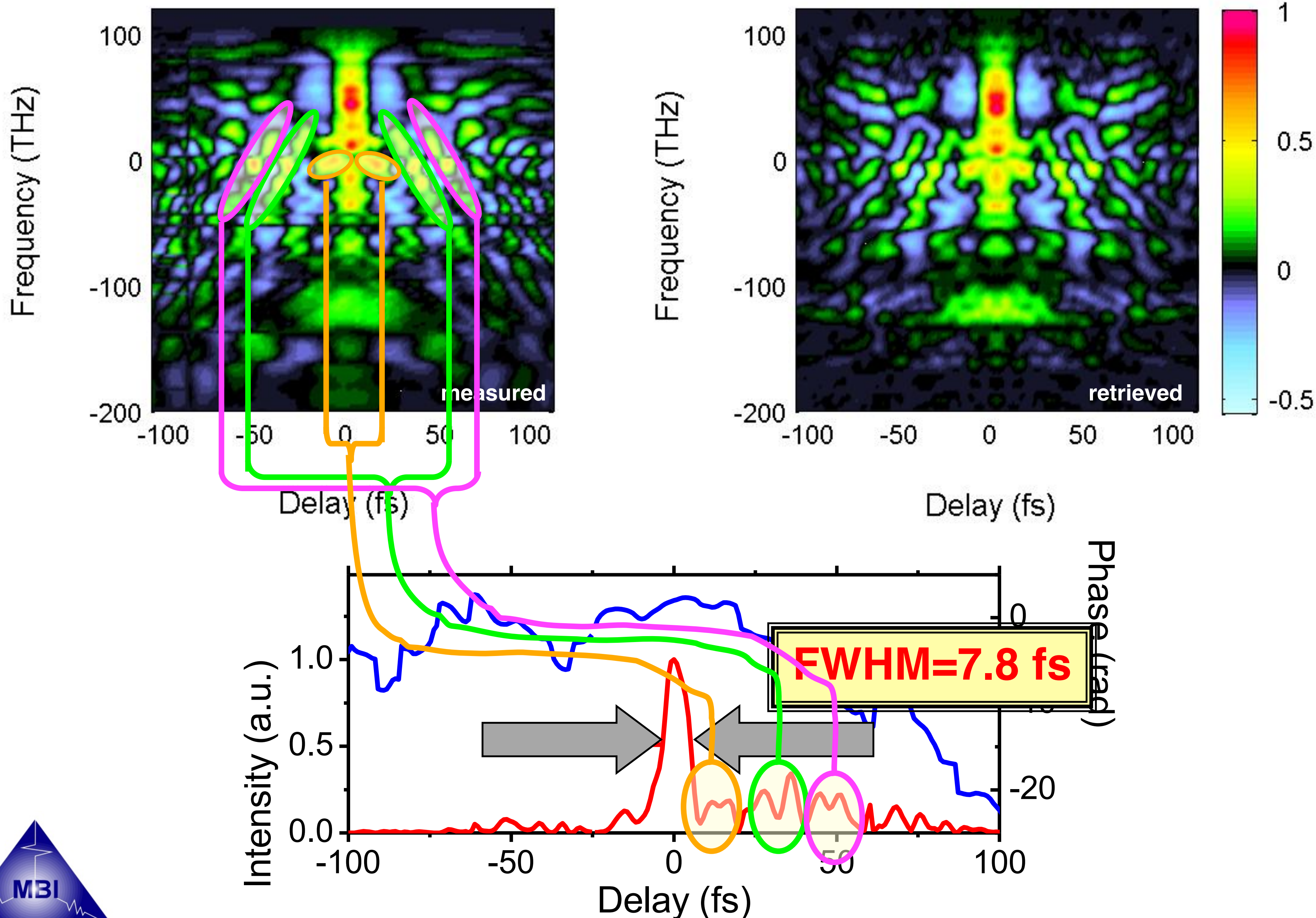

MBI

Method III

Spectral phase interferometry for direct electric-field reconstruction

SPIDER

Ian Walmsley

Characterization via spectral Interferometry

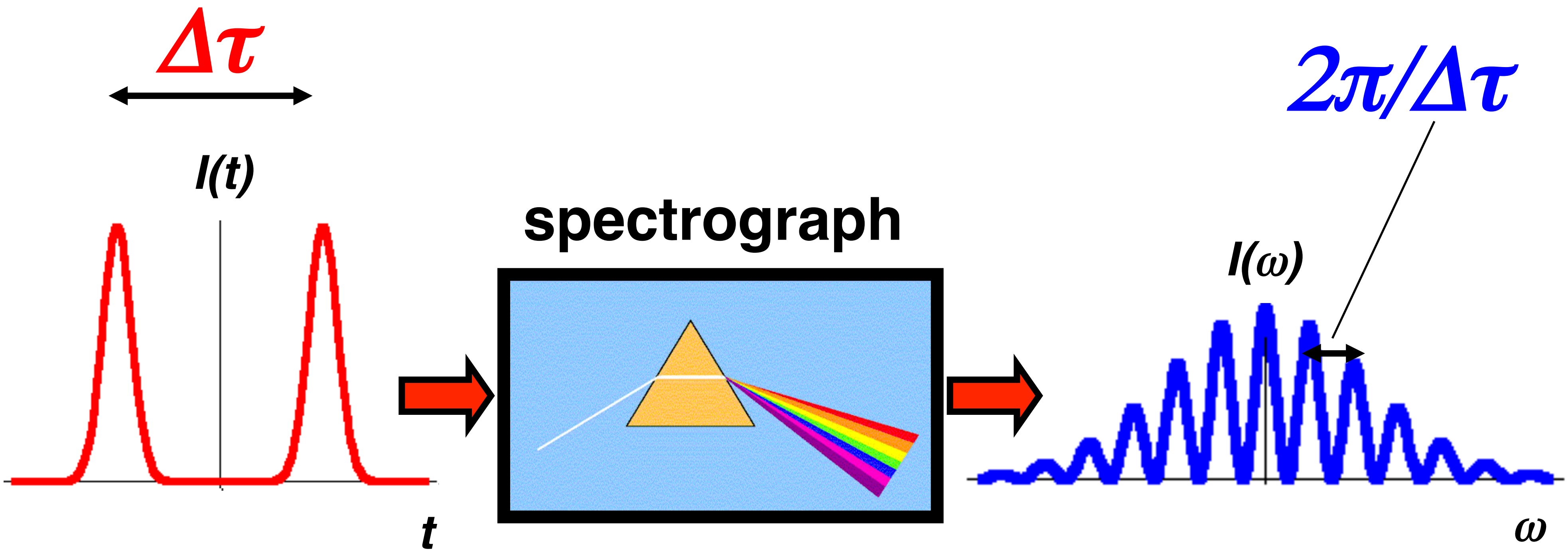

Important: **Modulation period independent of ω !**

Spectral Interference of phase fronts

$$E(\omega) = |A(\omega)| \cdot \exp(i\underbrace{\varphi(\omega)}), \qquad \varphi = \omega \cdot \Delta t$$

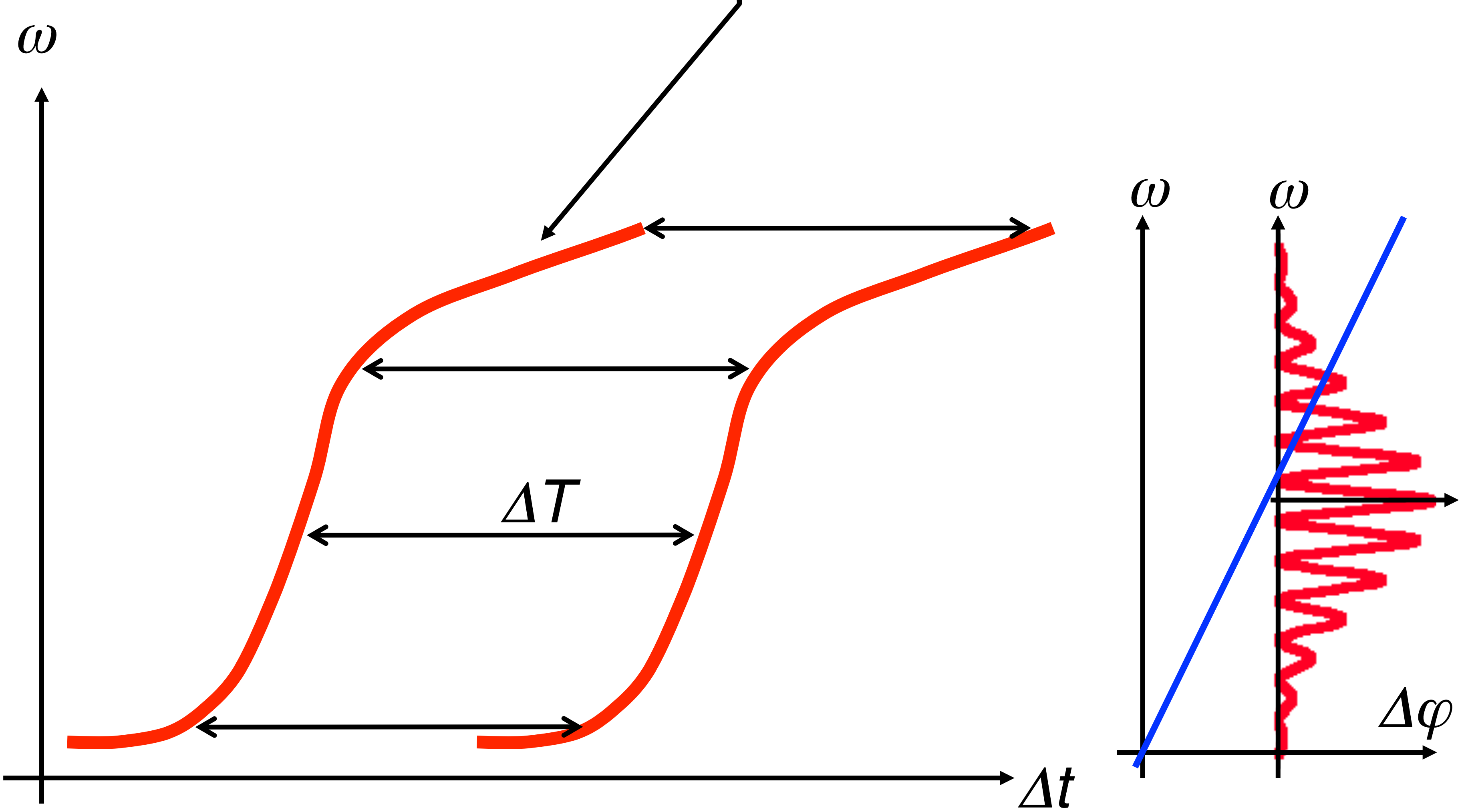

Introducing the spectral shear

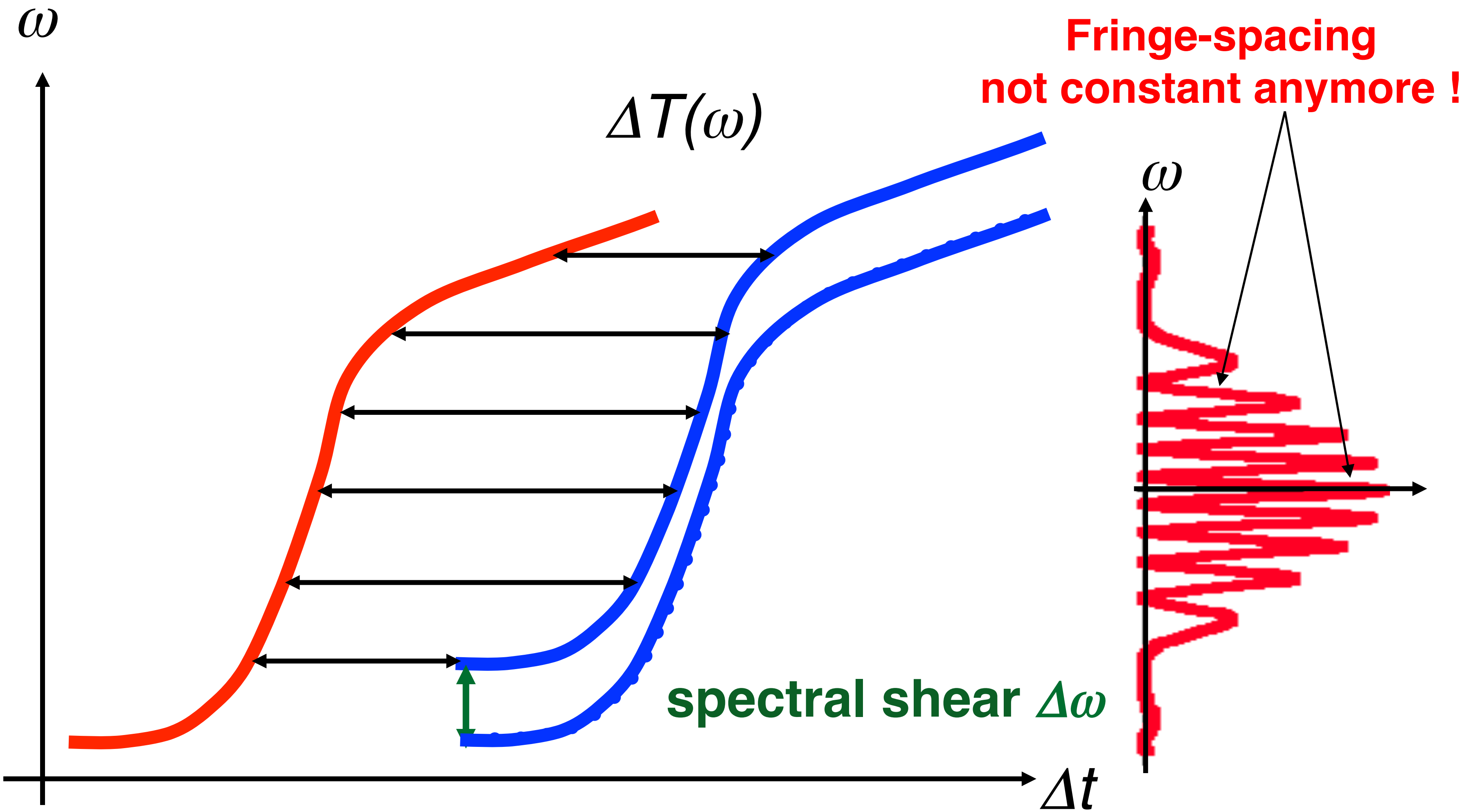

Reconstruction of the spectral phase

$$\varphi(\omega) = \omega \cdot \Delta T(\omega)$$

Sampling the spectral phase according to $\dfrac{\Delta\varphi(\omega)}{\Delta\omega} = (\Delta T(\omega) - \Delta T_0)$

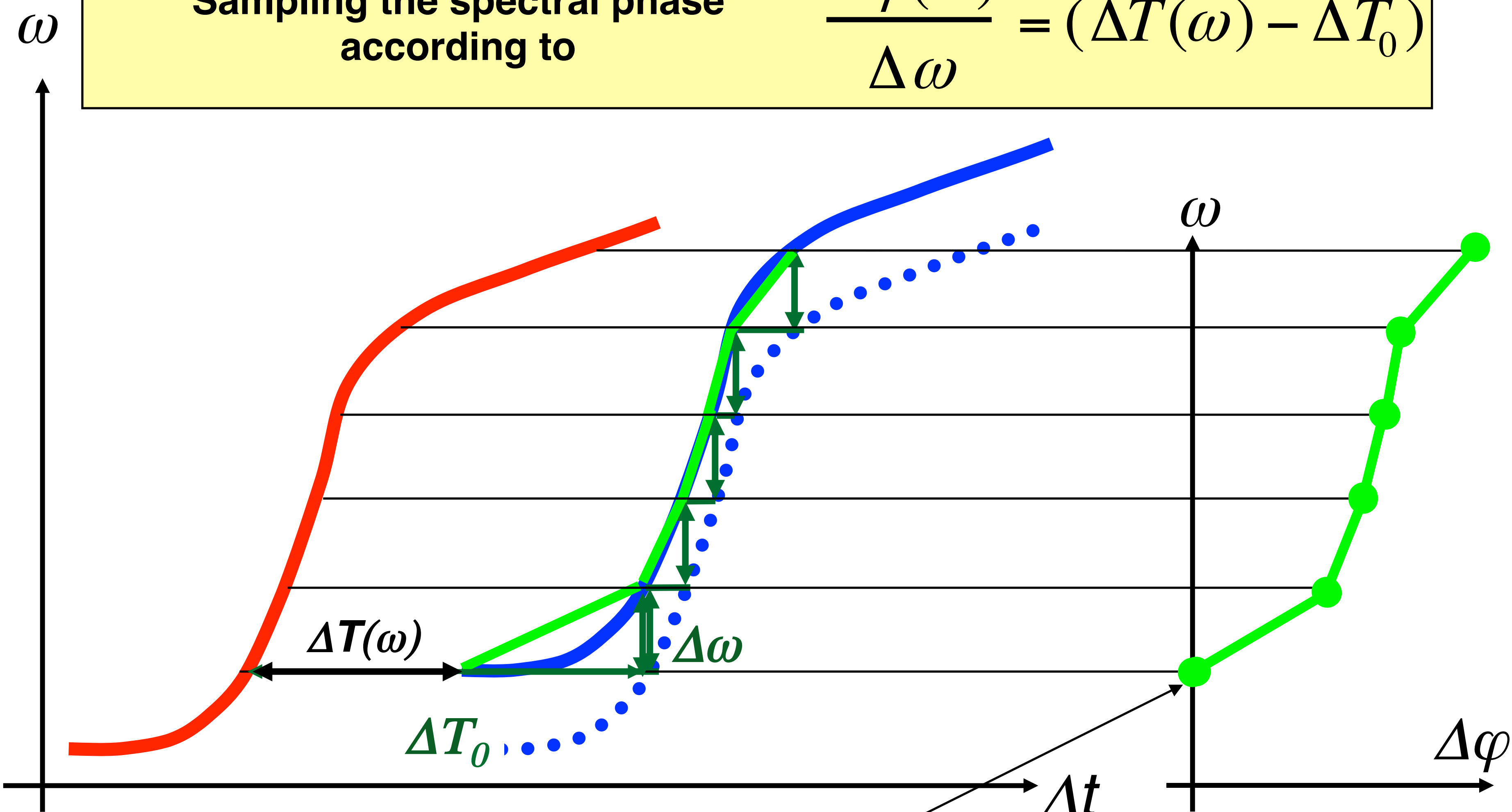

Choose phase start value arbitrarily

Spectral interference pattern

- Chirp causes spectrally dependent fringe spacing

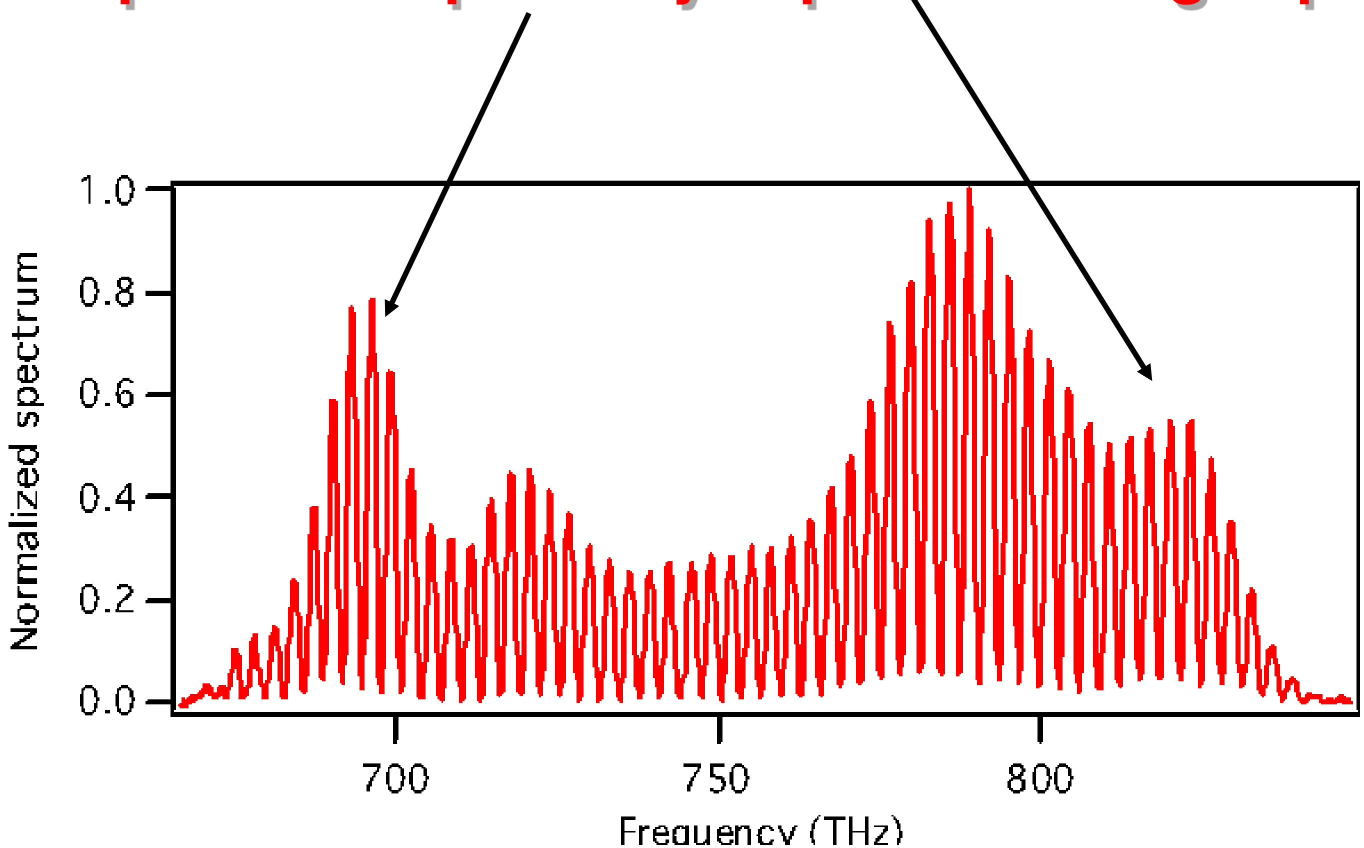

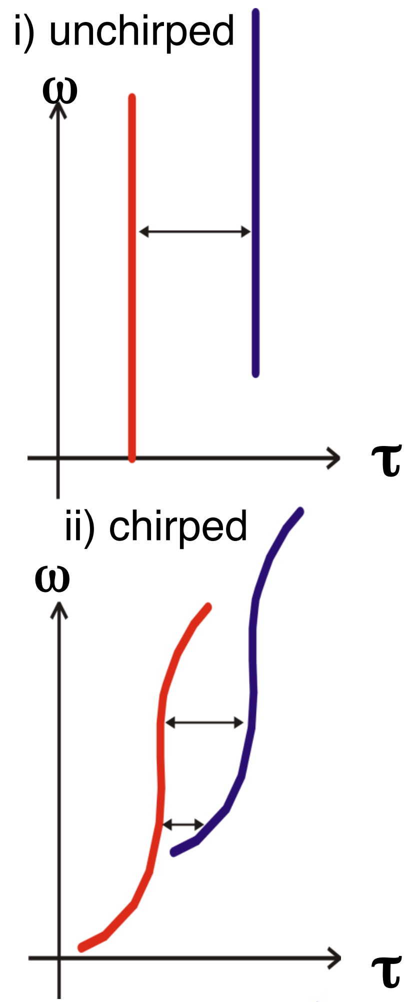

- Phase information of spectral modulation
- Phase extraction does not require amplitude information

Gallmann et al.: Opt. Lett. **24** , 1314 (1999)

SPIDER

(Spectral Phase Interferometry for Direct E-field Reconstruction)

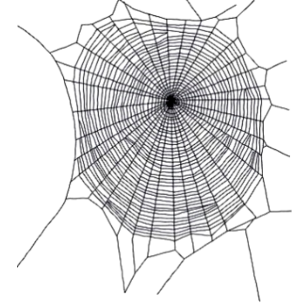

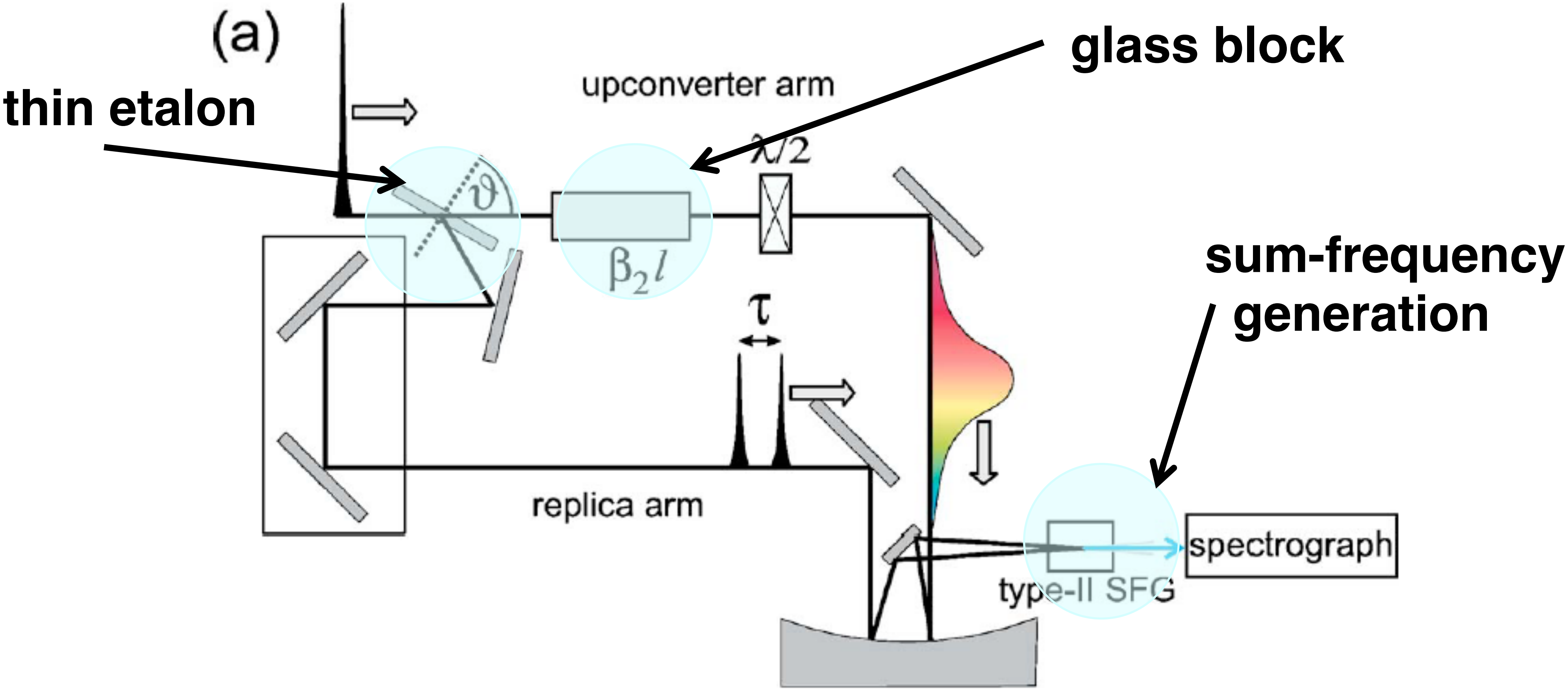

C. Iaconis, I.A. Walmsley, IEEE JQE **35**, 501 (1999)
Gallmann et al.: Opt. Lett. **24** , 1314 (1999)
Stibenz & Steinmeyer, Rev. Sci. Instrum. **77**, 073105 (2006)

Calibration step

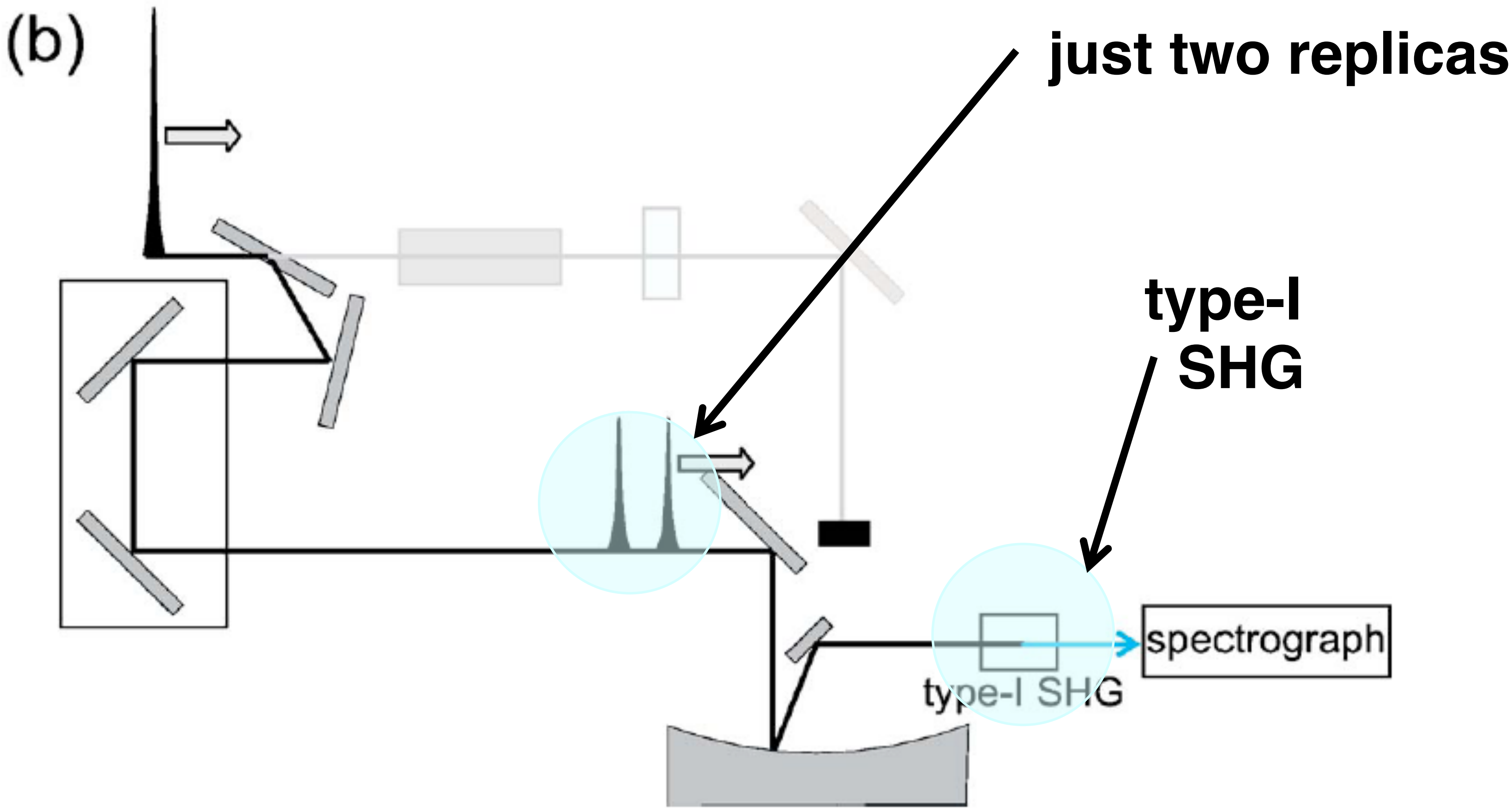

C. Iaconis, I.A. Walmsley, IEEE JQE **35**, 501 (1999)
Gallmann et al.: Opt. Lett. **24** , 1314 (1999)
Stibenz & Steinmeyer, Rev. Sci. Instrum. **77**, 073105 (2006)

Etalon for optimum beam splitting

s polarization !

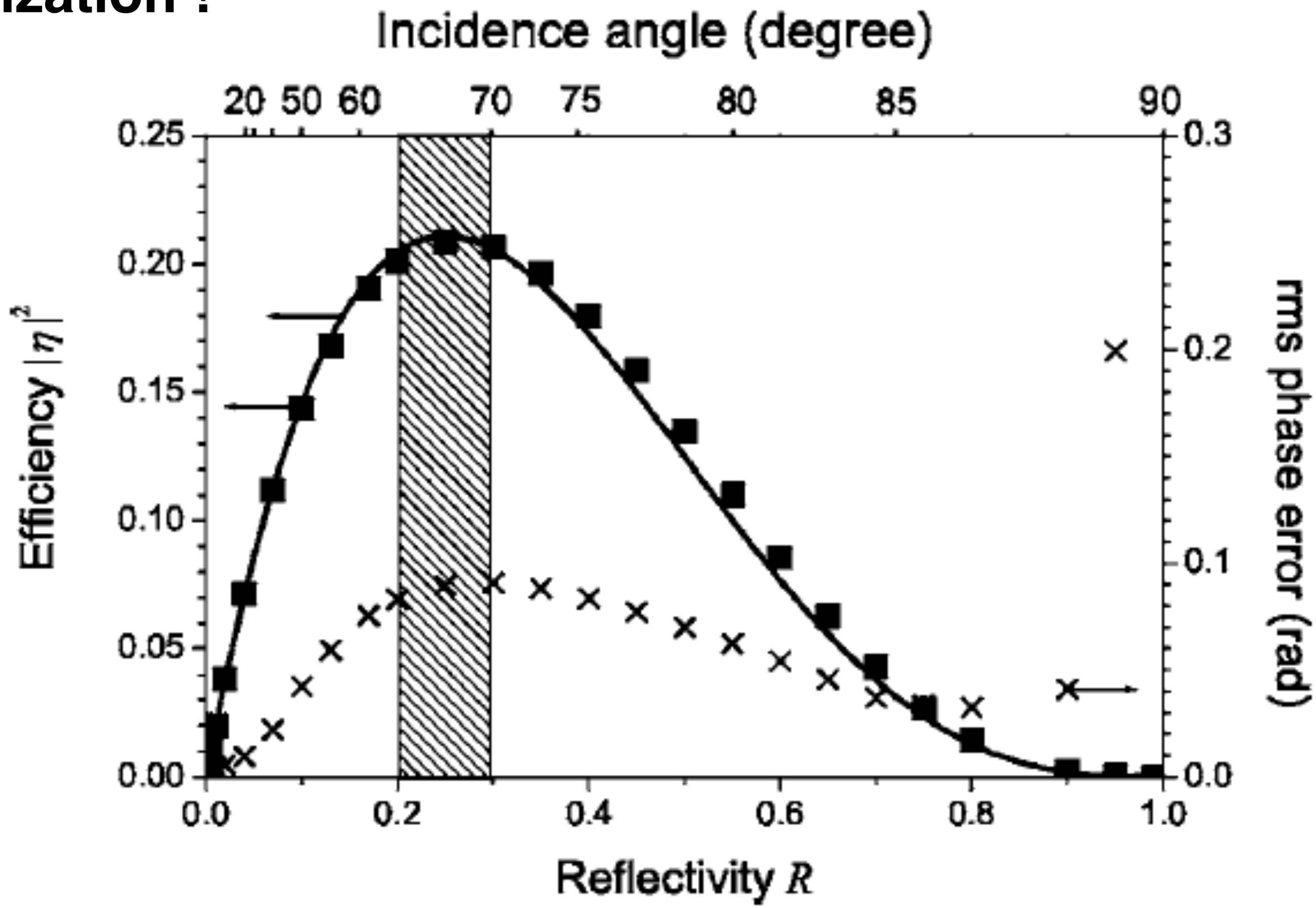

Stibenz & Steinmeyer, Rev. Sci. Instrum. **77**, 073105 (2006)

SPIDER-Results

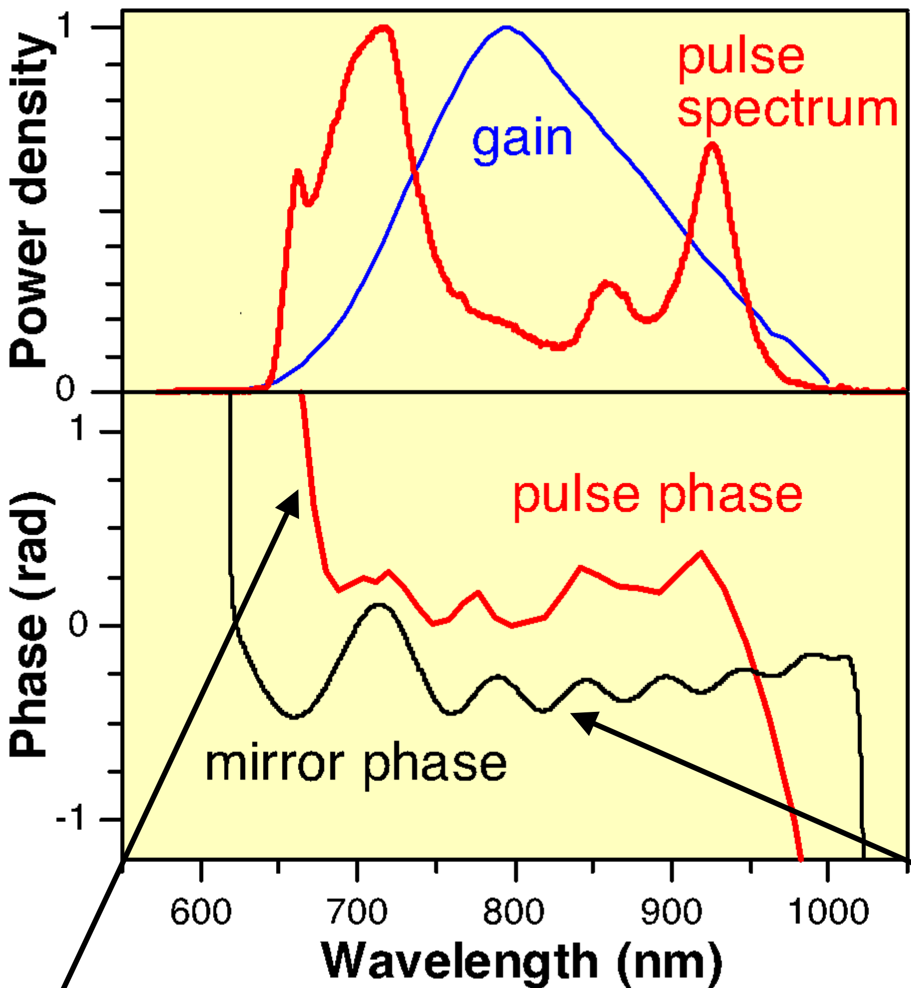

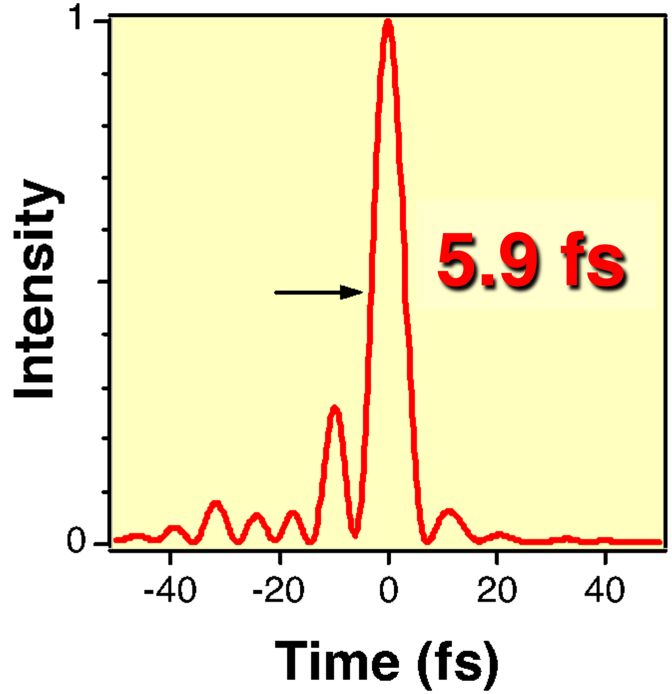

Dispersion oscillations

Output coupler phase response (λ/4 single stack)

Gallmann et al.: Opt. Lett. **24** , 1314 (1999)

SPIDER-Measurements

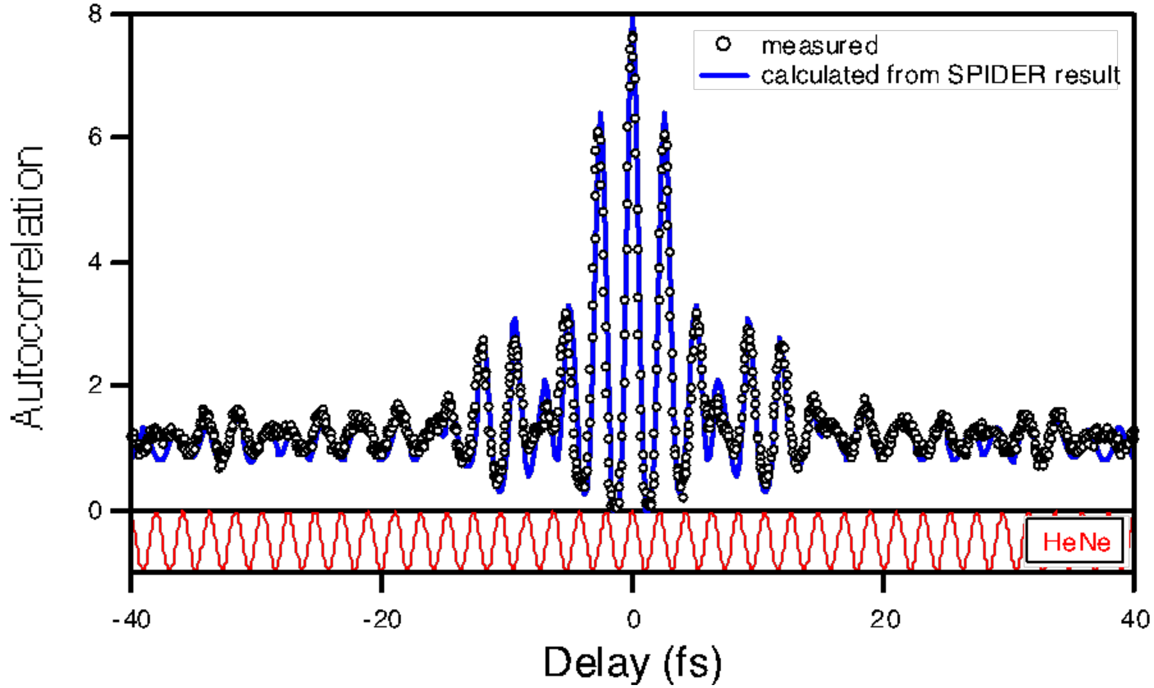

SPIDER yields excellent agreement with independently measured IAC

SPIDER enables measurement of a GDD<2 fs^2 (≈ 10 cm air path...)

.. Gallmann et al., Appl. Phys. B 70 [Suppl.], S67–S75 (2000)

Advanced SPIDER

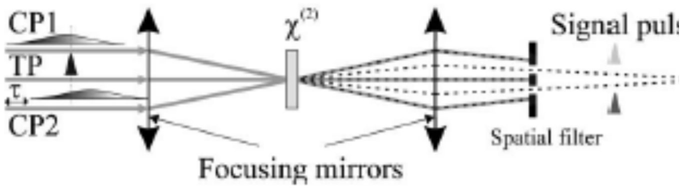

Fig. 1. SEA-SPIDER concept: TP, test p chirped pulse 1/2; τ, time delay.

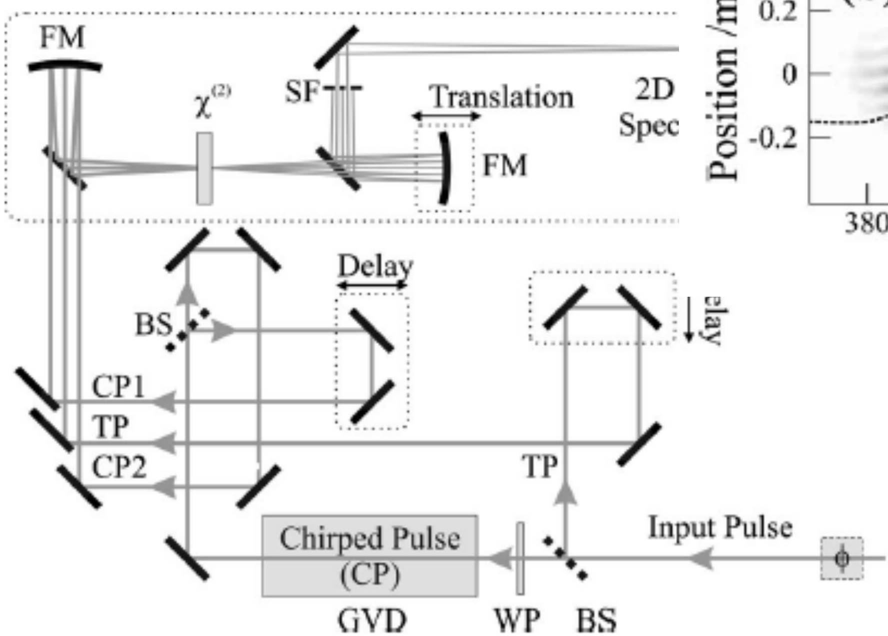

Fig. 2. SEA-SPIDER setup: BS, beam splitter; WP, $\lambda/2$ wave plate; GVD, dispersive glass block (10 cm SF10); FM, focusing mirror ($f = 100$ mm); $\chi^{(2)}$, nonlinear crystal (30 μm β-barium borate, type II); SF, spatial filter; ϕ, optional additional phase.

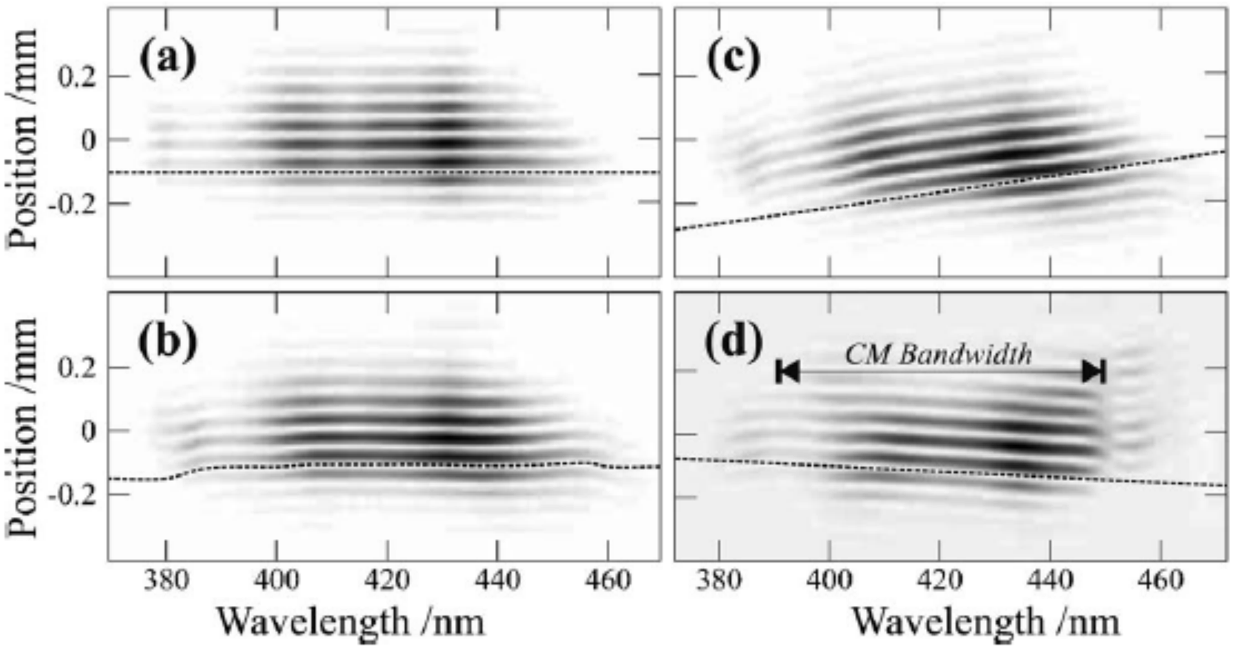

SEA-SPIDER = spatially encoded arrangement for SPIDER

A. S. Wyatt, et al. Opt. Lett. **31**, 1914-1916 (2006)

Comparison of characterization architectures

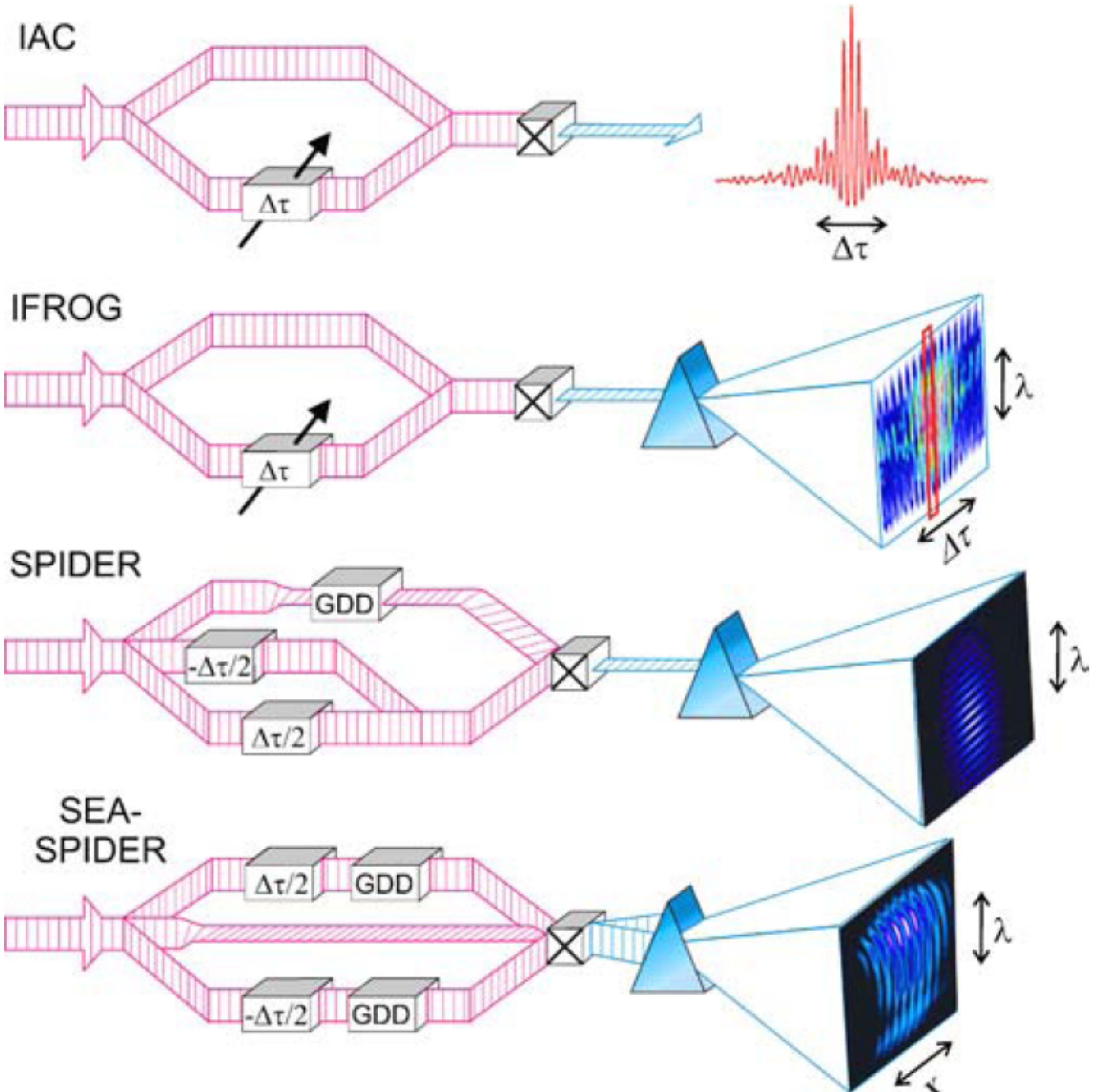

G. Stibenz et al., Appl. Phys. B 83, 511–519 (2006)

Comparison

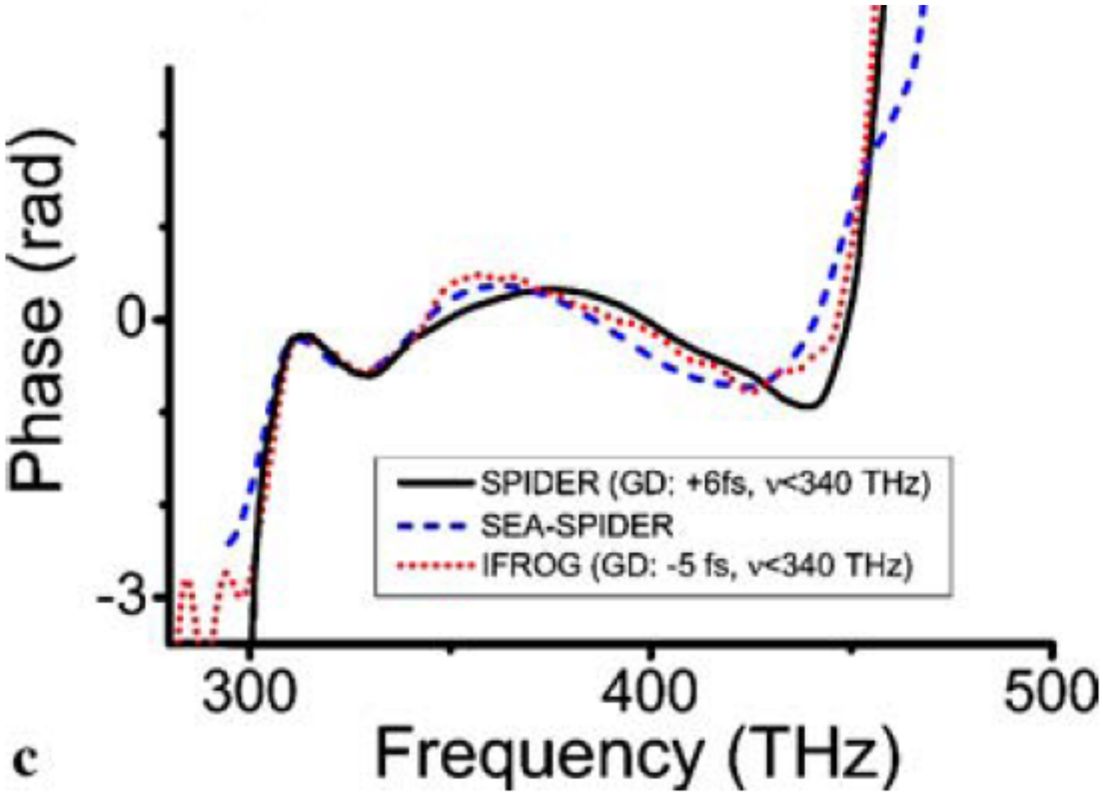

G. Stibenz et al., Appl. Phys. B 83, 511–519 (2006)

The coherent artifact

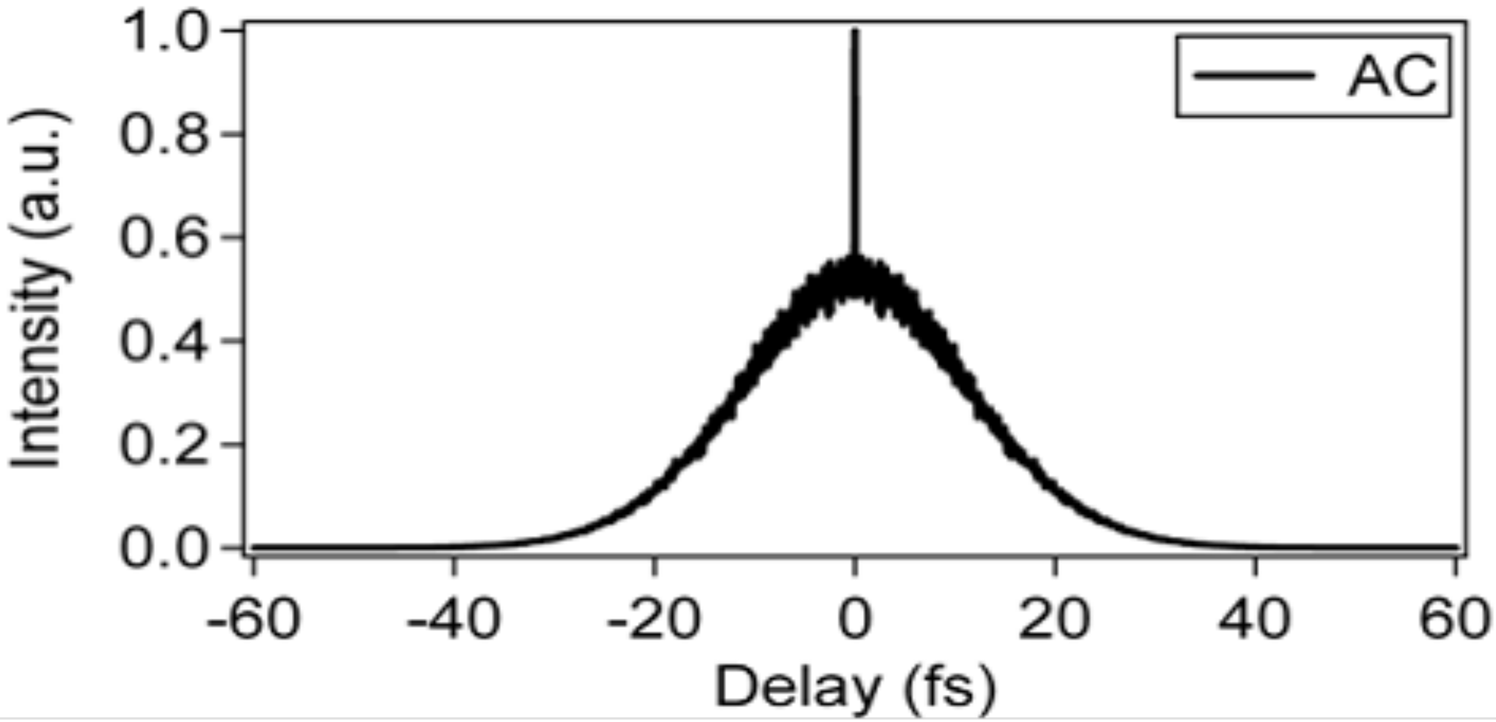

As the intensity increases in complexity, its autocorrelation approaches a broad smooth background and a coherence spike.

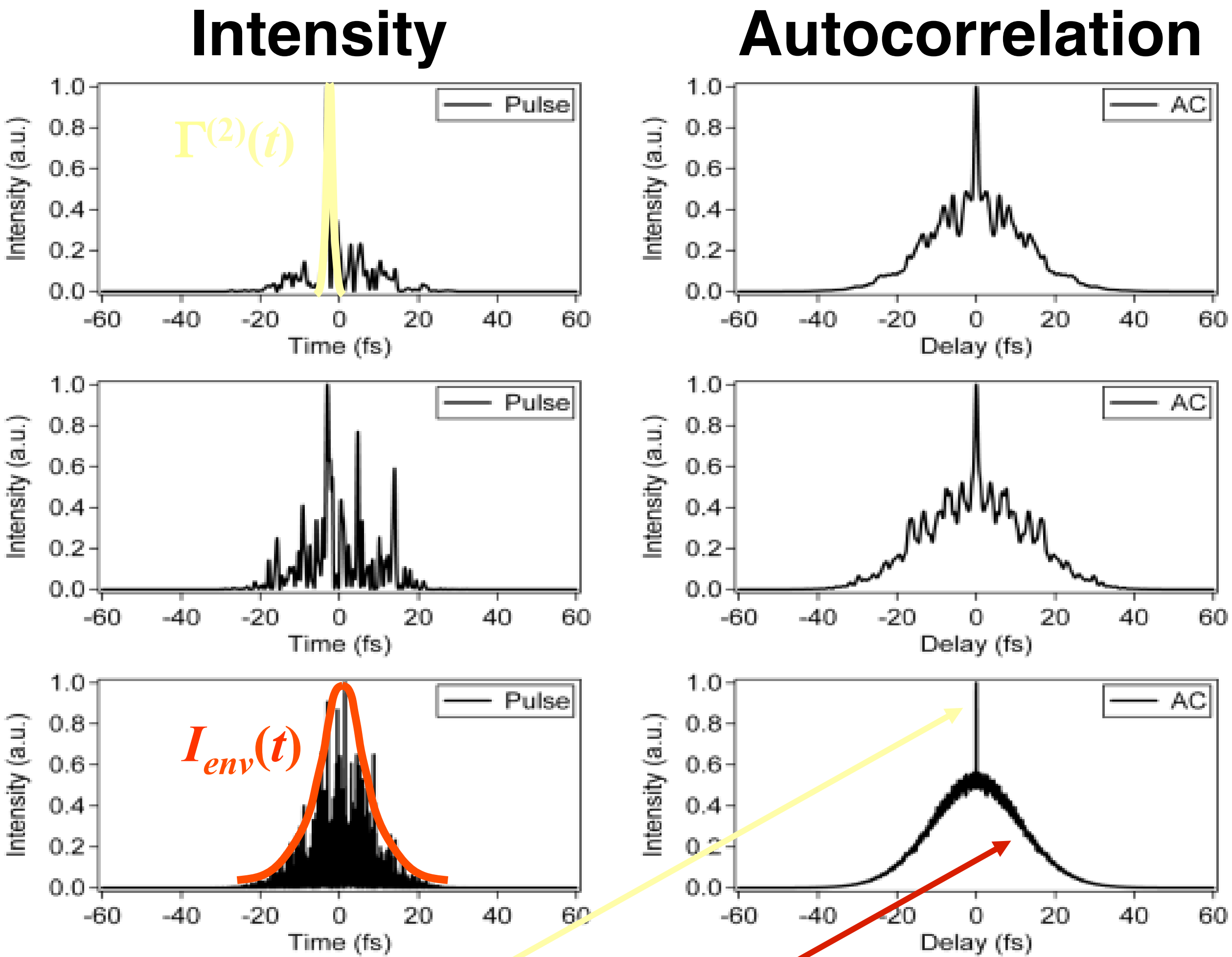

This shows why retrieving the intensity from the autocorrelation is fundamentally impossible!

$$A^{(2)}(\tau) = \left|\Gamma^{(2)}(\tau)\right|^2 + \int_{-\infty}^{\infty} I_{env}(t)\, I_{env}(t-\tau)\, dt$$

The coherent artifact

CW

mode-locked

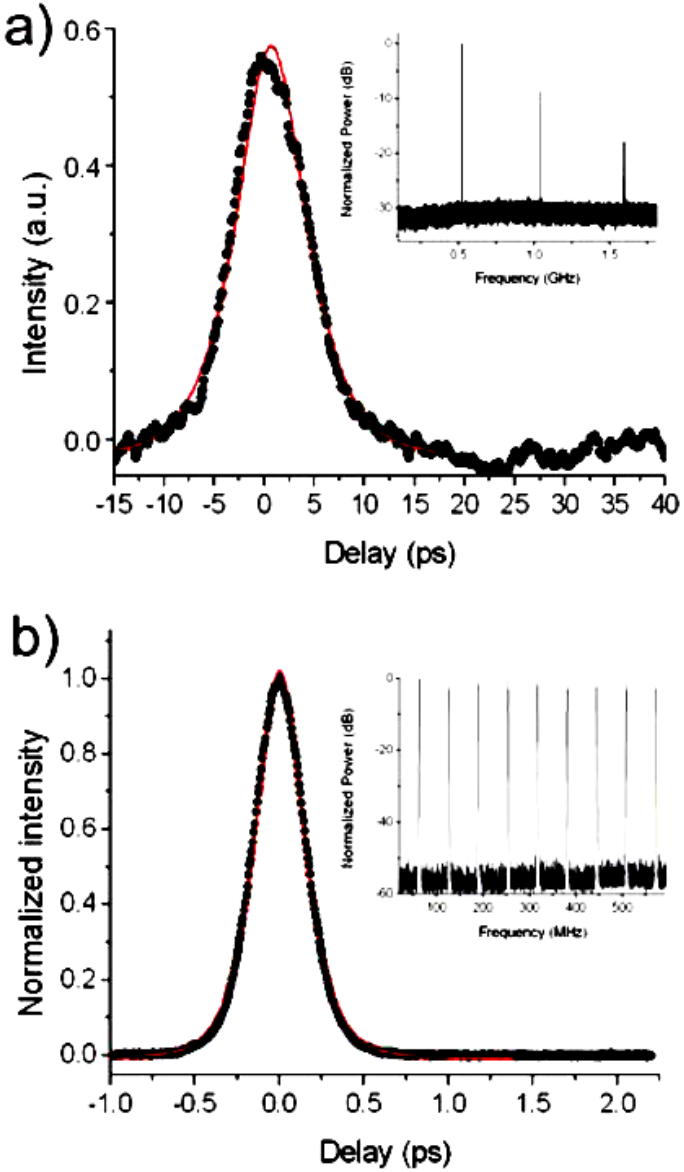

Figure 1 Autocorrelation and RF spectrum (inset) for a) a Nd:YLF CW laser and b) a mode-locked Yb:glass laser. Both autocorrelations include a sech2 fit to the data (red lines).

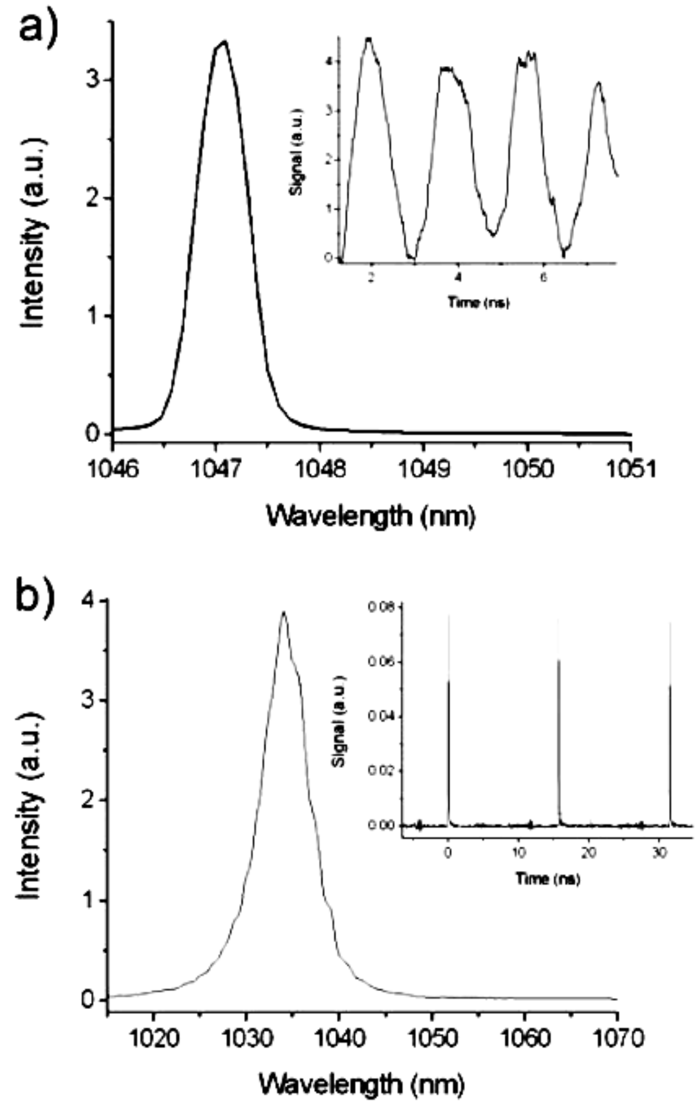

Figure 2 Optical spectrum and fast oscilloscope trace (inset) for a) a Nd:YLF CW laser and b) a mode-locked Yb:glass laser.

- Wilcox et al., Laser Photonics Rev. **7,** 422–423 (2013)

Coherent artifact in autocorrelation

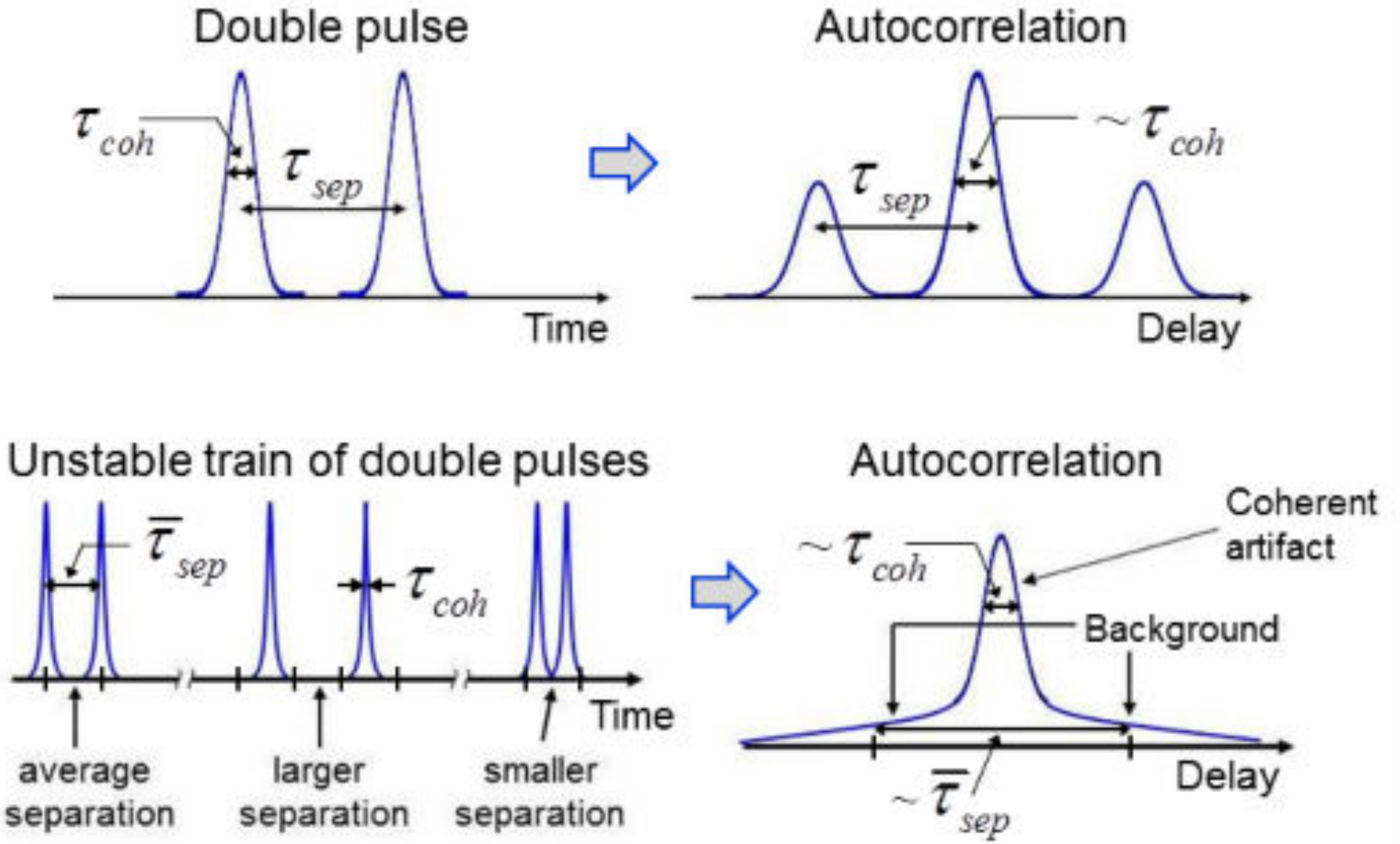

J. Ratner et al., Opt. Lett. 37, 2874-2876 (2012)

Coherent artifact in SPIDER and FROG

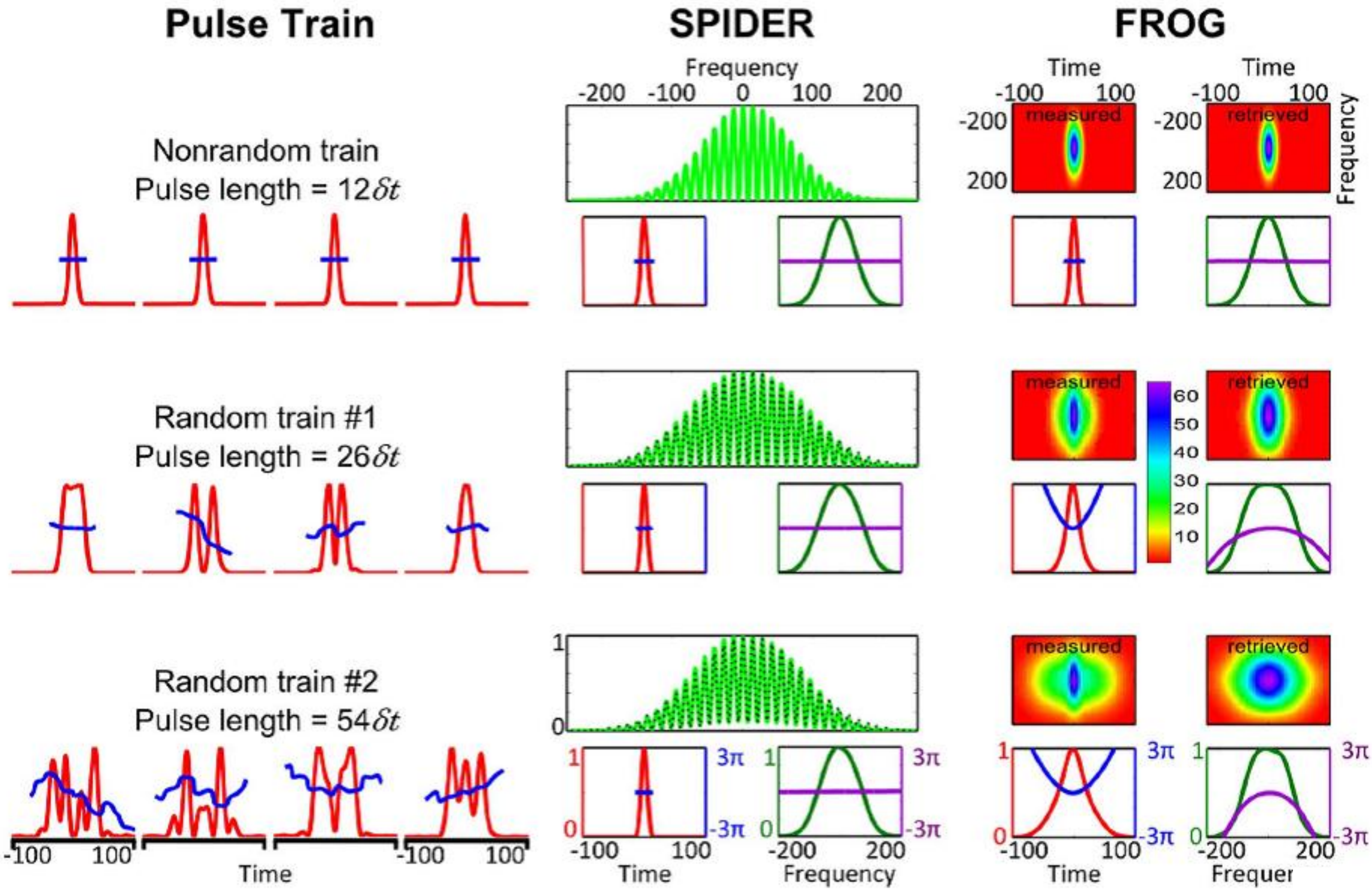

M. Rhodes et al., Laser Photonics Rev. **7,** 557–565 (2013)

High dynamic range autocorrelation

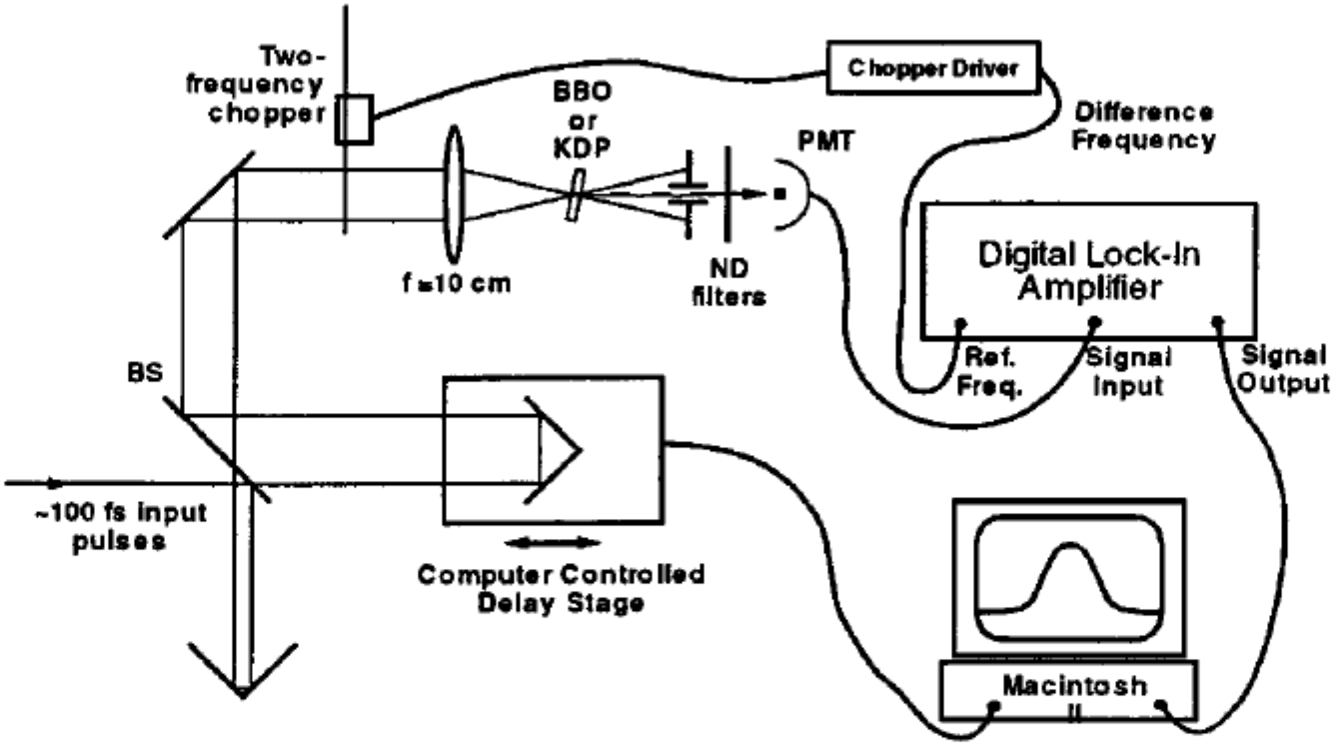

Ref: A. Braun et al., Opt. Lett. **20**, 1889-91 (1995)

Example for high dynamic range AC

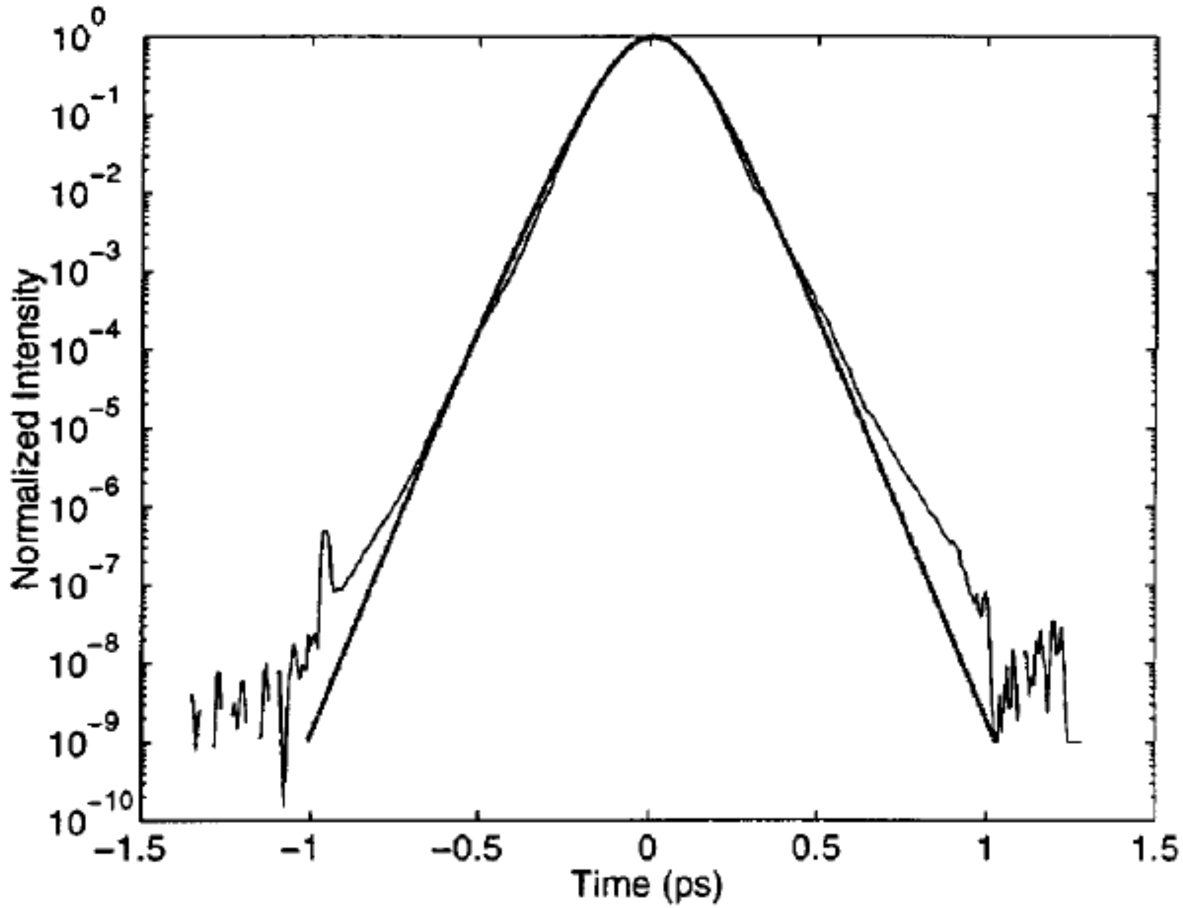

Fig. 4. Autocorrelation trace of a Nd:glass oscillator mode-locked by an A-FPSA sample fit to a 140 fs (FWHM) sech^2 pulse shape. The spectrum is centered at 1.058 μm.

Ref: A. Braun et al., Opt. Lett. **20**, 1889-91 (1995)

Multiphoton intrapulse interference phase scan

MIIPS

Marcos Dantus

MIIPS setup

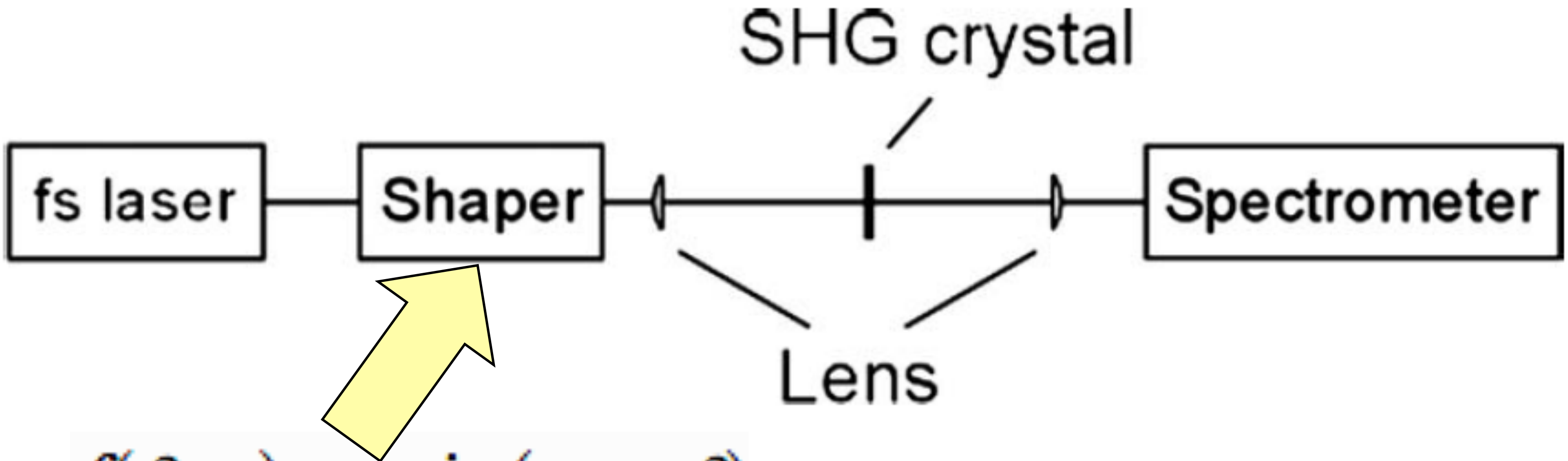

$$f(\delta,\omega)=\alpha\sin(\gamma\omega-\delta)$$

δ: phase scanned from 0 to 4π

α: **typically** 1.5π

γ: **estimated pulse duration**

B. Xu et al., J. Opt. Soc. Am. B **23**, 750-759 (2006)

Three MIIPS iterations

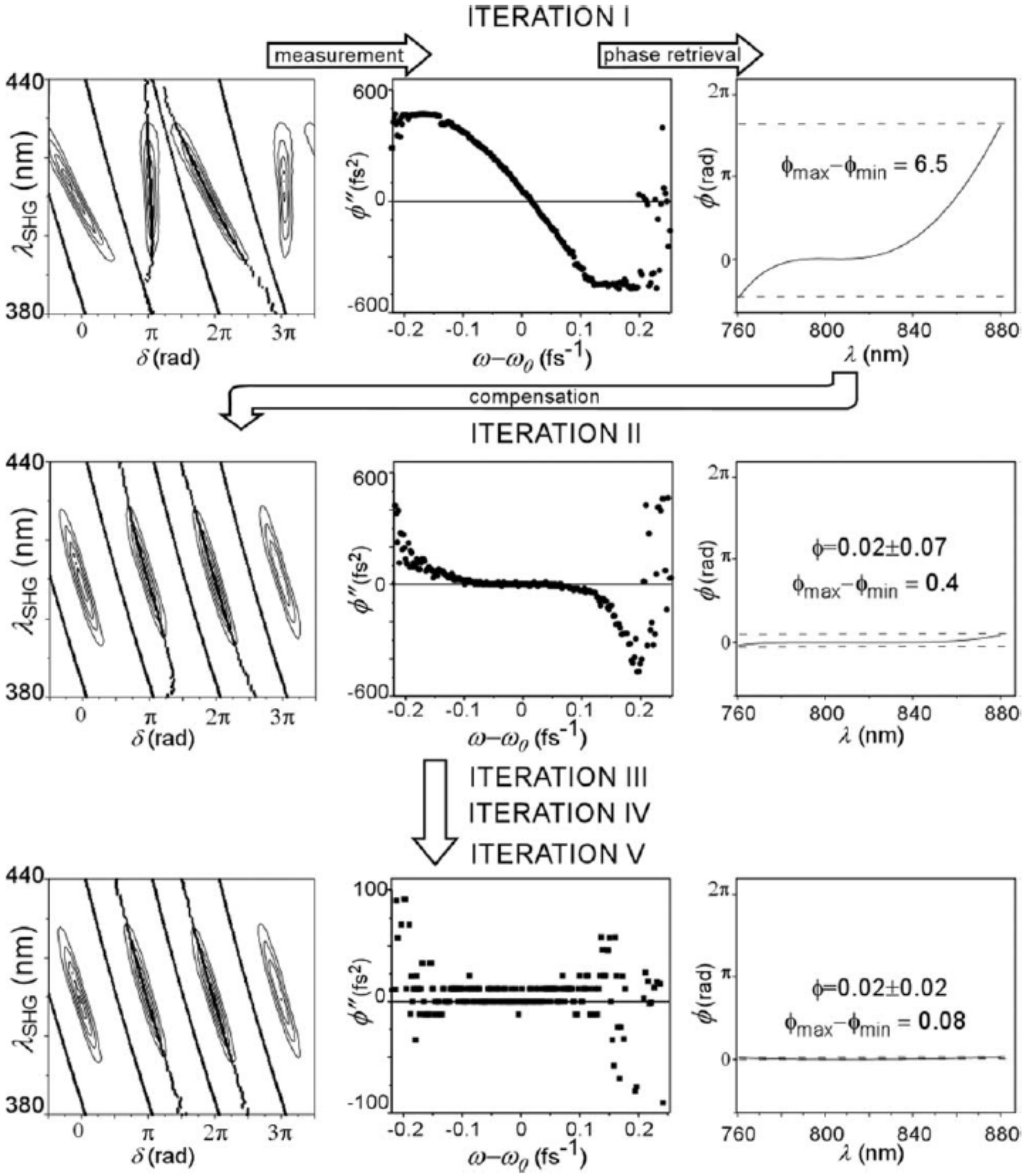

B. Xu et al., J. Opt. Soc. Am. B **23**, 750-759 (2006)

MIIPS may even master the coherent artifact…

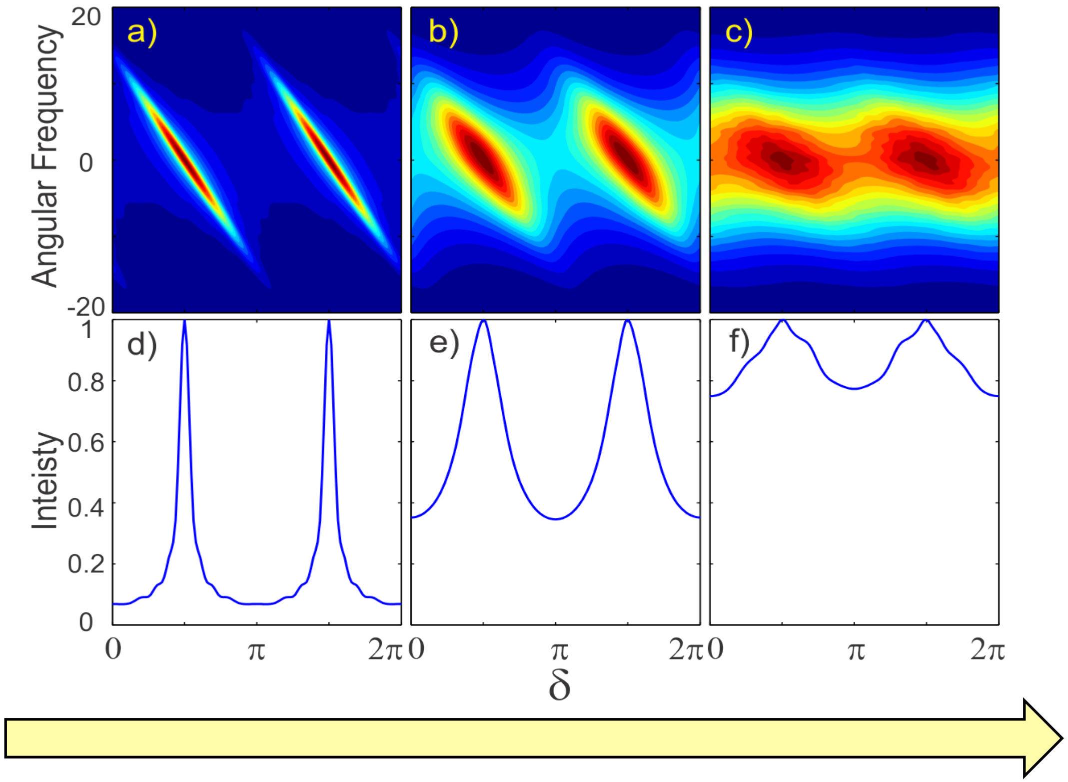

Loss of coherence, but constant pulse duration

Dantus & Trebino & Steinmeyer, to be submitted

Method V

Dispersion-scan

Dscan

Helder Crespo

D-scan

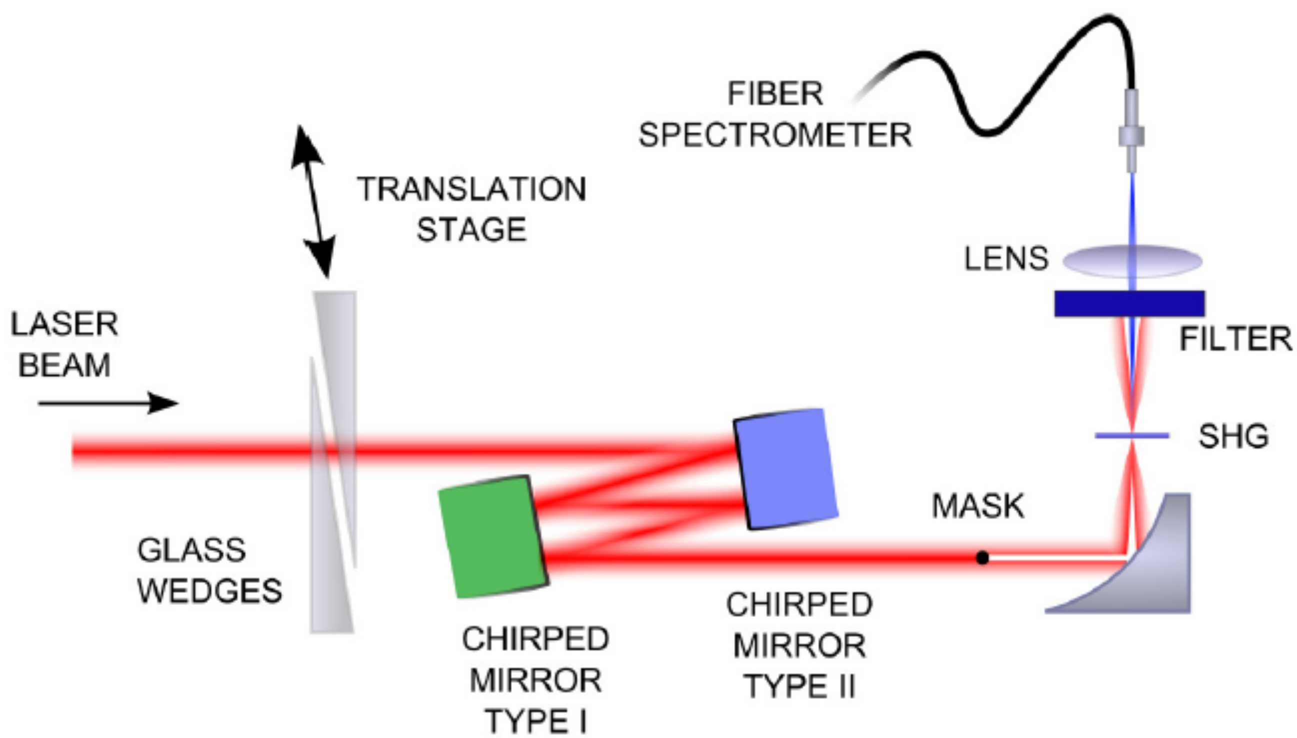

M. Miranda et al., Opt. Express **20**, 18732-18743 (2012)

D-scan

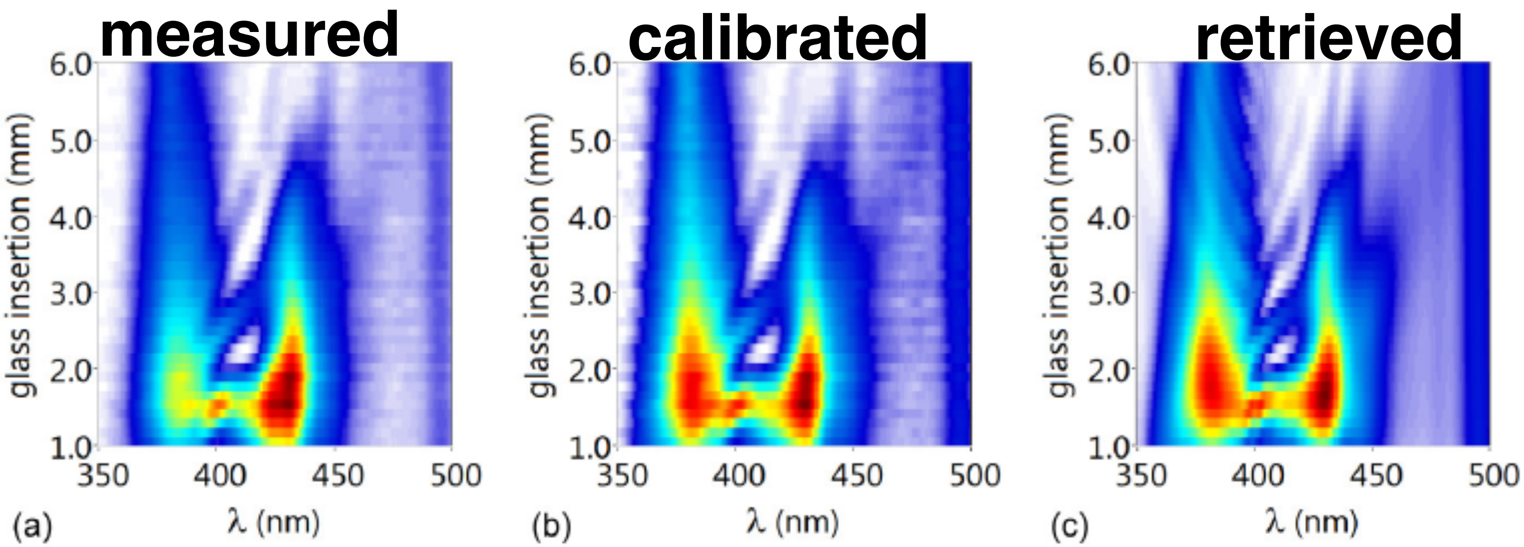

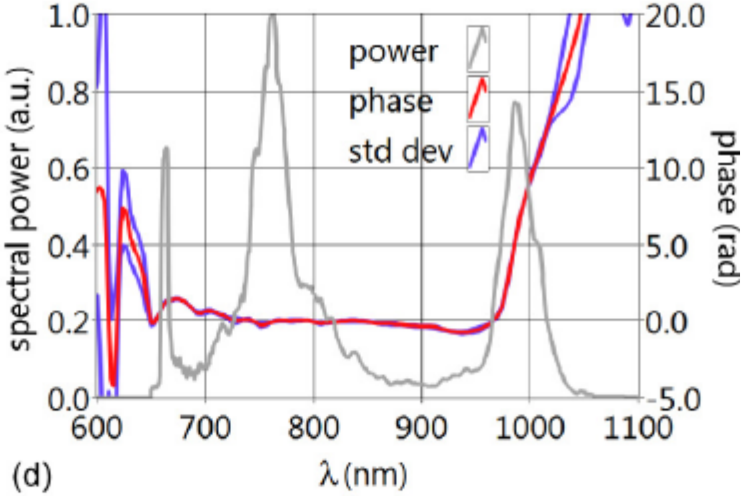

amplitude and phase

M. Miranda et al., Opt. Express **20**, 18732-18743 (2012)

Problem

The carrier-envelope phase

CEP

Carrier Envelope Offset (CEO)

Successive pulses from a Ti:sapphire laser

(100 MHz repetition rate)

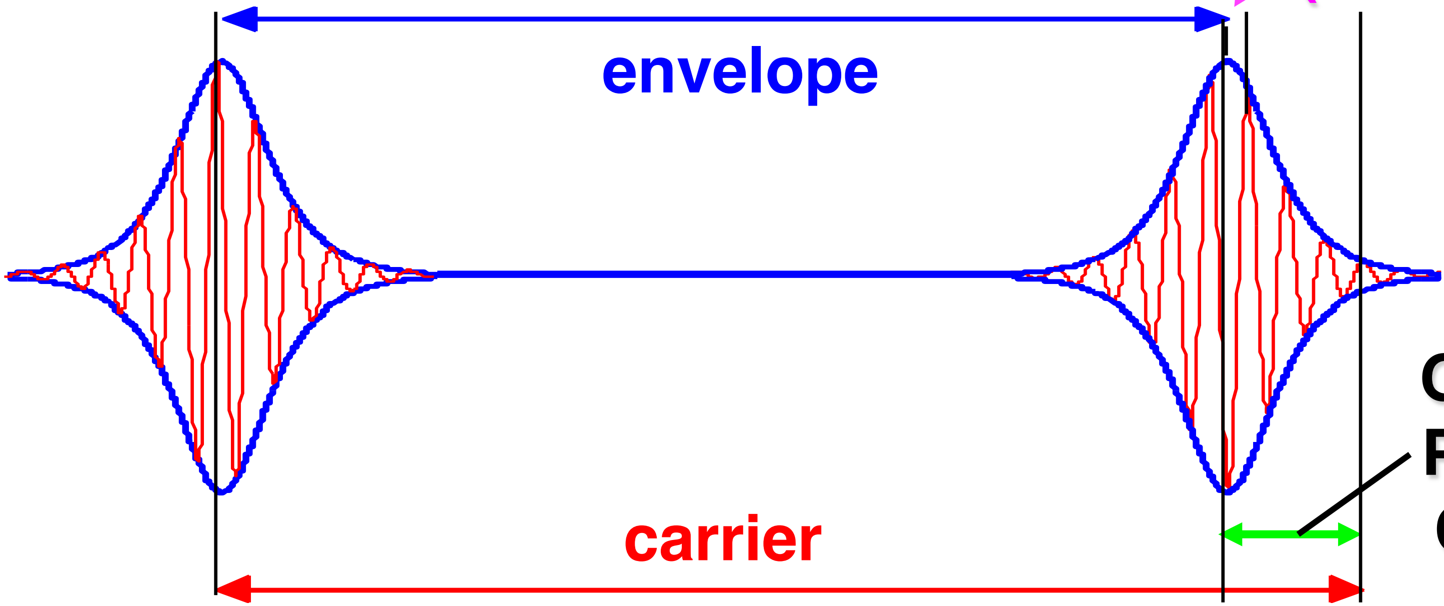

4.6 mm Ti:sapphire:	120.X cycles
3 m air:	20.X cycles
Prism compressor:	140.X cycles
	260.X cycles

Carrier-Envelope Offset (CEO)

$$\nu(m) = \nu_{\mathrm{CEO}} + m \cdot f_{\mathrm{rep}}$$

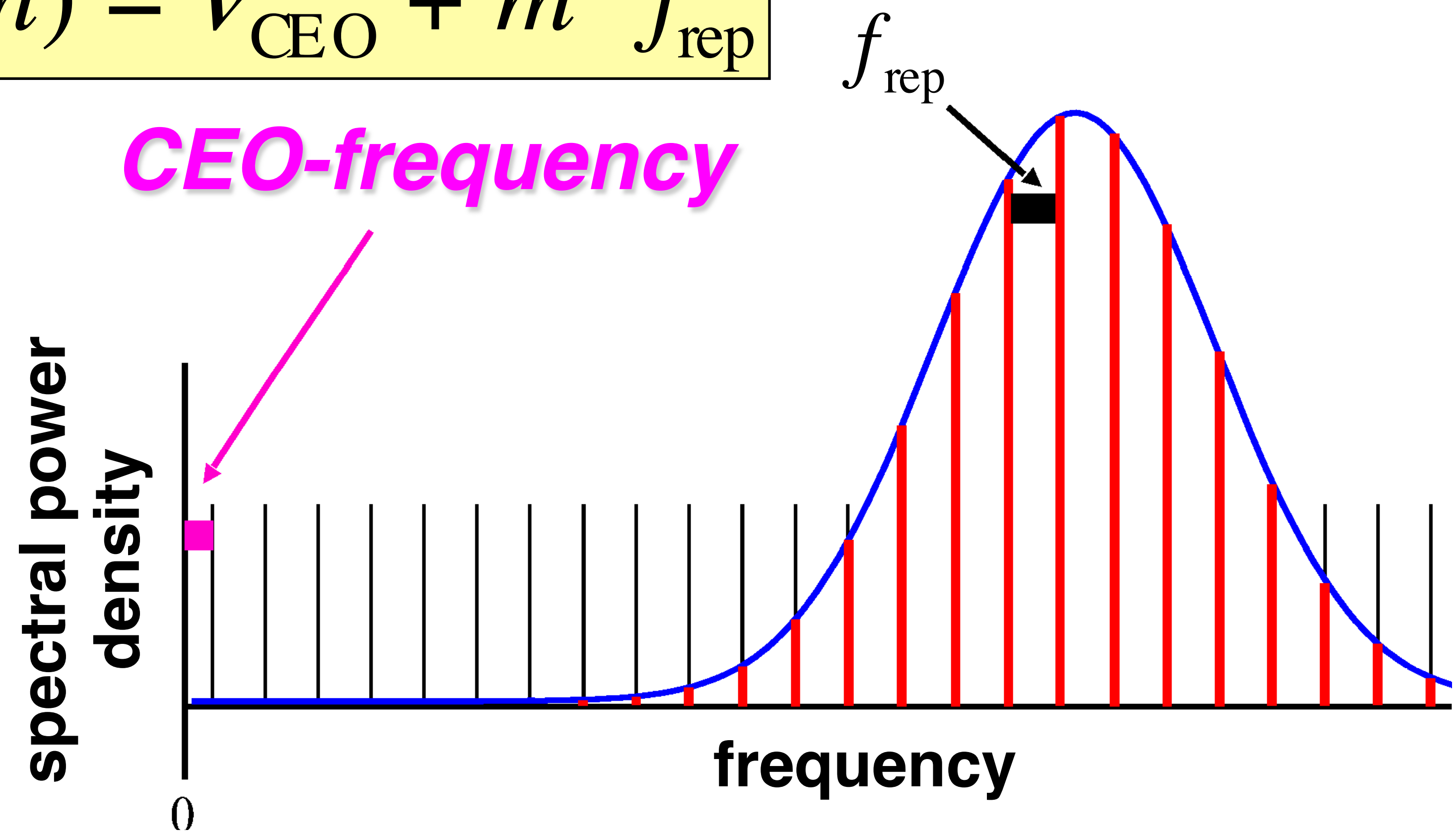

- **mode-locked laser = optical frequency ruler**

- mode comb uniformity better than 10^{-15}

- otherwise rep-rate would be function of wavelength

- 2 degrees of freedom: "translation" and "breathing"

T.Udem et al., *Opt. Lett.* 24, 881 (1999)

Measuring the CEO: f-2f interferometer

A simple scheme based on SHG:

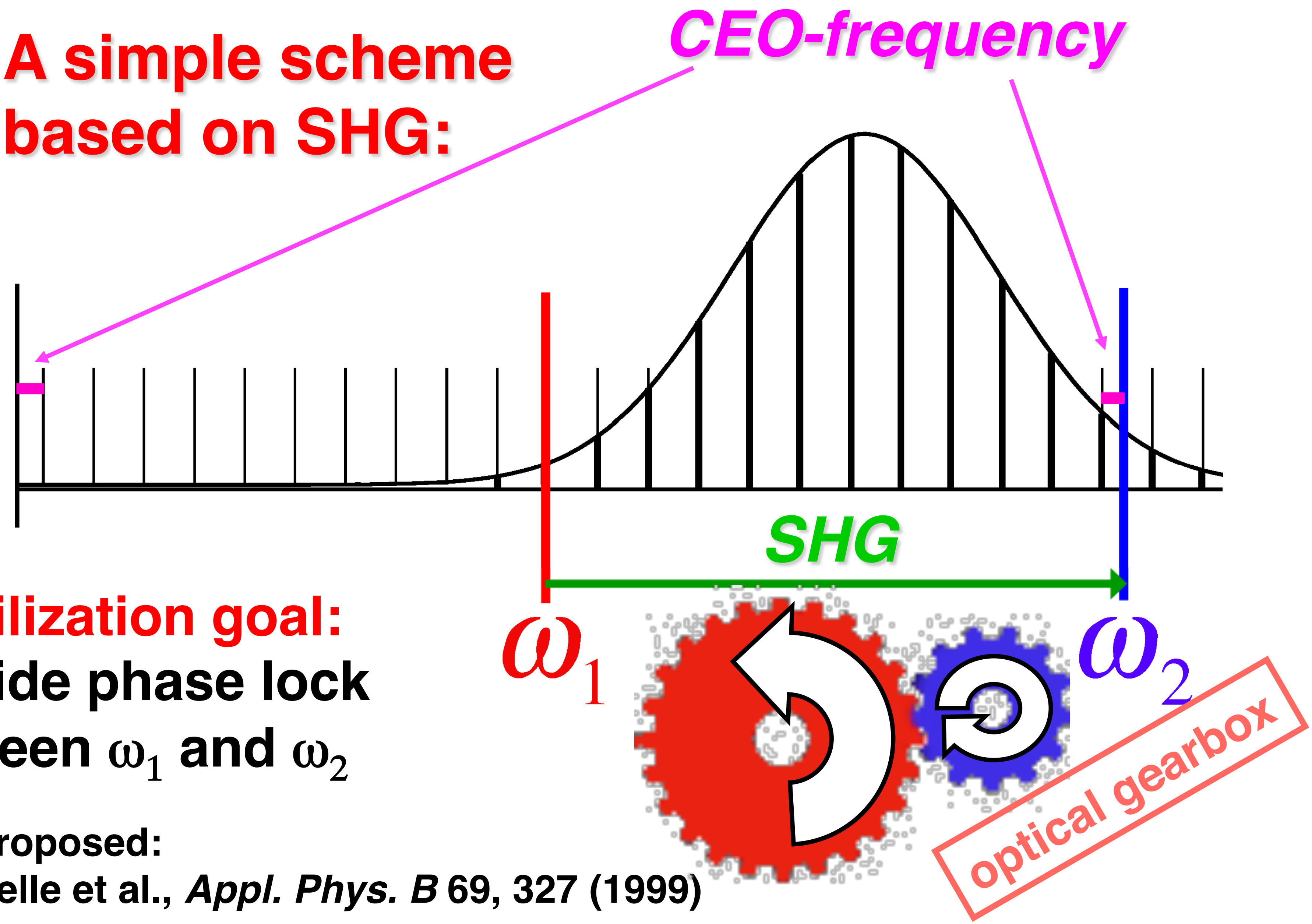

Stabilization goal:
provide phase lock between ω_1 and ω_2

first proposed:
H.R. Telle et al., *Appl. Phys. B* 69, 327 (1999)

Measuring the CEO: 0-f interferometer

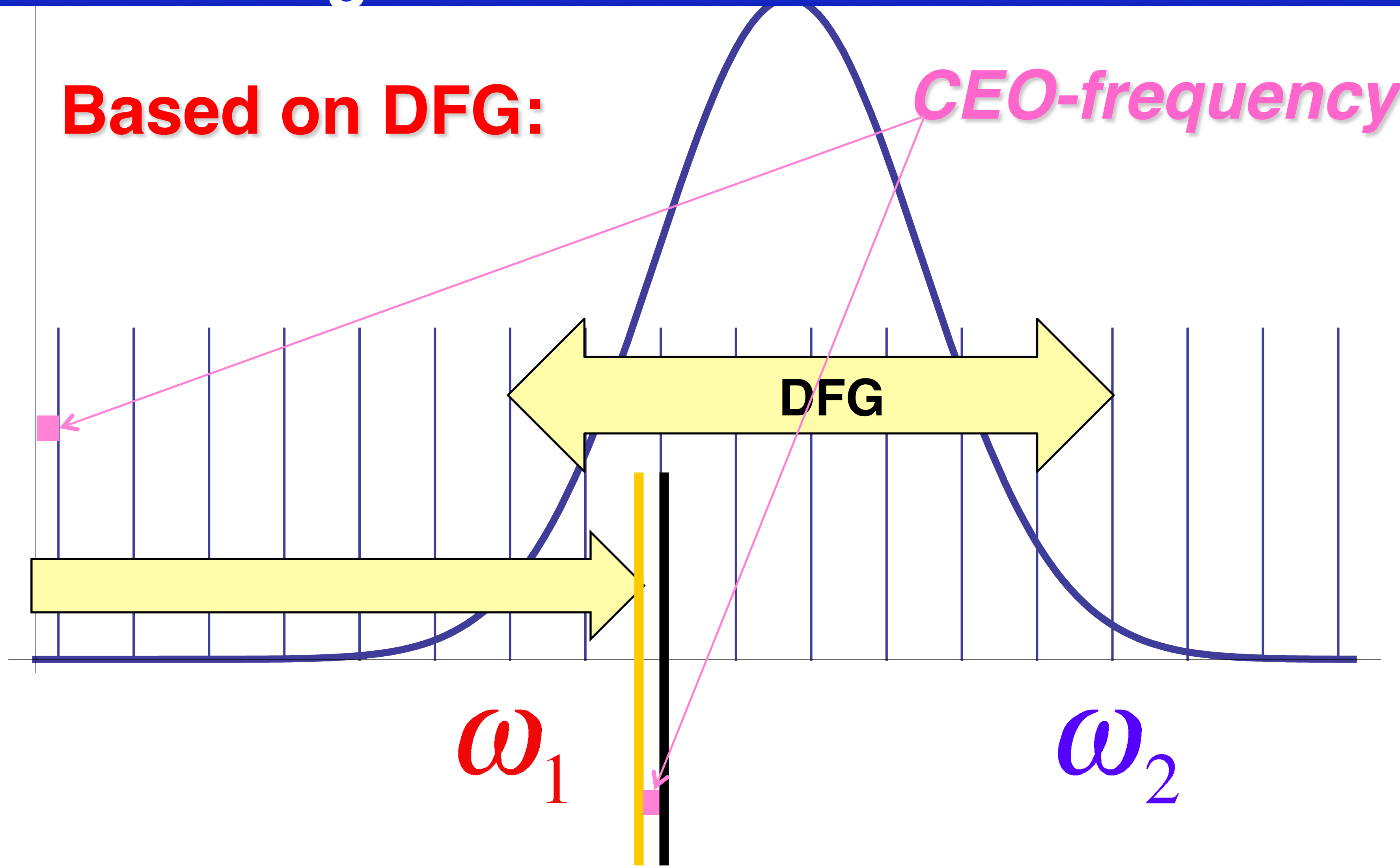

proposed: T. Fuji et al., Opt. Lett. 30, 332 (2005).

Setup Schematic f-2f

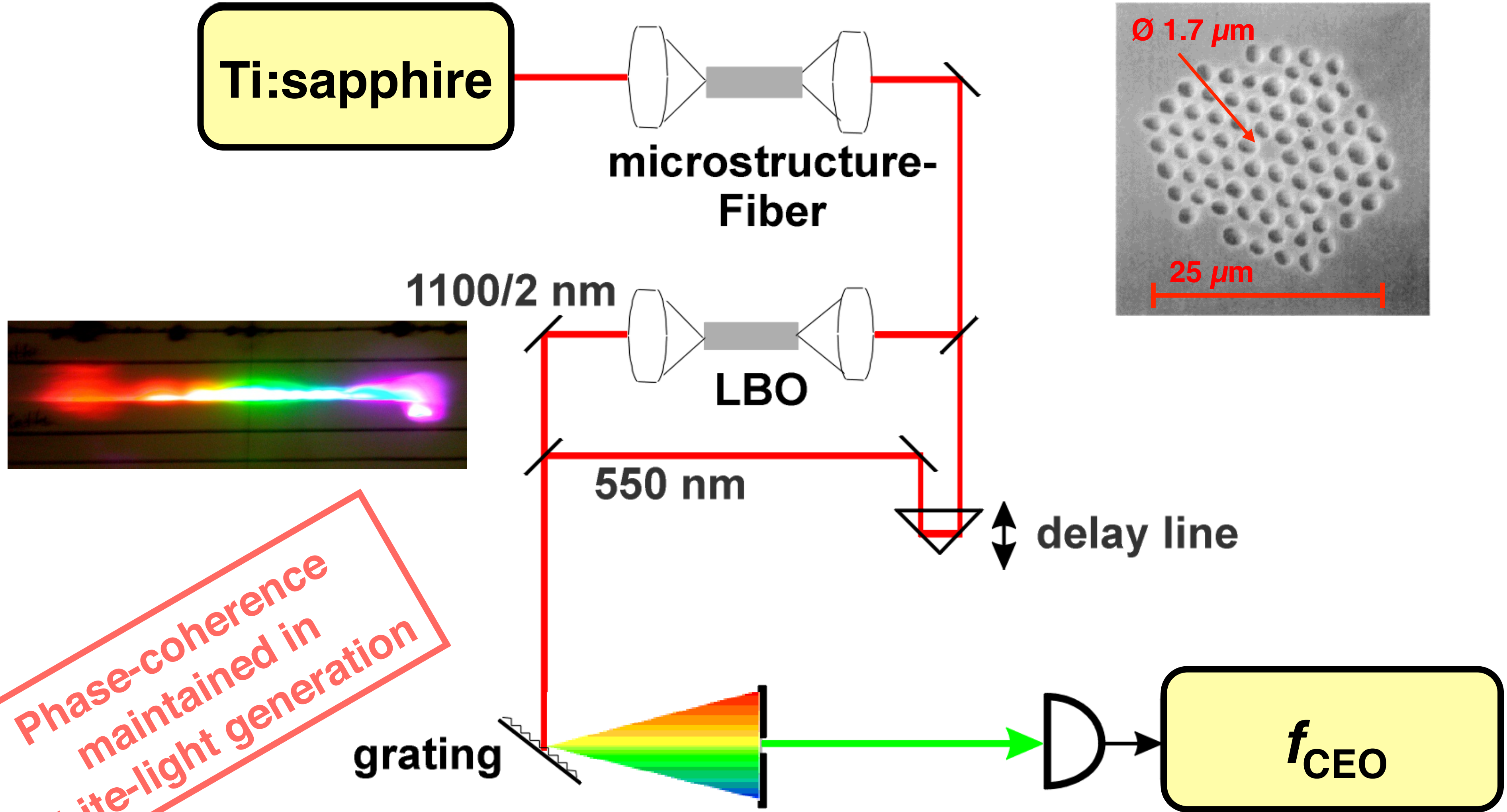

Phase-coherence maintained in white-light generation

SHG bottleneck

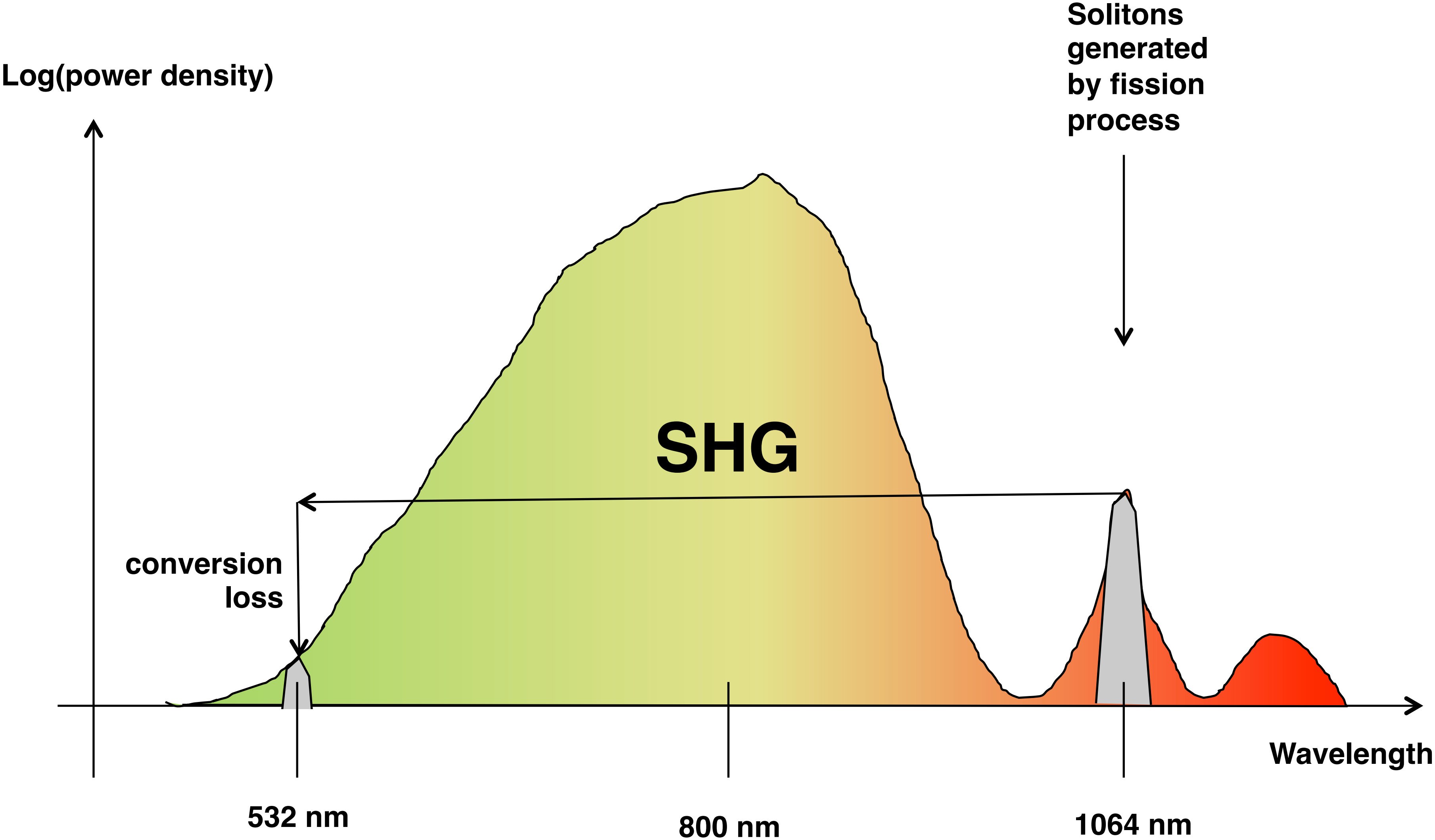

Lessons learned:

- **Use material w/ highest available nonlinearity for SHG**
- **Match spectral broadening process, shorter fibers are better**

Shot noise

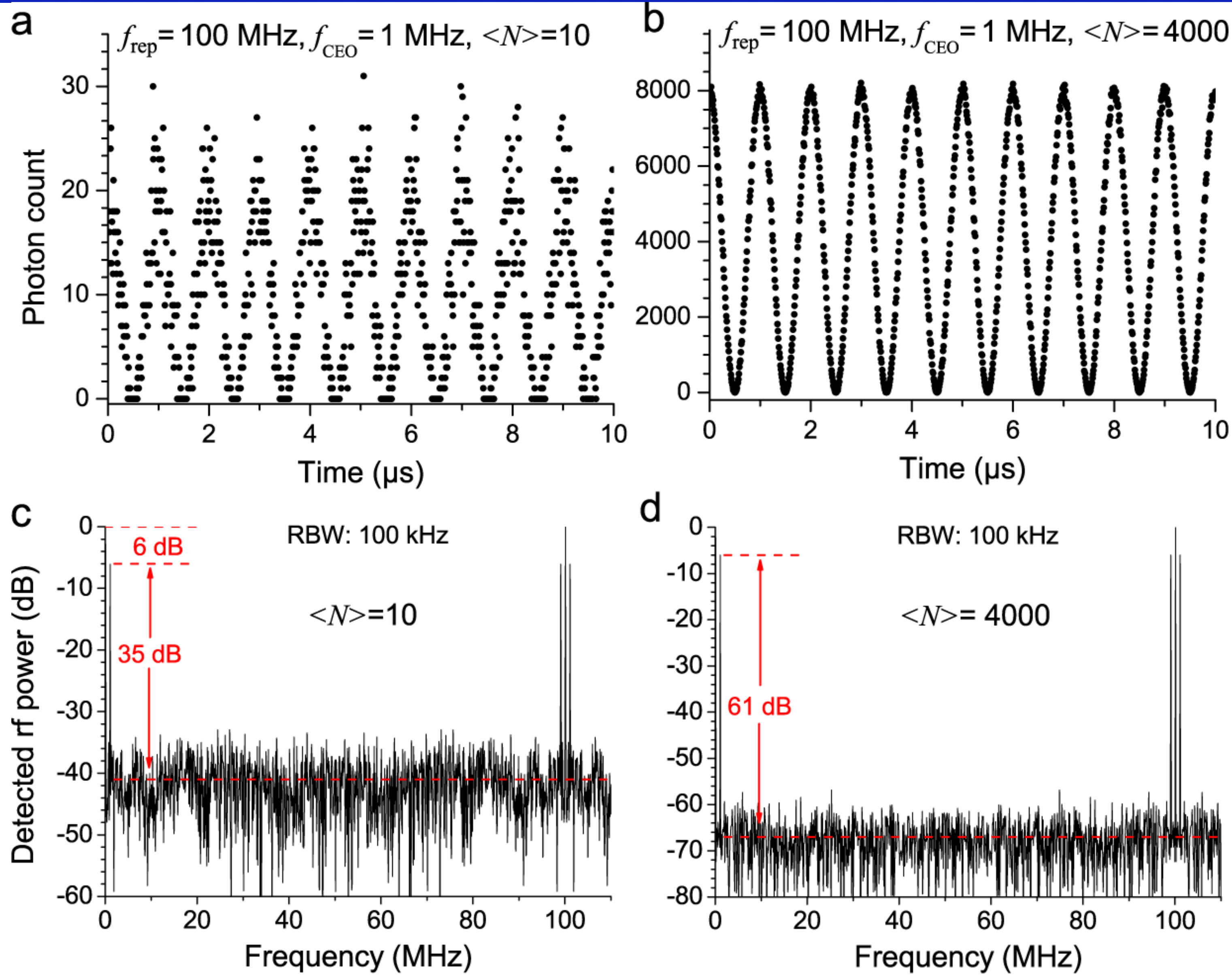

B. Borchers et al., Laser Photon. Rev. 8, 303-315 (2014)

Shot noise

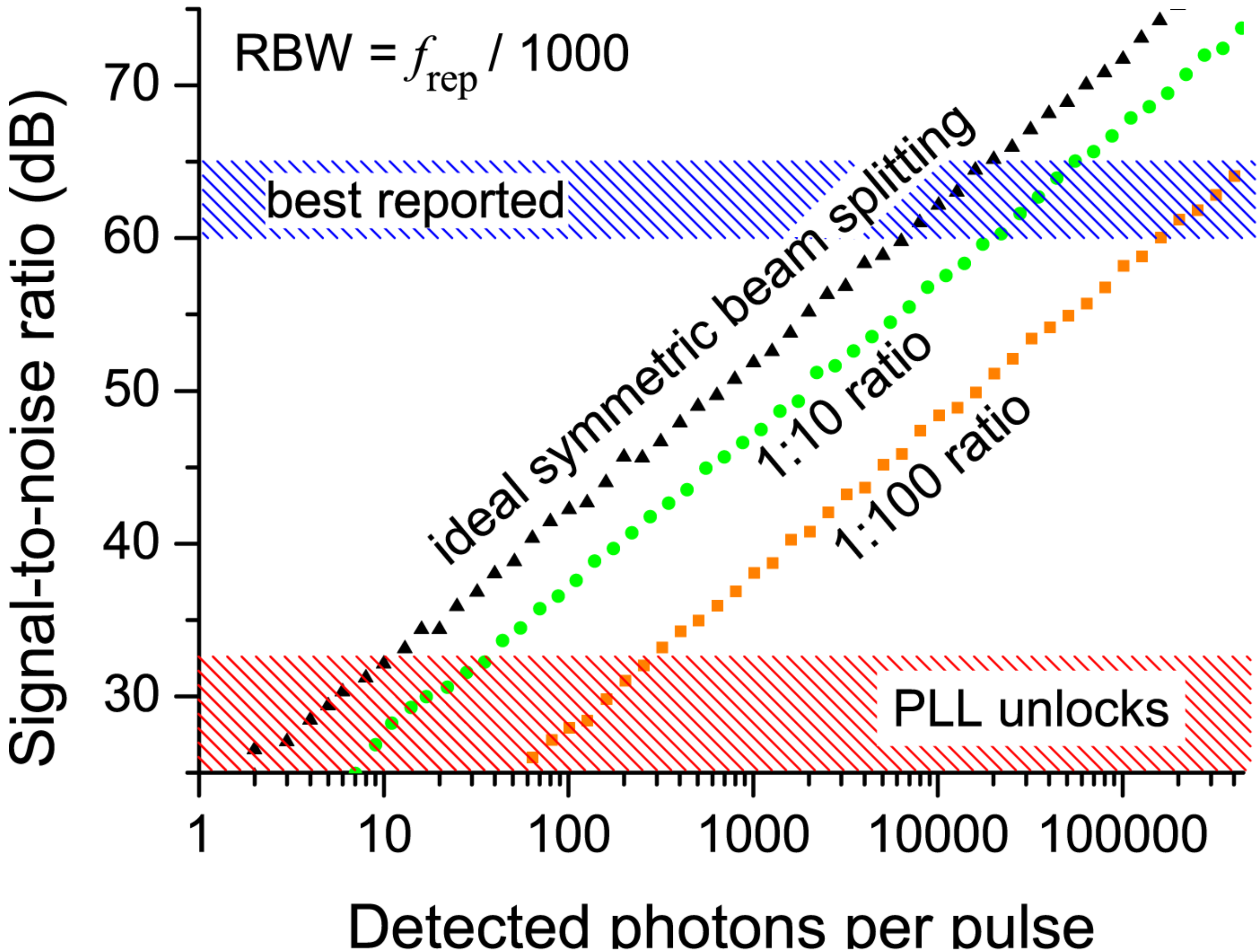

B. Borchers et al., Laser Photon. Rev. 8, 303-315 (2014)

Optimizing the f-2f interferometer

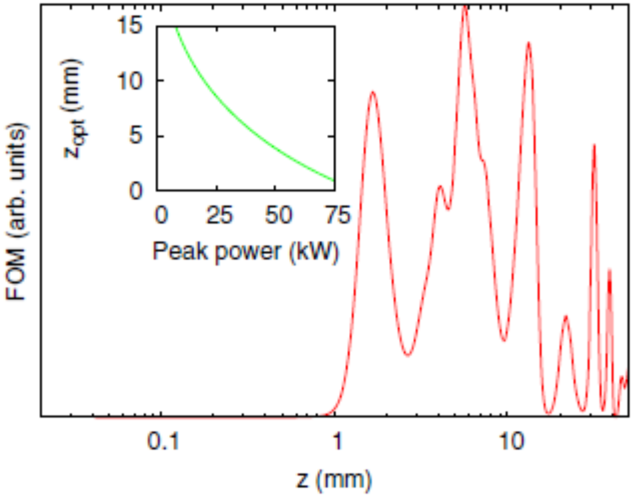

Fig. 1. (Color online) Dependence of the FOM on the propagation length for 15 fs input pulse at 770 nm with peak power of 22 kW. The inset illustrates the dependence of the optimum fiber length on the input power.

Simulation by A. Husakou

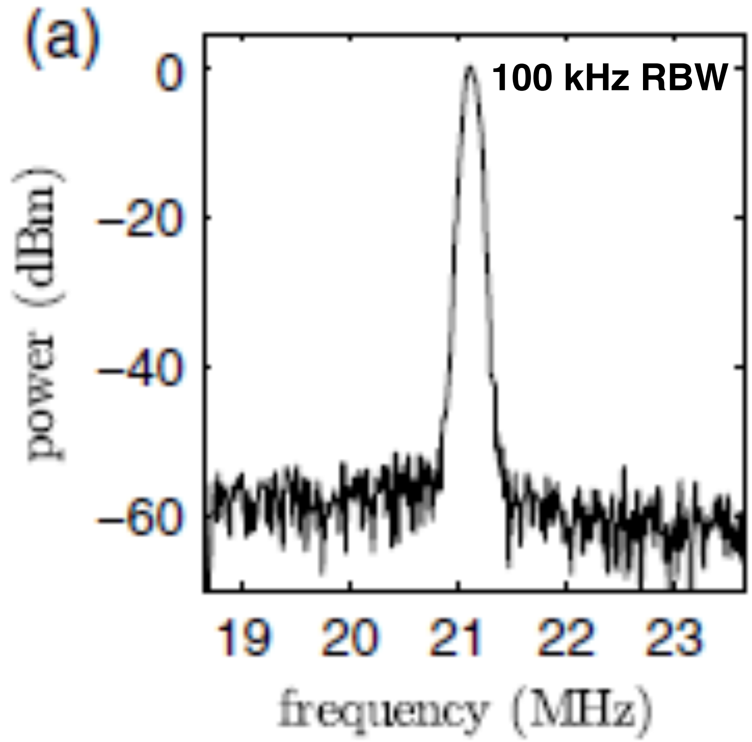

B. Borchers, S. Koke, A. Husakou, J. Herrmann, and G. Steinmeyer, "Carrier-envelope phase stabilization with sub-10 as residual timing jitter," Opt. Lett. 36, 4146-4148 (2011)

Interferometer topology - drift

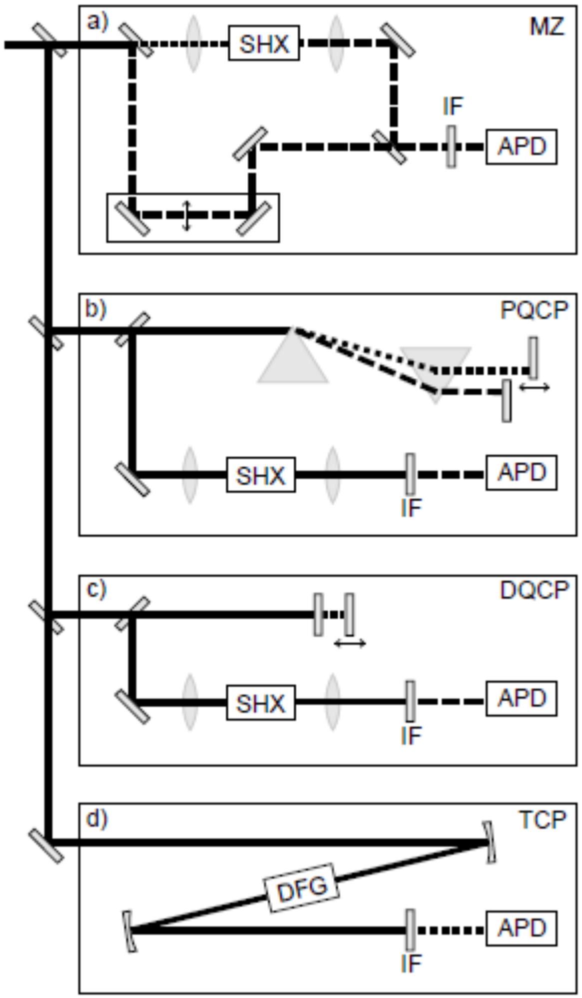

Traditional Mach-Zehnder

Prism based quasi-common path

Dichroic quasi-common path

True common path

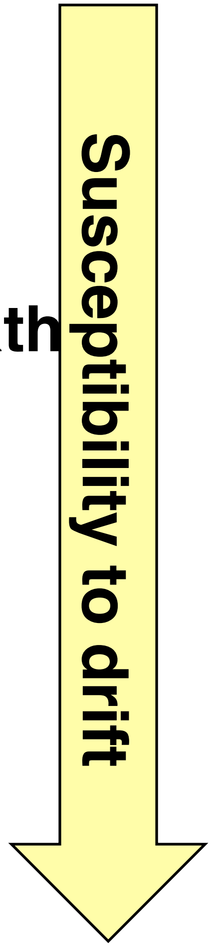

C. Grebing, et al., *Performance comparison of interferometer topologies for carrier-envelope phase detection*, Appl. Phys. B 95, 81 (2009).

Ultimate jitters depend on beat note visibility

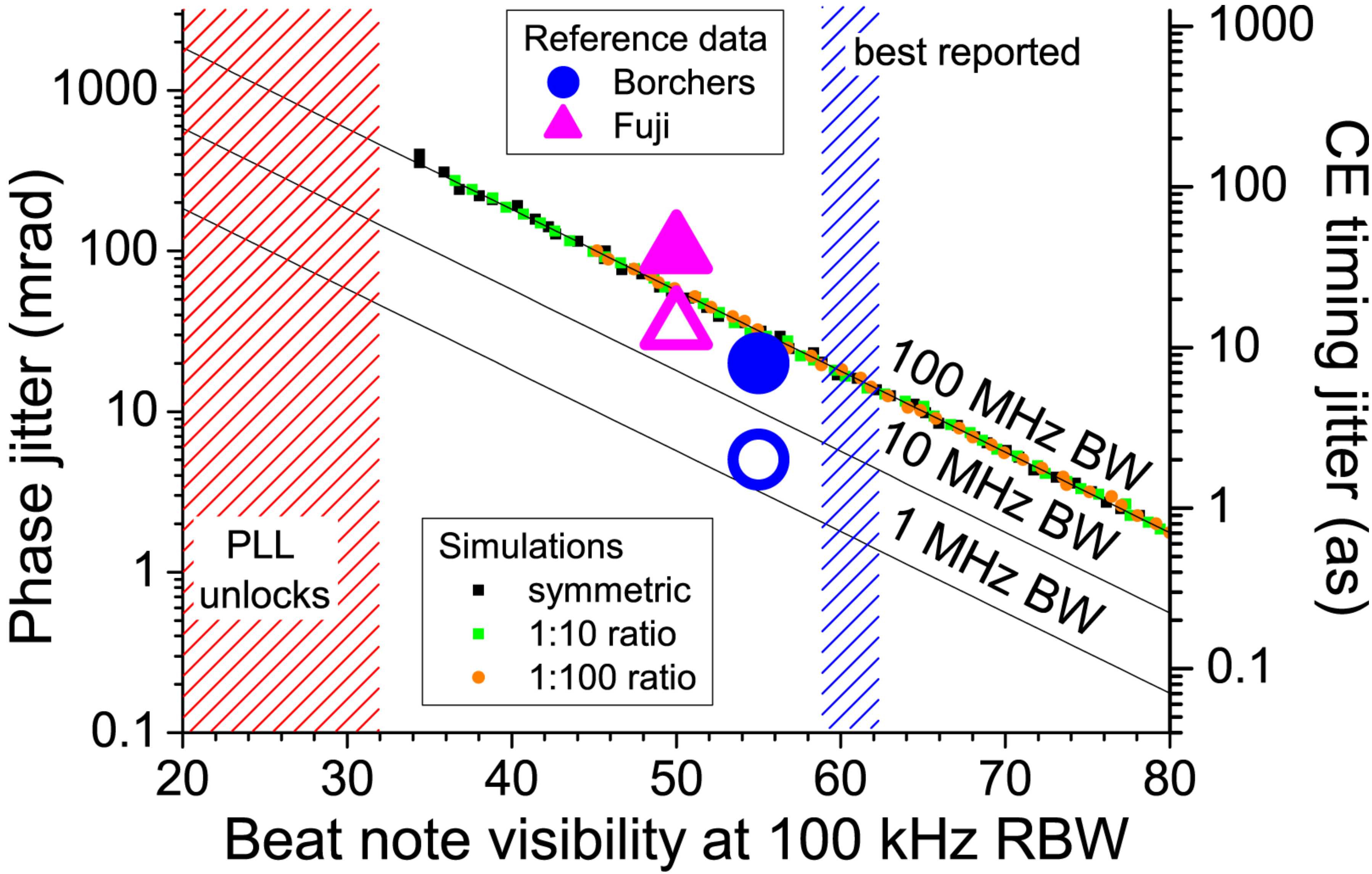

B. Borchers et al., Laser Photon. Rev. **8**, 303-315 (2014)

Phase stabilization via feedback

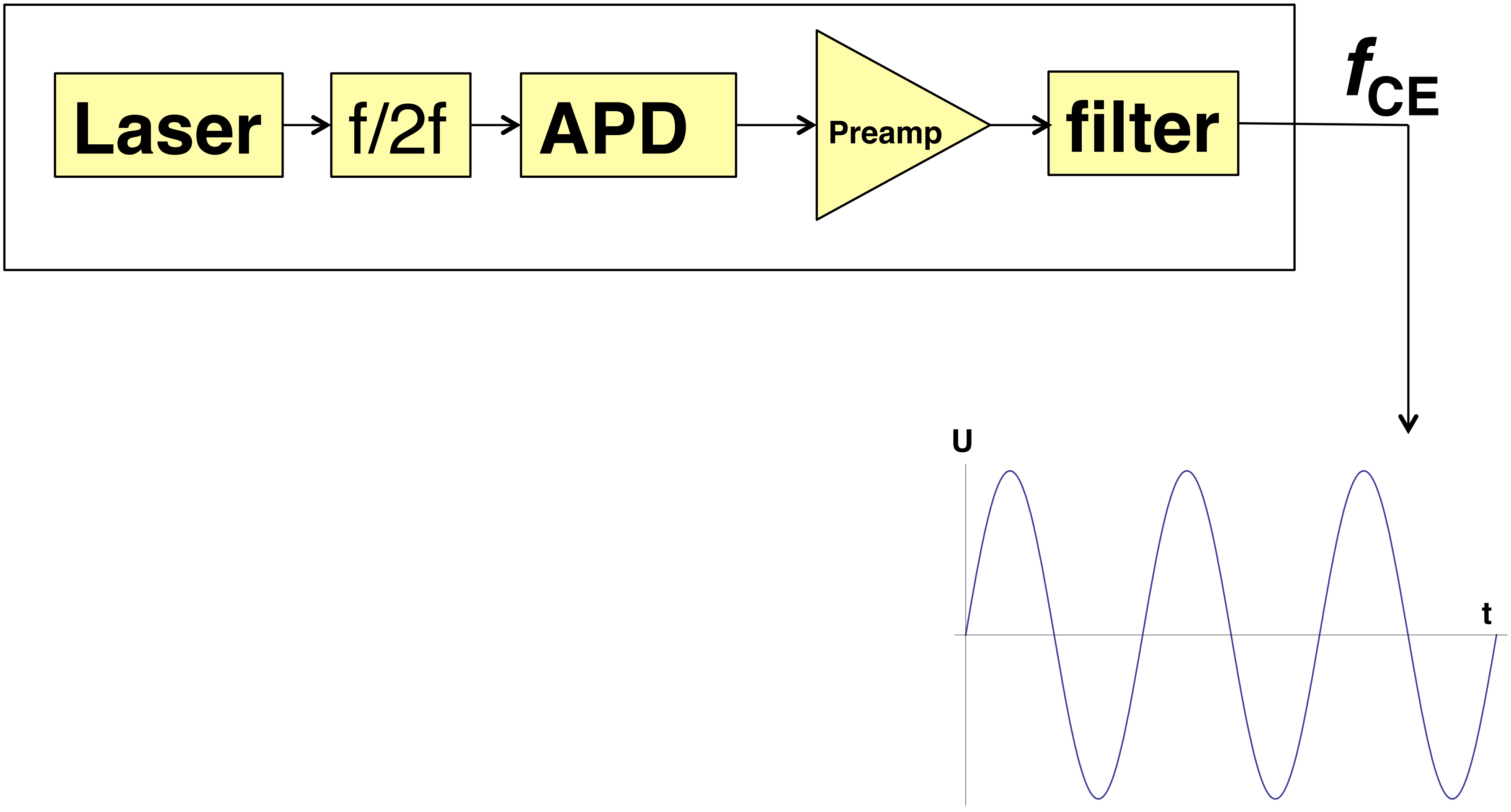

How can we change the CE frequency?

Servo mechanisms

Environmental (temperature, pressure)

- very slow (a few Hertz at best)
- secondary mechanism for drift compensation

Nonlinearity induced (pump power mod.)

- Kerr effect is dispersive
- can be made very fast (>100 kHz w/ AOM or EOM)
- most established way

The laser as a VCO

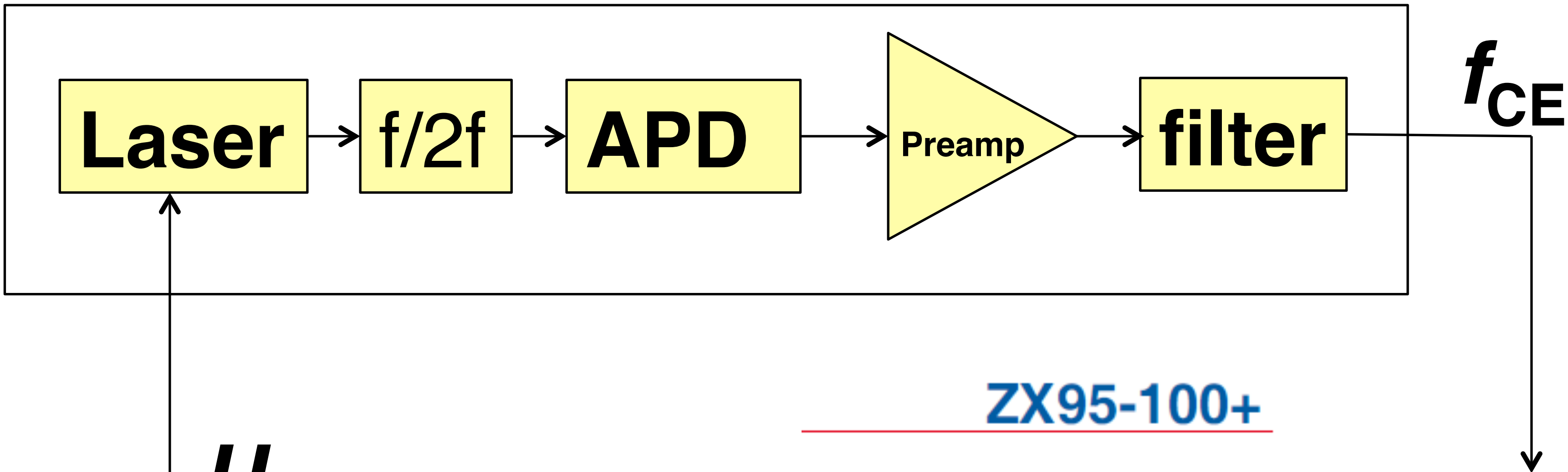

ZX95-100+

CASE STYLE: GB956

Connectors	Model	Price	Qty.
SMA	ZX95-100-S+	$37.95 ea.	(1-9)

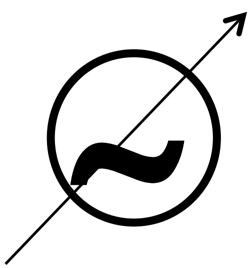

VCO = voltage controlled oscillator

Closing the loop

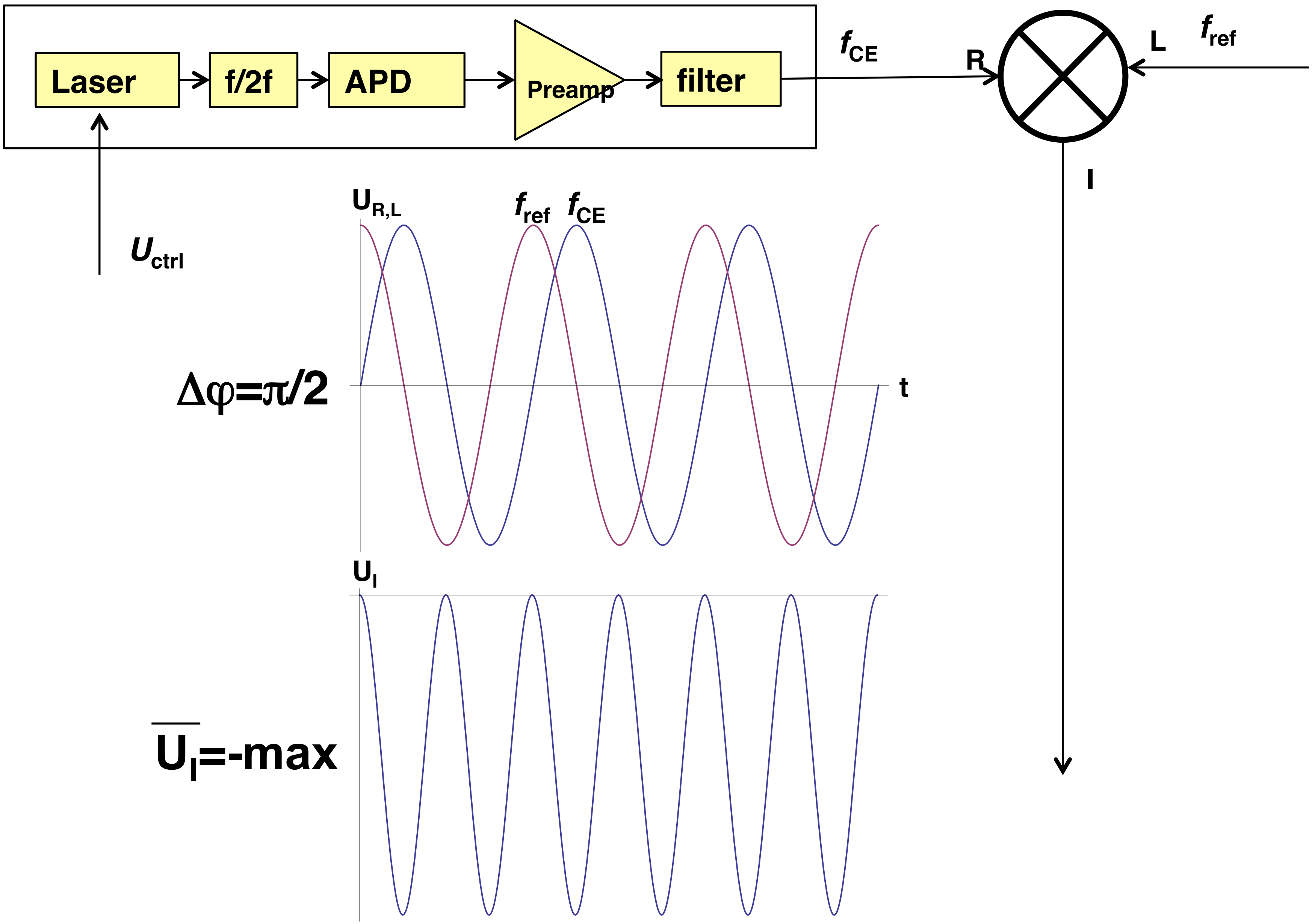

Closing the loop

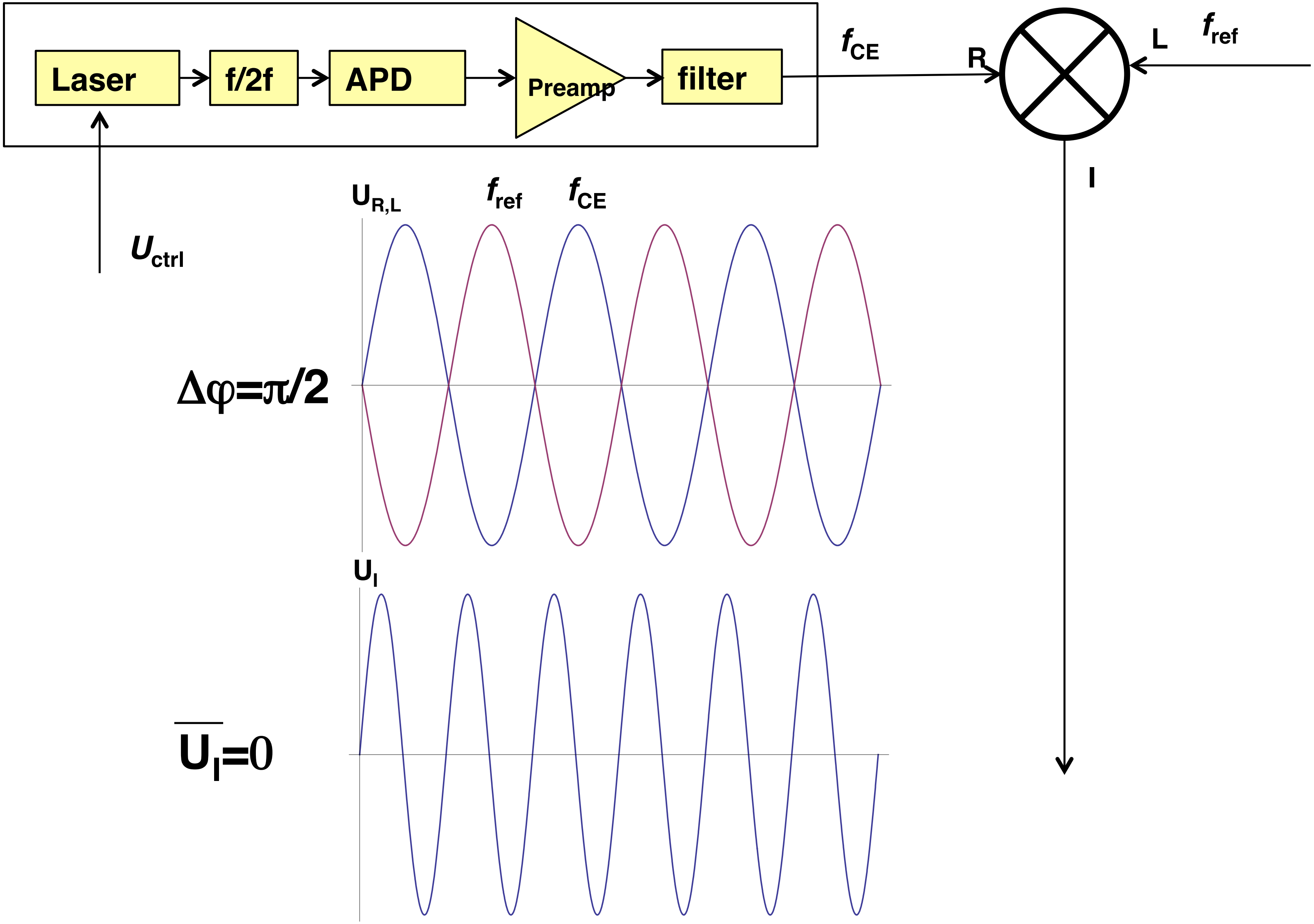

Closing the loop

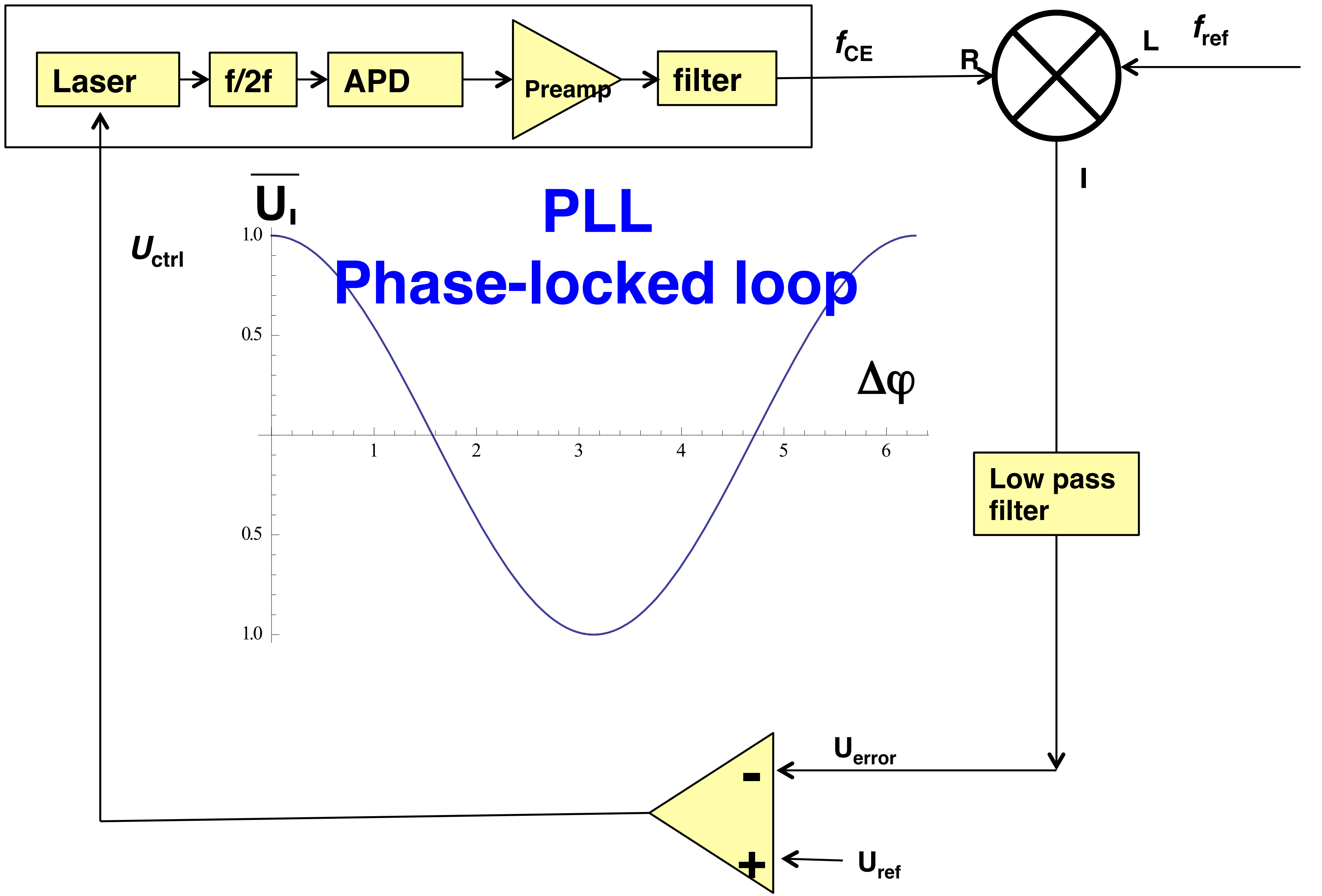

Stabilization with servo loop

PLL= phase-locked loop

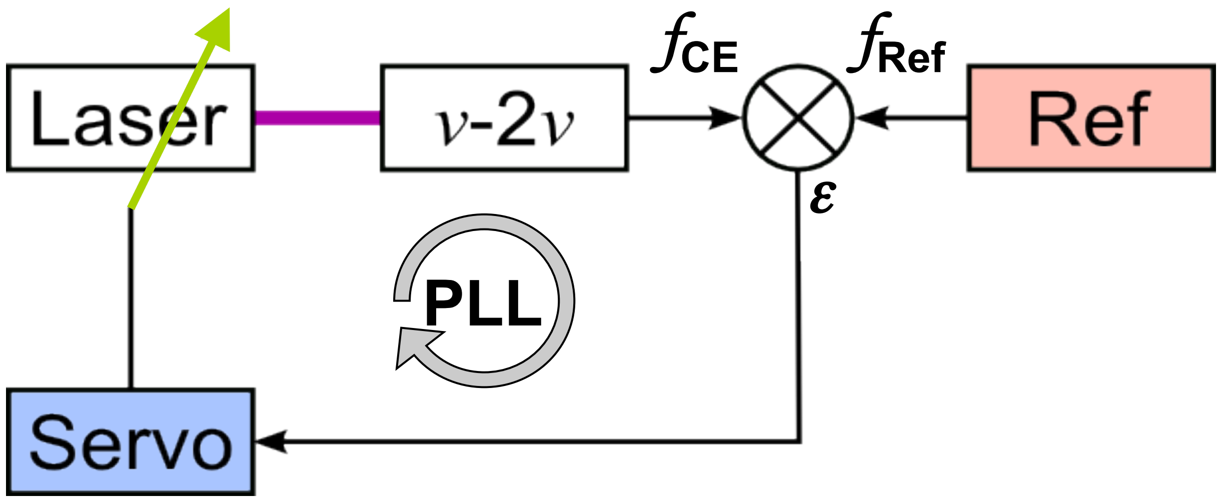

PLL prevents stabilization to zero offset

Complex locking electronics required (Phase margin!)

Feedback compromises laser performance

Tradeoff: phase capture range vs. precision

Best performance achieved with feedback scheme

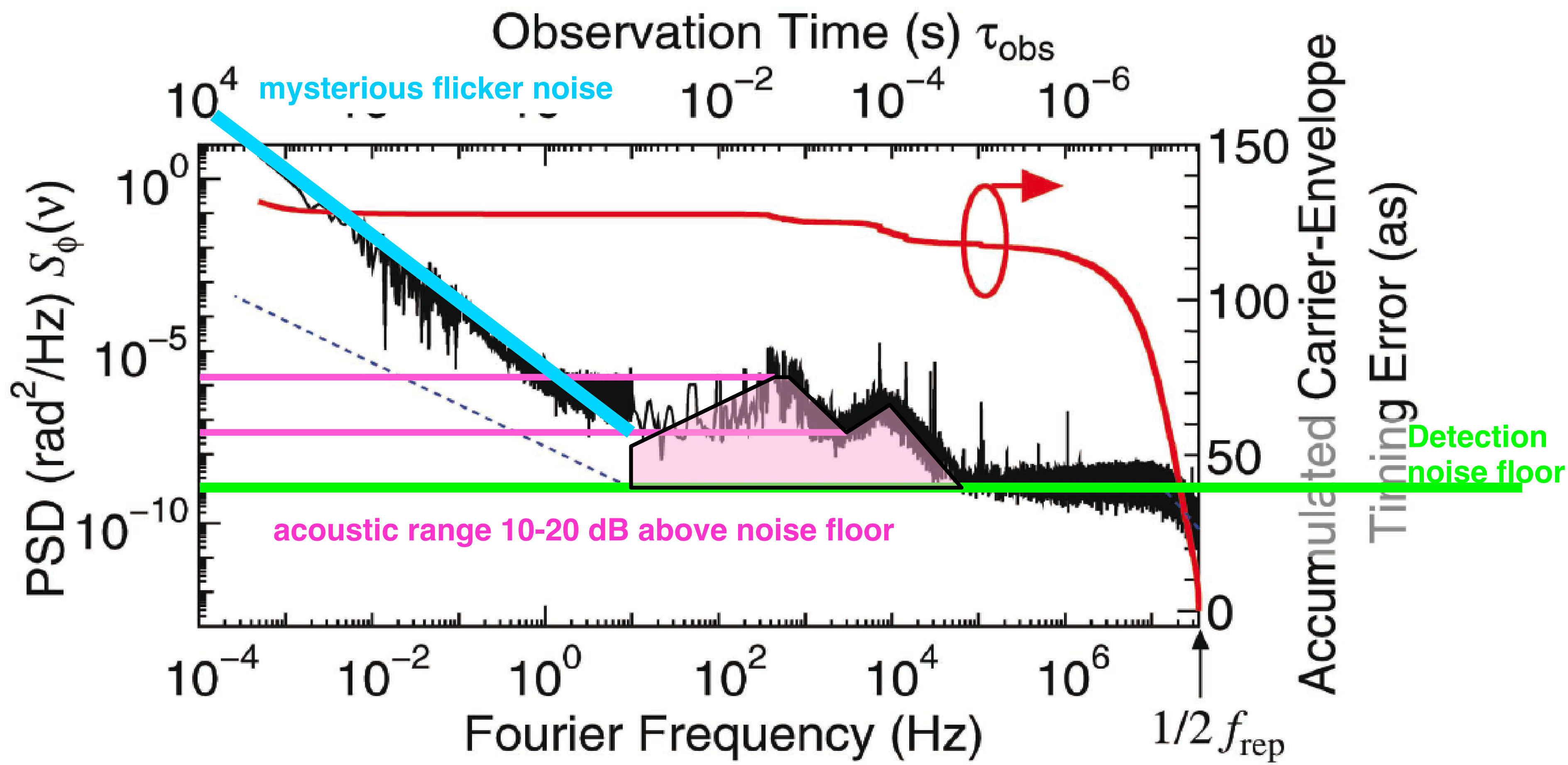

residual jitter: 180 mrad=70 attoseconds (0.2Hz-2MHz))

monolithic scheme: Takao Fuji et al., Opt. Lett. 30, 332 (2005).
similar excellent results obtained by Tara Fortier, Opt. Lett. 27, 1436 (2002).

Direct feed-forward scheme

Koke et al., *Nature Photonics* 4, 462 (2010).
B. Borchers et al. Opt. Lett. **36**, 4146-4148 (2011)

Idea

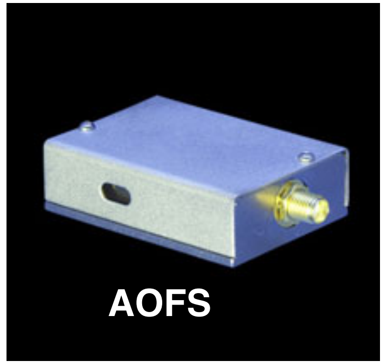

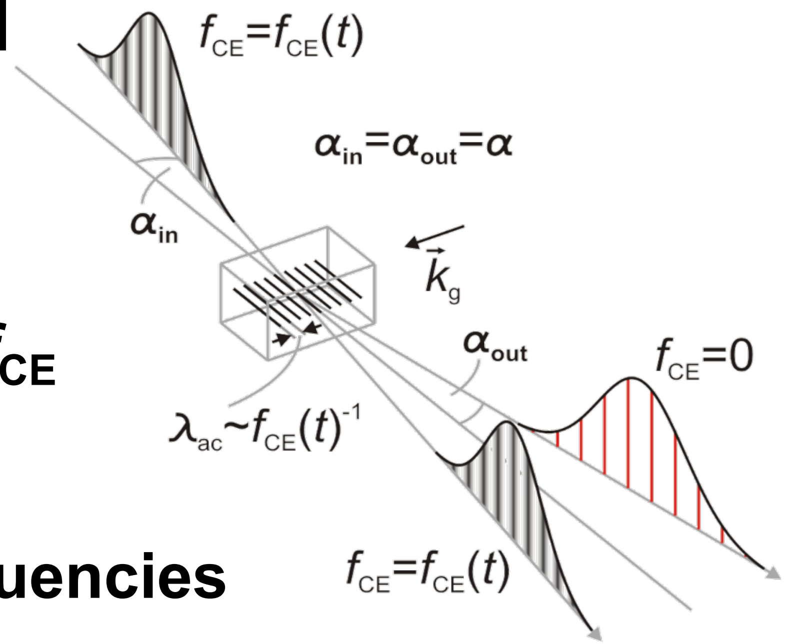

1. **We can measure the comb offset f_{CE}**

2. **There exist devices to shift laser frequencies by radio frequencies**

3. **Why don‘t we simply shift the entire comb by f_{CE}**

Experimental set-up

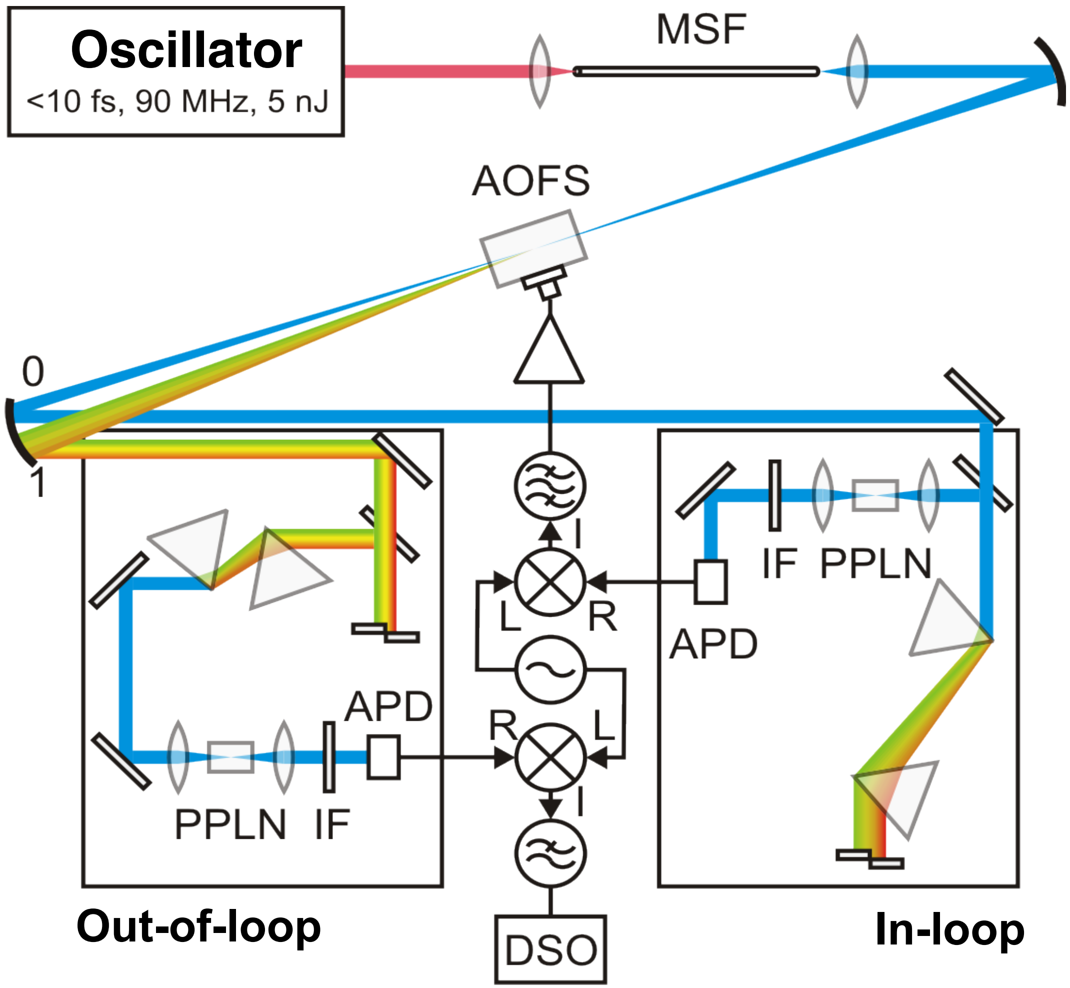

AOFS center frequency:
f= 70 MHz
(2.7 cm fused silica @ 1000 fs²)

Out-of-loop measurement scheme

MSF...microstructured fiber

IF...interference filter

AOFS...acousto-optical frequency shifter

APD...avalanche photo diode

PPLN...periodically poled lithium niobate

DSO...digital sampling oscilloscope

Results

Koke et al., *Nature Photonics* 4, 462 (2010).

Fuji et al., *Opt. Lett.* 30, 332 (2005)

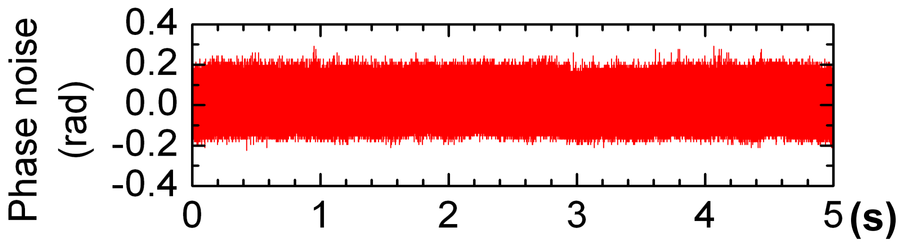

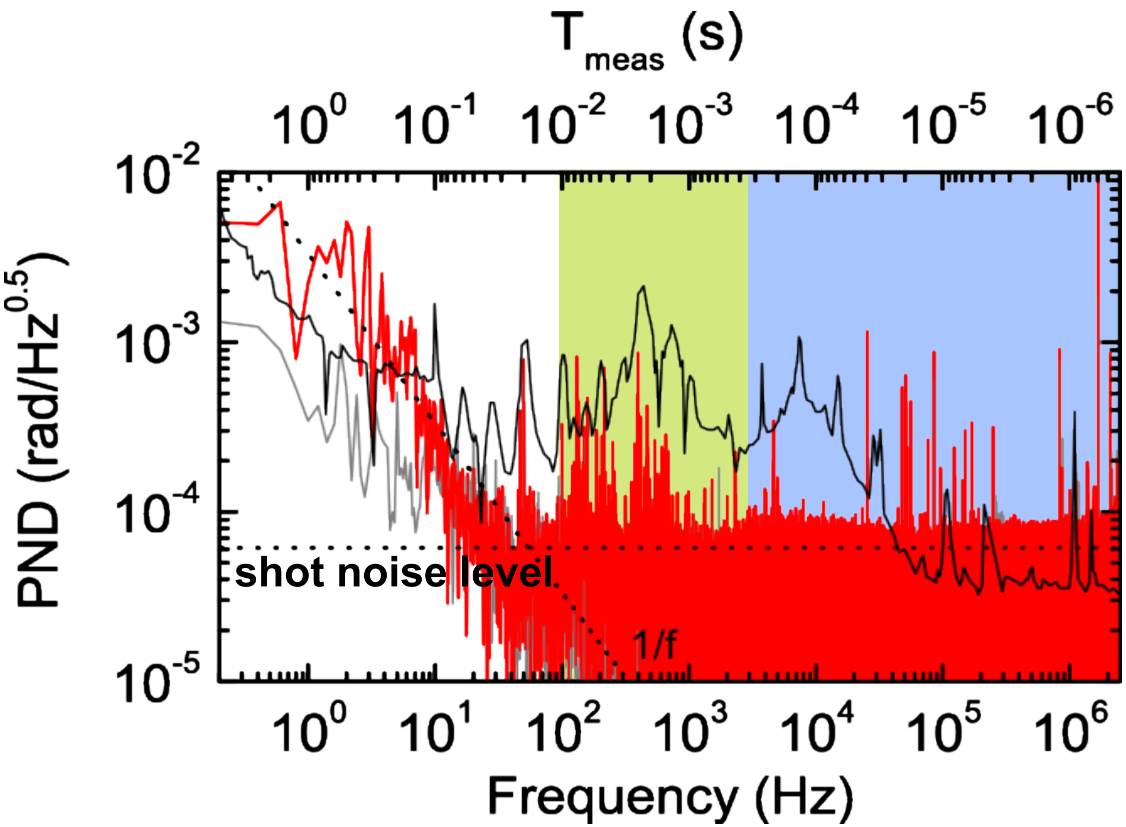

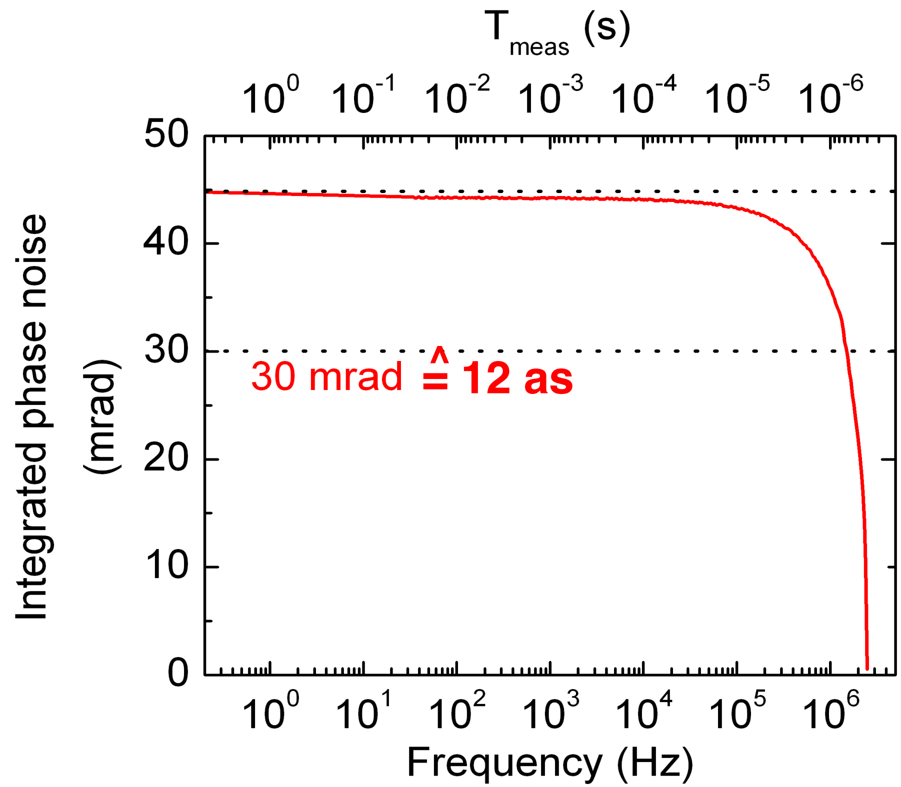

>kHz: technical noise

100 Hz – 3kHz: acoustical range

<100 Hz: flicker noise

CEP measurement of amplified systems

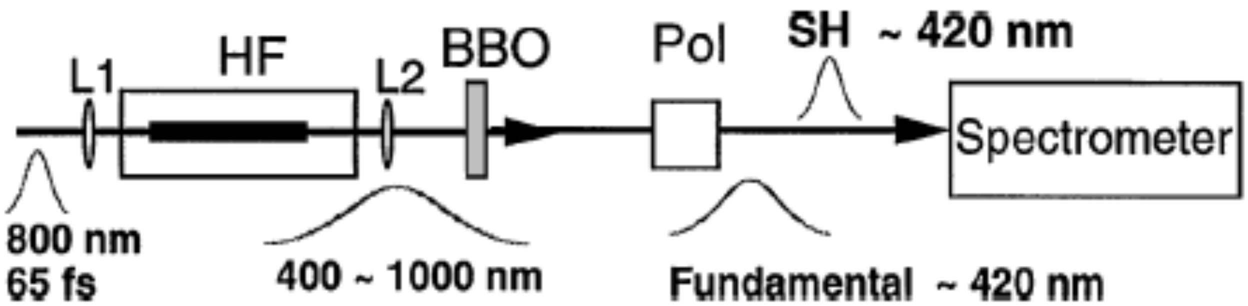

Fig. 2. Experimental setup: L1, 250-mm focal-length lens; L2, 600-mm focal-length lens; HF, hollow fiber; BBO, 300-μm-thick BBO crystal; Pol, polarizer.

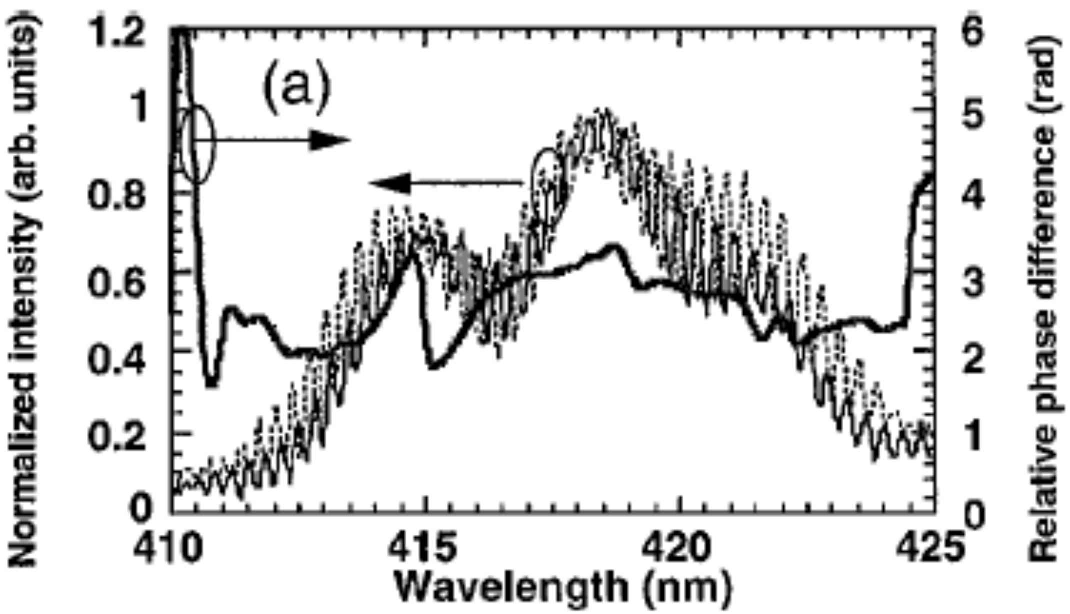

M. Kakehata et al., Opt. Lett. **26**, 1436-1438 (2001)

Fast f-to-2f

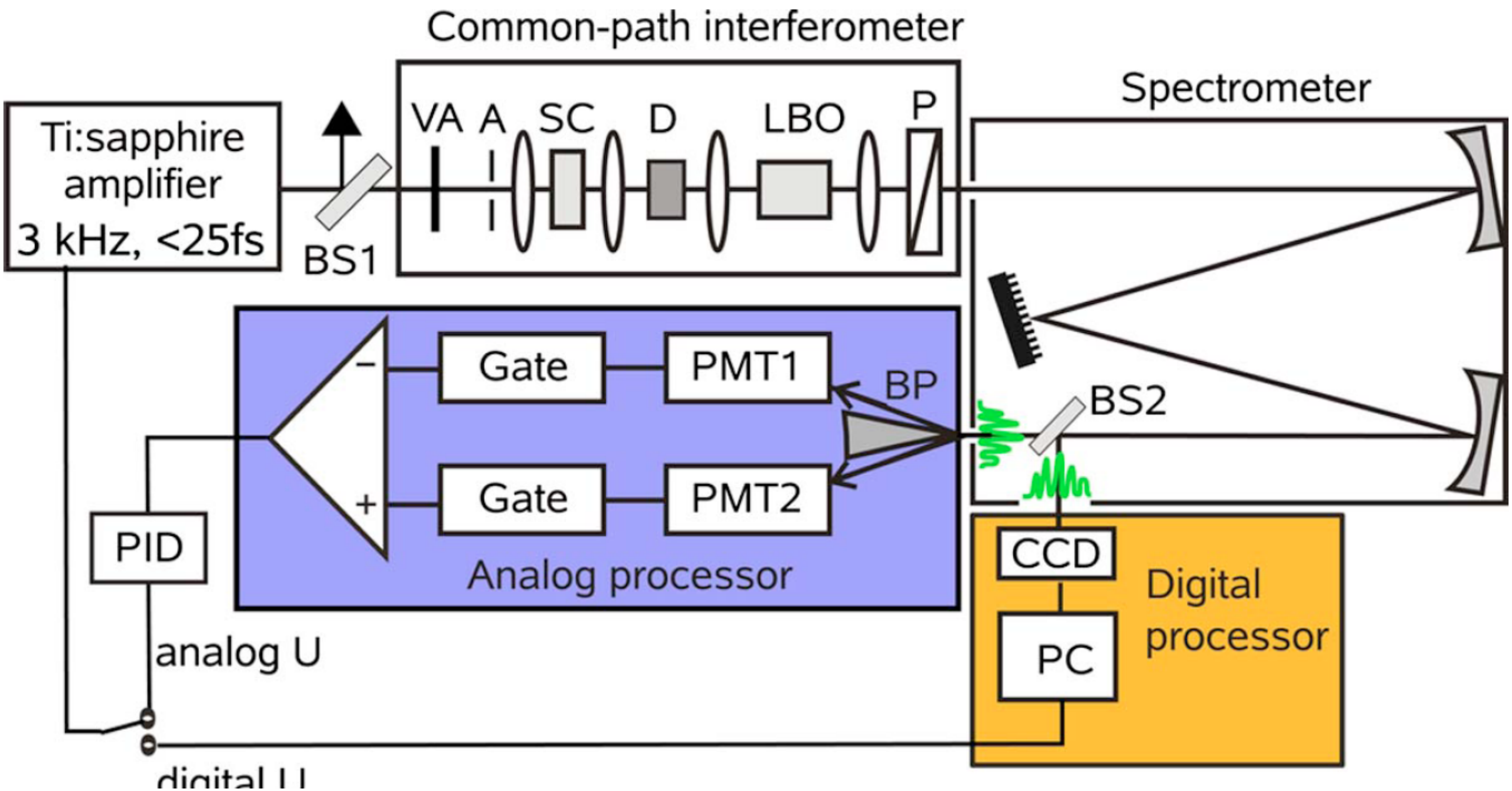

S. Koke et al., Opt. Lett. **33**, 2545-2547 (2008)

Optimizing single-shot detection

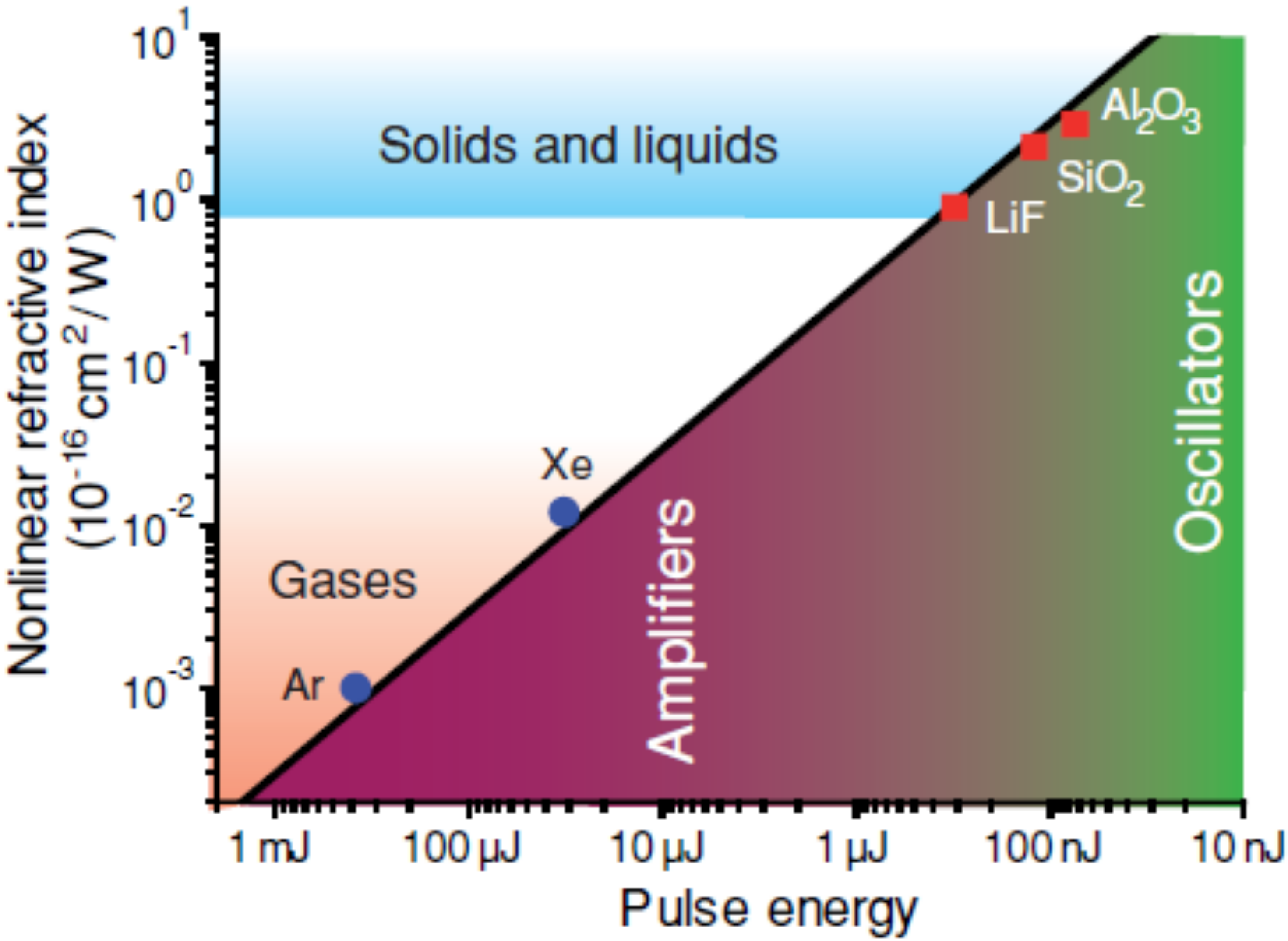

B. Borchers et al., Laser Photon. Rev. **8**, 303-315 (2014)

Combining FROG and CEP measurement

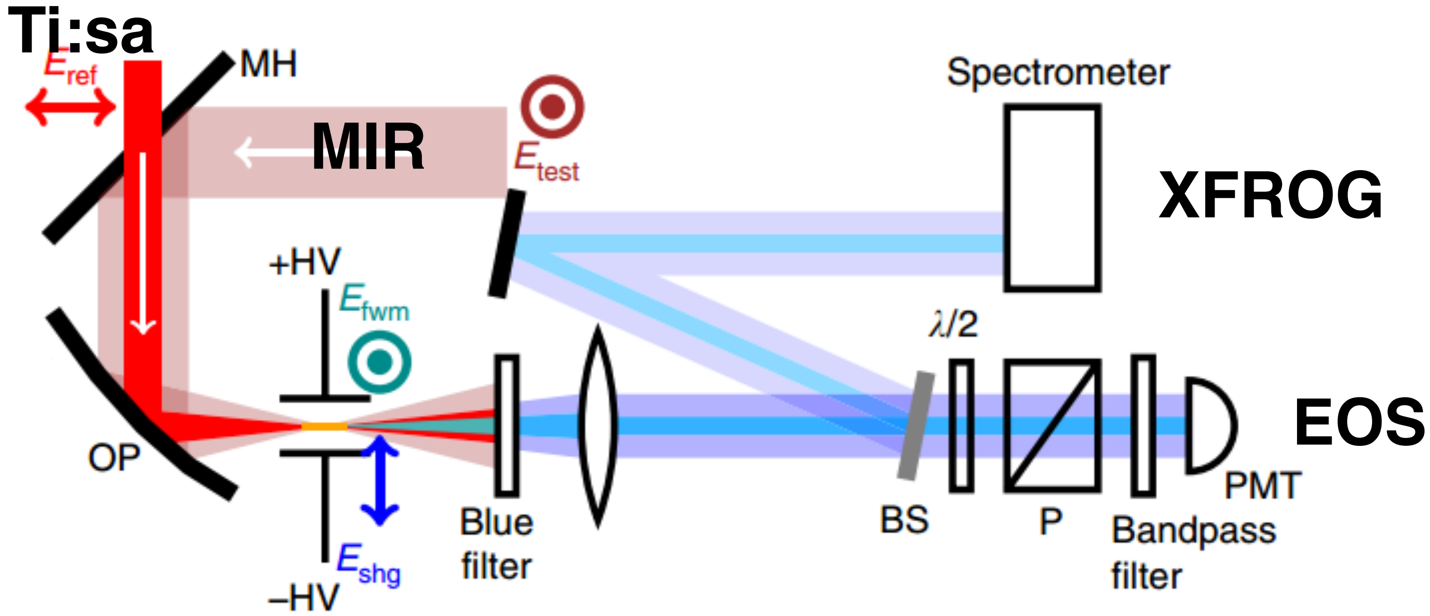

Figure 1 | Schematic of the system for scanning operation. BS, 7% beam splitter; HV, high voltage (4 kV); MH, mirror with a hole; OP, off-axis parabolic mirror; P, calcite polariser; PMT, photomultiplier tube.

Use electro-optic sampling for CEP detection
Use FROG at the same time

FWM and SHG are generated at crossed polarization

Y. Nomura et al., Nature Communications **4**, 2820 (2013)

Combining FROG and CEP measurement

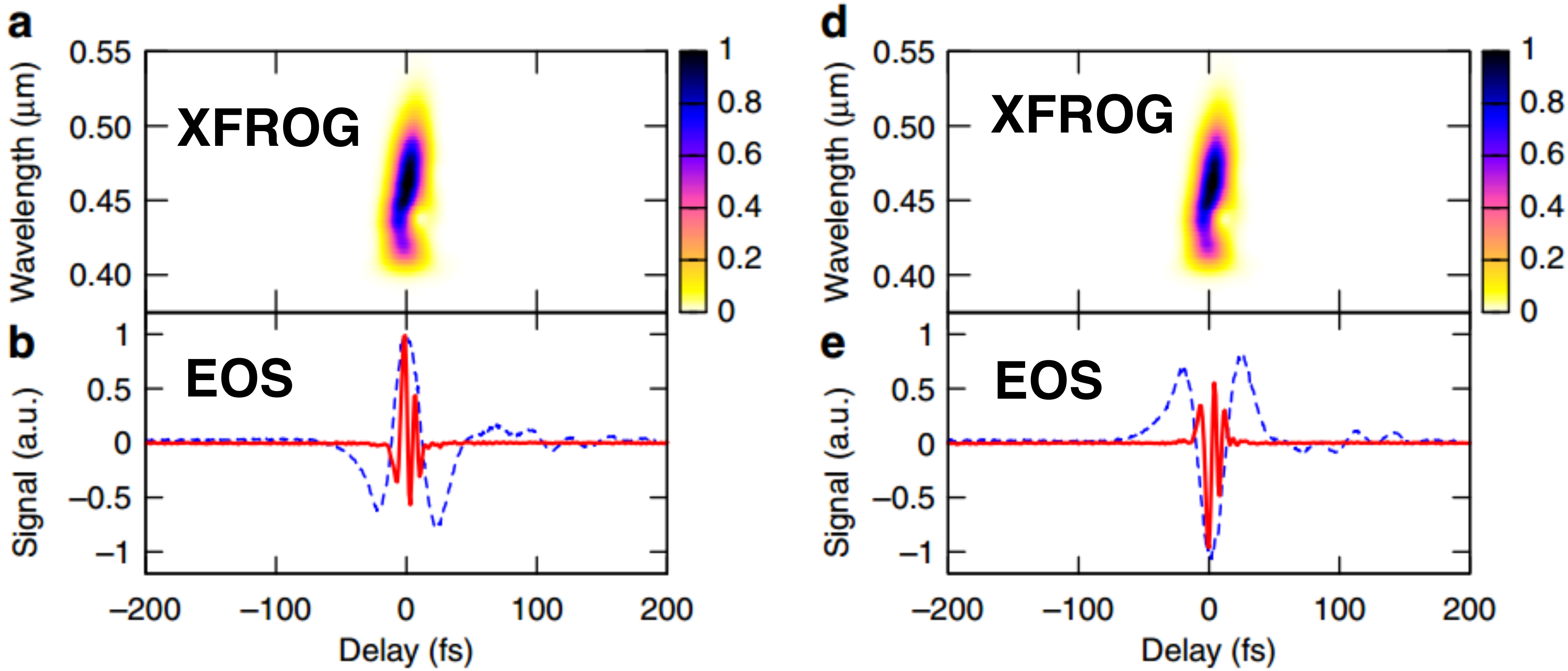

Y. Nomura et al., Nature Communications **4**, 2820 (2013)